

Modeling of cloud microphysics: from simple concepts to sophisticated parameterizations

Part II: ice microphysics

Wojciech Grabowski

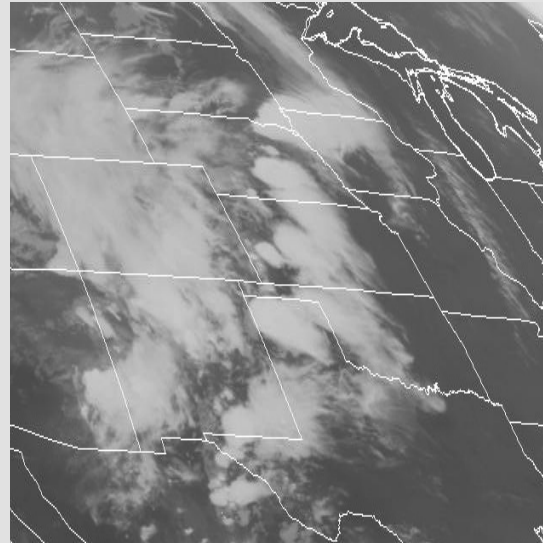
National Center for Atmospheric Research, Boulder, Colorado



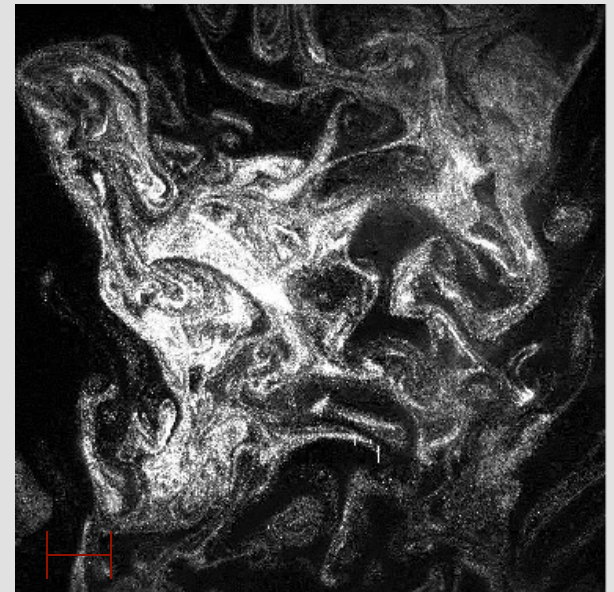
Mesoscale convective systems over US



1,000 km

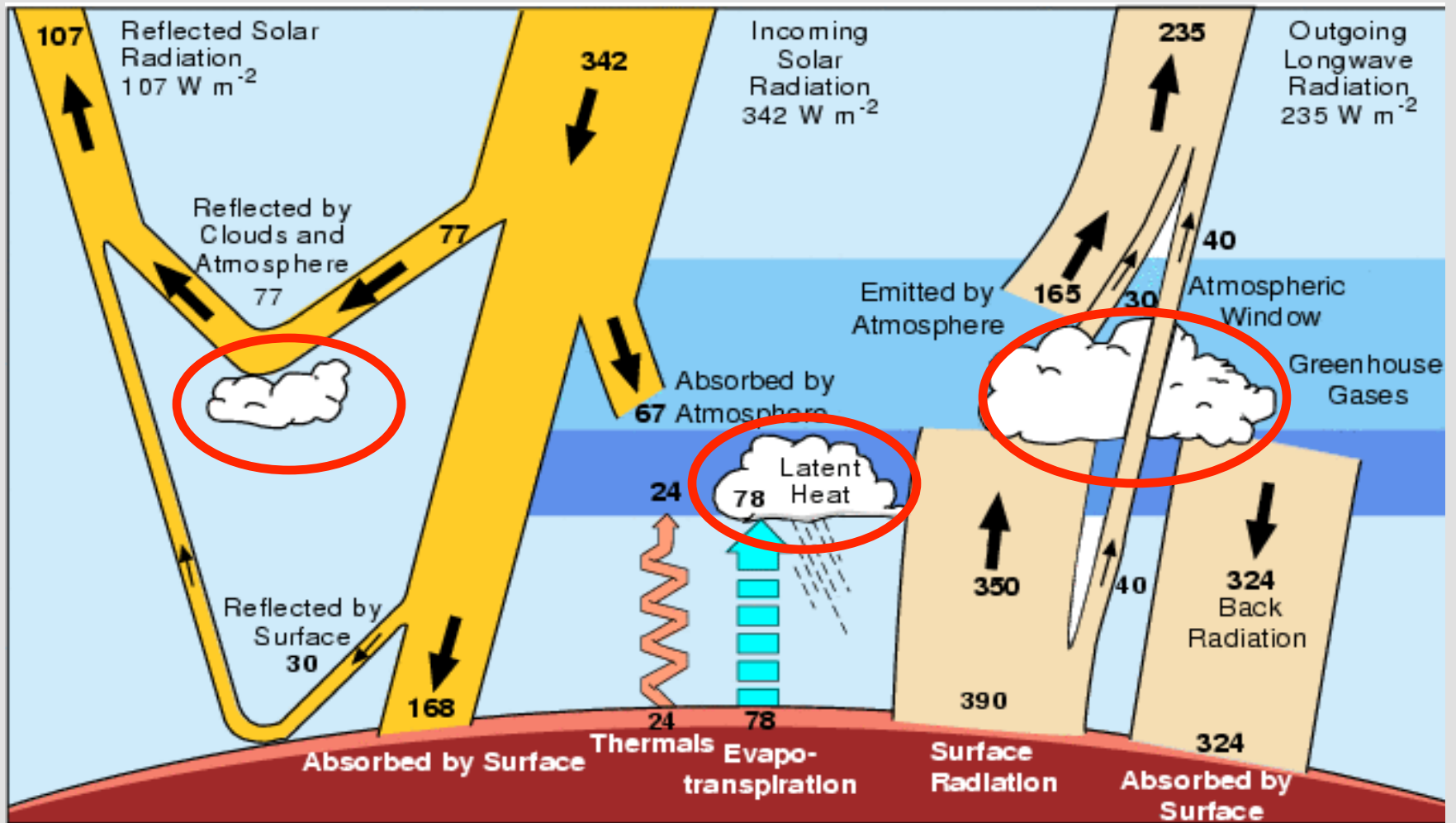


Mixing in laboratory cloud chamber



10 cm

*Clouds and climate:
the range of scales...*



Kiehl and Trenberth 1997

The Earth annual and global mean energy budget

Fundamentals of cloud physics

ELEMENTARY CLOUD PHYSICS:

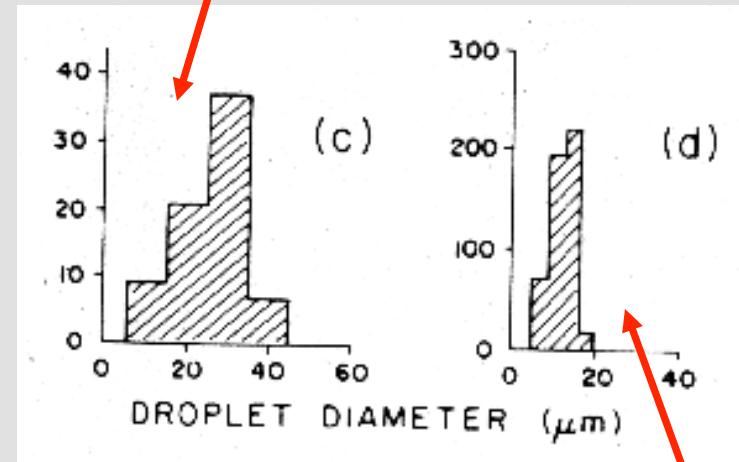
clouds form due to cooling of air (e.g., adiabatic expansion of a parcel of air rising in the atmosphere)

- *condensation*: water vapor \rightarrow cloud droplets

heterogeneous nucleation on atmospheric aerosols called Cloud Condensation Nuclei (CCN); typically highly soluble salts (sea salt, sulfates, ammonium salts, nitrates)

typically, only a small percentage of CCN used by clouds (i.e., water clouds form just above saturation)

Maritime cumulus



Continental cumulus

ELEMENTARY CLOUD PHYSICS, cont.:

- *formation of ice particles*

heterogeneous nucleation on atmospheric aerosols called Ice-forming Nuclei (IN); dominates for temperatures higher than about -40 deg C (233 K); poorly understood; various modes (contact, deposition, condensation-freezing)

IN are typically silicate particles (clays) or other compounds with crystallographic lattice similar to ice, highly insoluble (contact nucleation) or coated with soluble compound (condensation-freezing)

IN are scarce, their number depends strongly on temperature (typically, 1 per liter at -20 deg C, 10 per liter at -25 deg C).

homogeneous freezing is possible once droplet temperature is smaller than about -40 deg C.

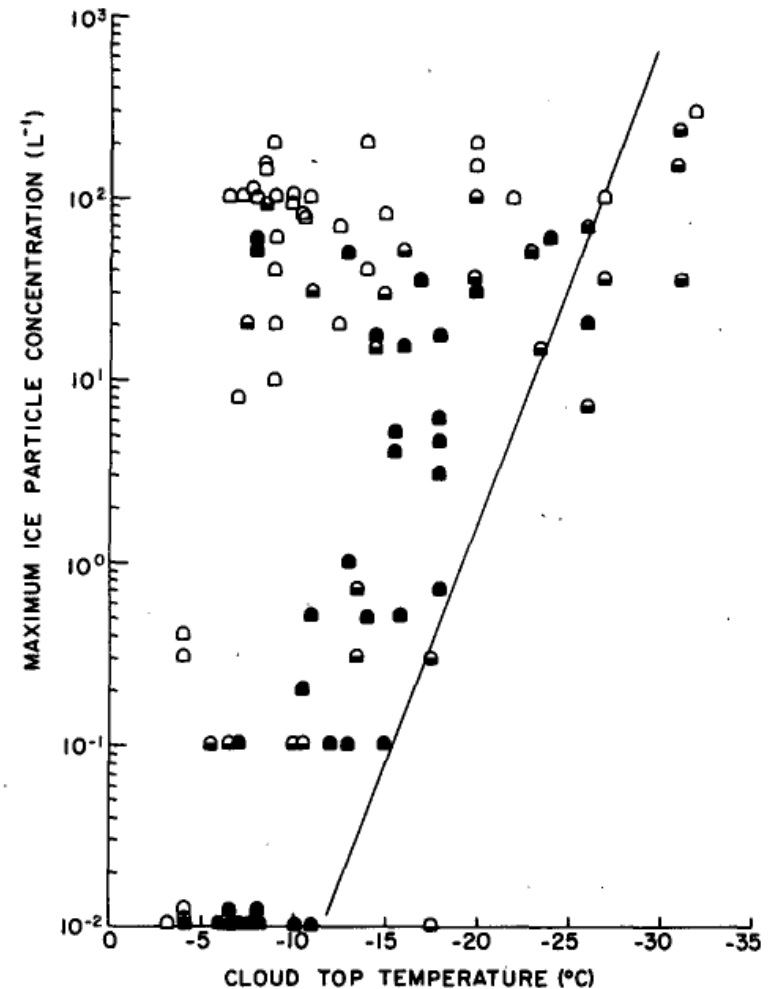


FIG. 2. Measurements of the maximum ice particle concentrations in mature and aging maritime (open humps), continental (closed humps) and transitional (half-open humps) cumuliiform clouds. The line represents the concentrations of ice nuclei given by Eq. (1).

From cloud droplets and ice crystals to precipitation:

WARM RAIN:

→ gravitational collision and coalescence between
cloud droplets

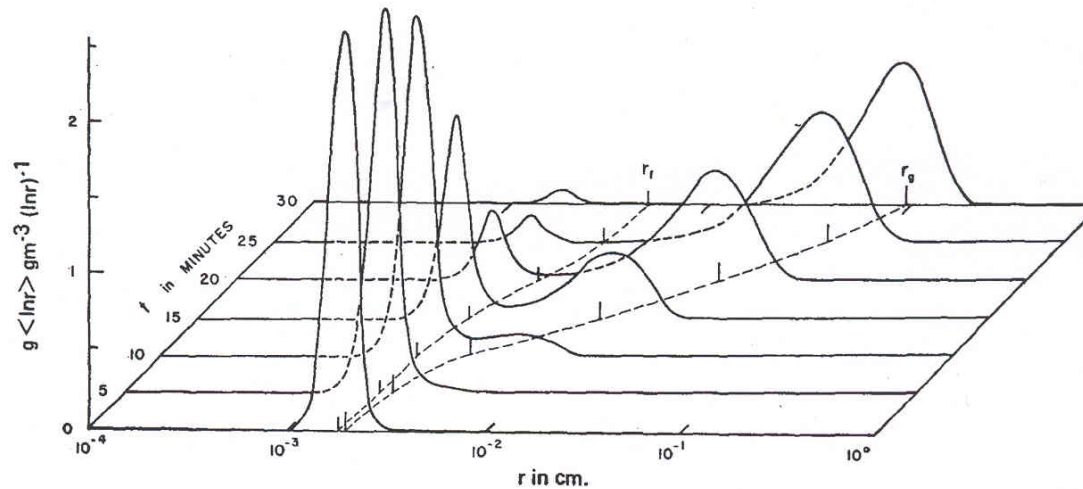


FIG. 5. Time evolution of the initial spectrum for $r_r^0 = 18 \mu\text{m}$, var $\alpha = 0.25$.

THE DISTRIBUTION OF RAINDROPS WITH SIZE

By *J. S. Marshall and W. McK. Palmer*¹

McGill University, Montreal

(Manuscript received 26 January 1948)

$$N_D = N_0 e^{-\Lambda D}$$

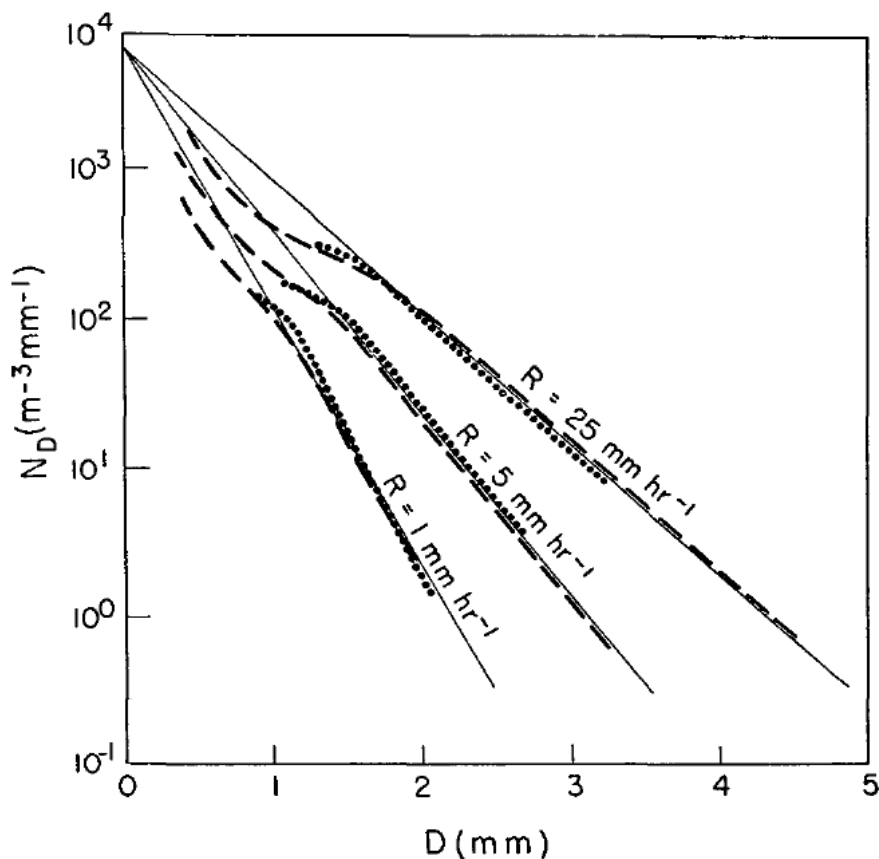


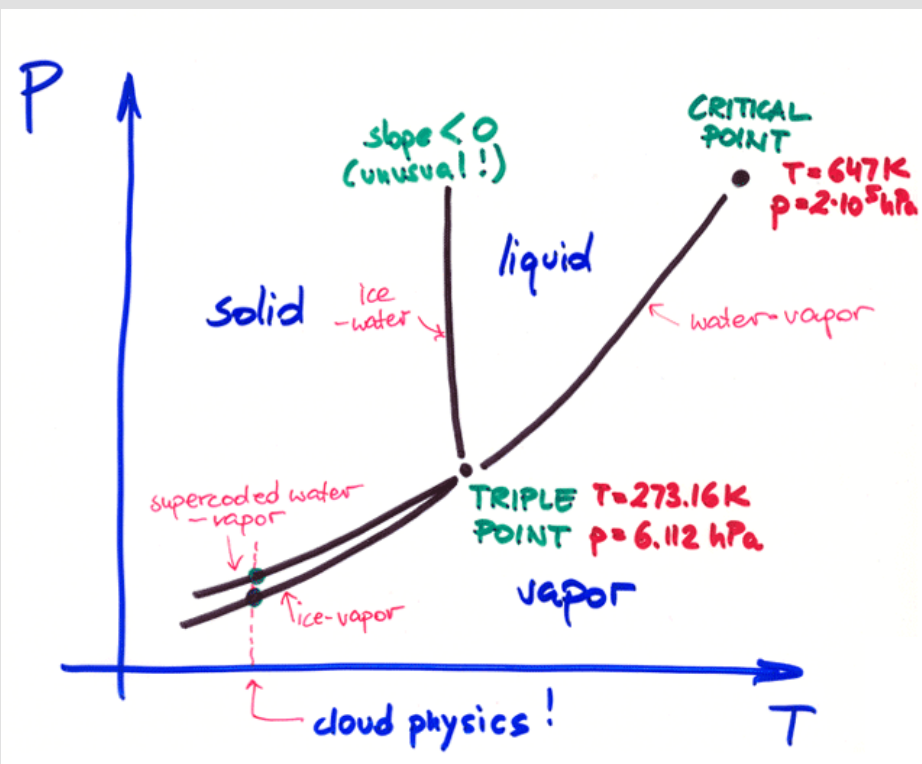
FIG. 2. Distribution function (solid straight lines) compared with results of Laws and Parsons (broken lines) and Ottawa observations (dotted lines).

From cloud droplets and ice crystals to precipitation:

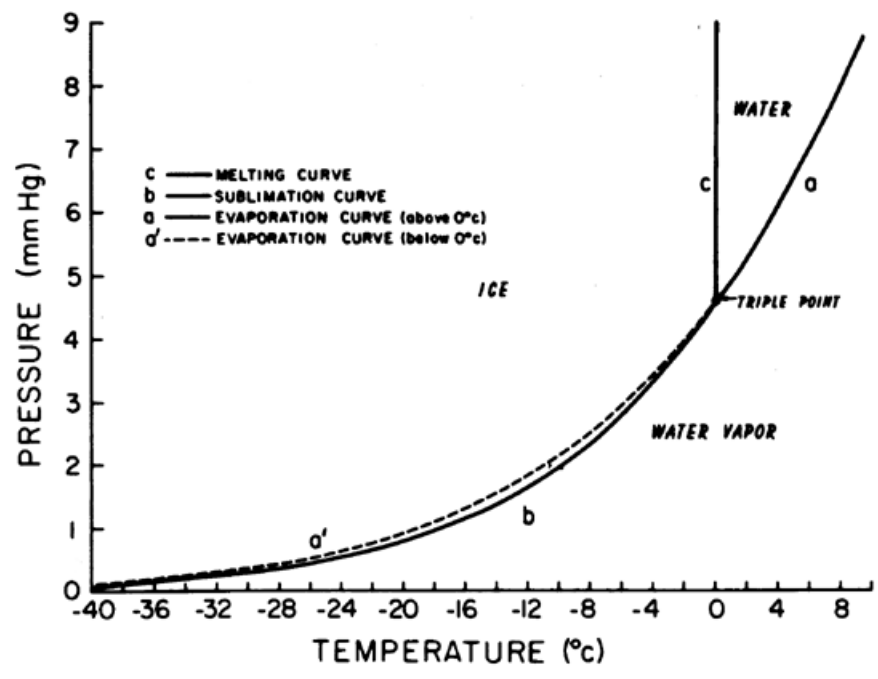
ICE PROCESSES:

→ Findeisen-Bergeron process: water vapor pressure at saturation is lower over ice than over water; it follows that once ice crystal is formed from supercooled droplet, it grows rapidly through diffusion of water vapor at the expense of cloud droplets

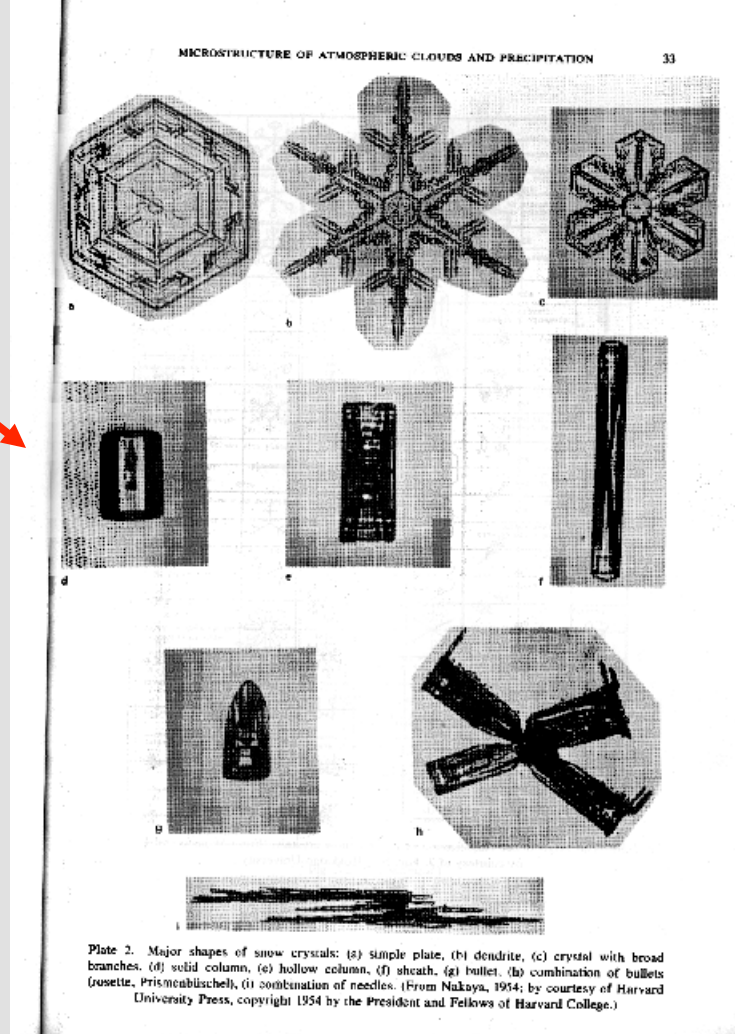
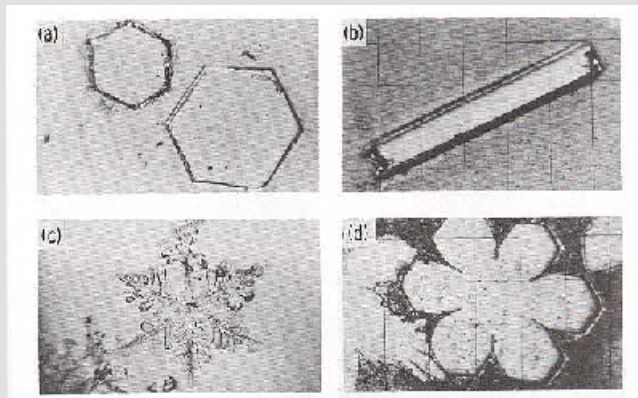
→ riming: falling ice crystal collects supercooled droplets that freeze upon contact (graupel, hail, etc).



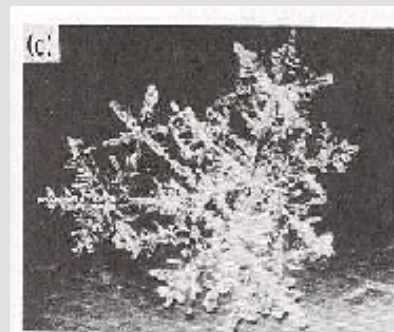
p-T phase equilibrium diagram for water substance



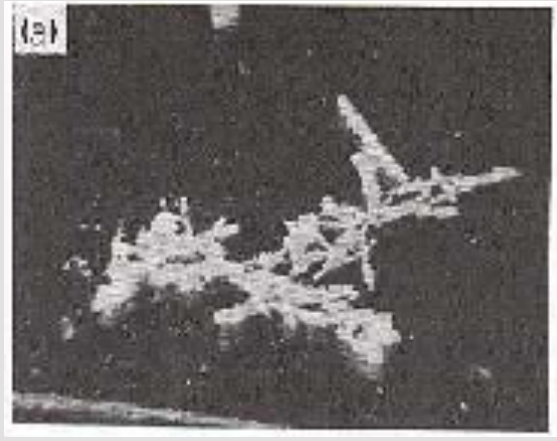
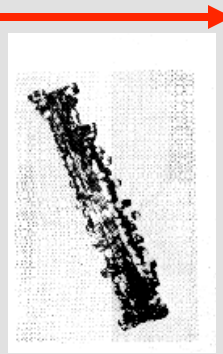
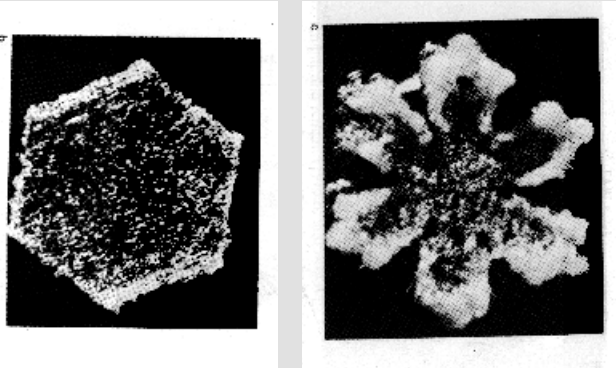
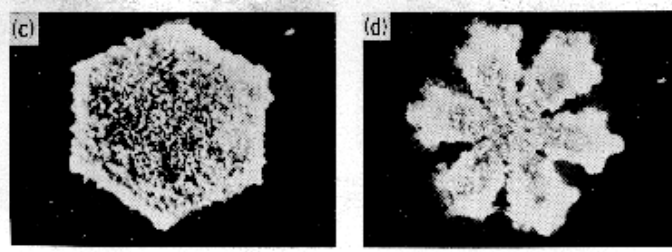
Pristine ice crystals,
grown by diffusion of
water vapor (water
vapor between ice-
and water-saturation)



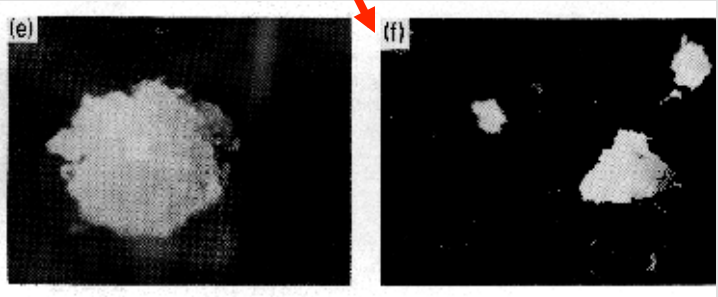
Snowflakes, grown by
aggregation



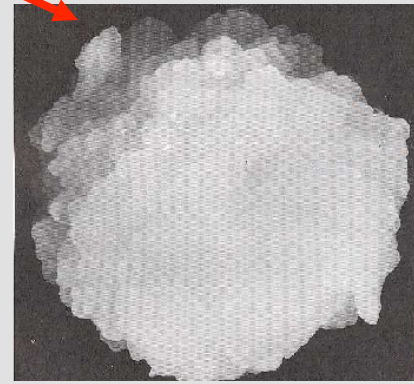
**Rimed ice crystals
(accretion of
supercooled cloud
water)**



**Graupel (heavily
rimed ice crystals)**



Hail (not to scale)



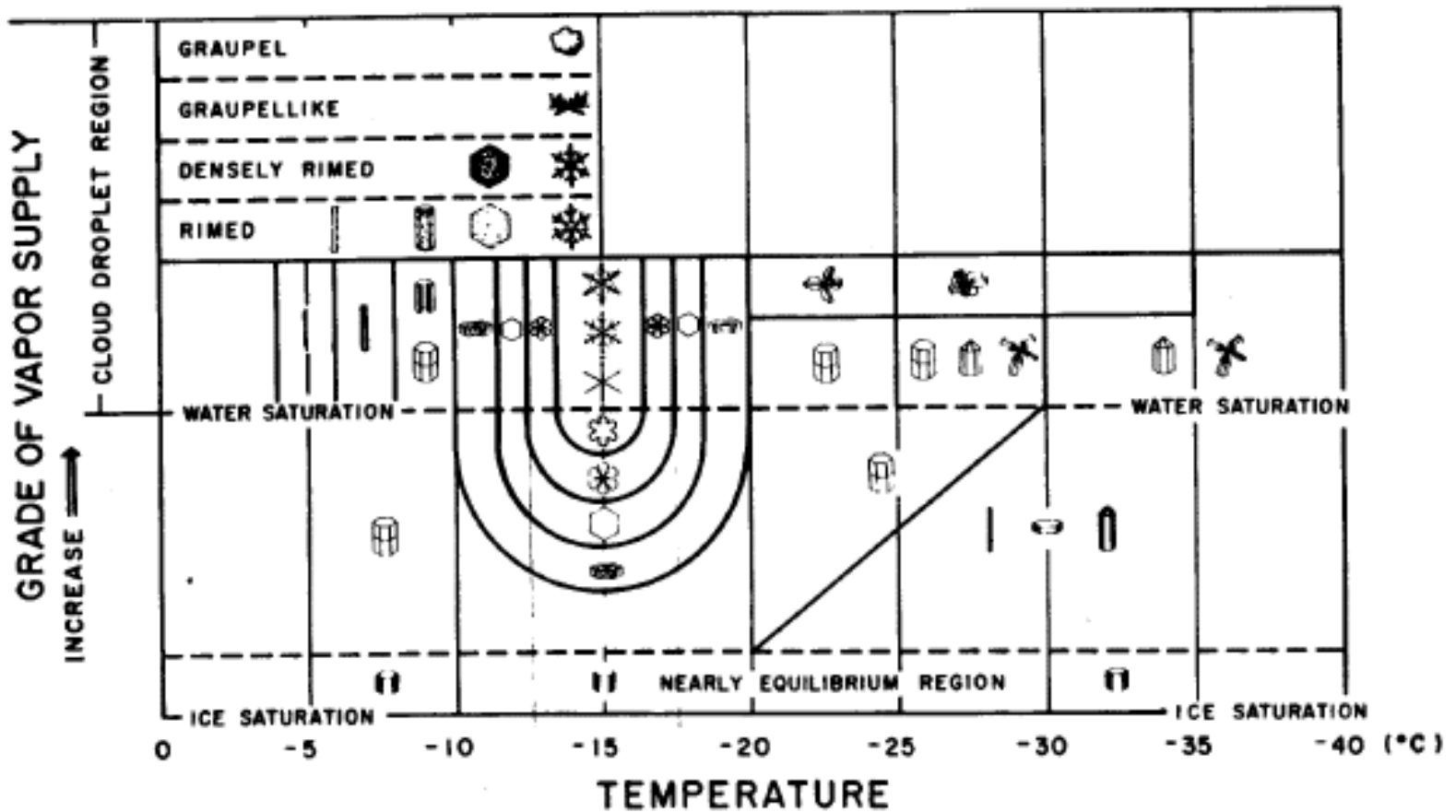
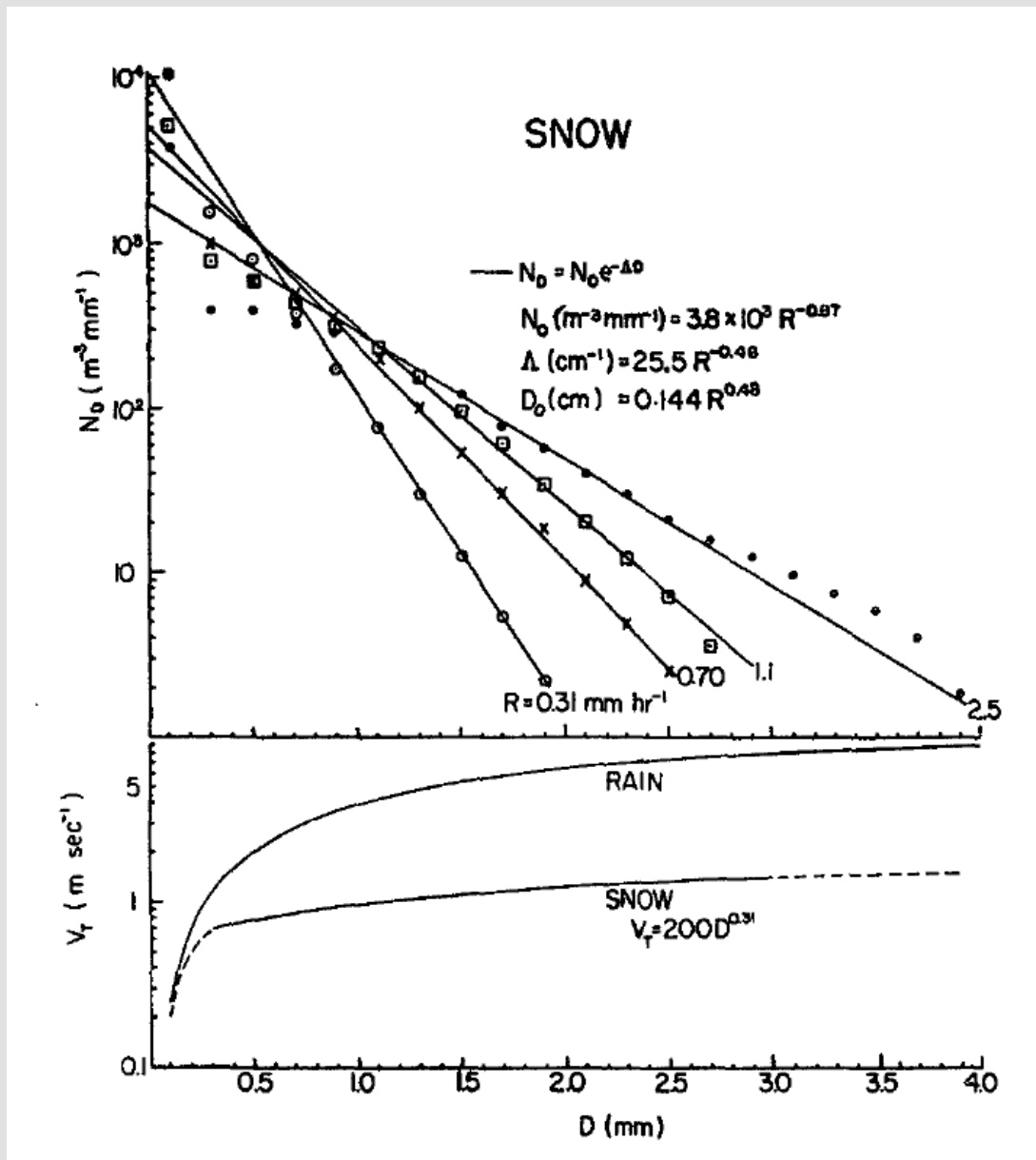


Fig. 2-26. Temperature and humidity conditions for the growth of natural snow crystals of various types. (From Magono and Lee, 1966; by courtesy of *J. Fac. Sci., Hokkaido University.*)

Magono and Lee (1966) classification of ice crystals and their growth regimes

$$N_D = N_0 e^{-\Delta D}$$



Gunn and Marshall JAS 1958

Fundamentals of cloud thermodynamics modeling

Water vapor is a minor constituent:

mass loading is typically smaller than 1%; thermodynamic properties (e.g., specific heats etc.) only slightly modified;

Suspended small particles (cloud droplets, cloud ice):

mass loading is typically smaller than a few tenths of 1%, particles are much smaller than the smallest scale of the flow; multiphase approach is not required, but sometimes used (e.g., DNS with suspended droplets, Lagrangian Cloud Model)

Precipitation (raindrops, snowflakes, graupel, hail):

mass loading can reach a few %, particles are larger than the smallest scale the flow; multiphase approach needed only for very-small-scale modeling

Continuous medium approach: density (i.e., mass in the unit volume) is the main field variable (density of water vapor, density of cloud water, density of rainwater, etc...)

$$\frac{\partial \rho_v}{\partial t} + \nabla(\rho_v \mathbf{u}) = S \quad \text{or} \quad \frac{d\rho_v}{dt} + \rho_v \nabla \mathbf{u} = S$$

$$\frac{d\psi}{dt} = \frac{\partial \psi}{\partial t} + \mathbf{u} \cdot \nabla \psi$$

In practice, mixing ratios are typically used. Mixing ratio is the ratio between the density (of water vapor, cloud water...) and the air density.

**Mixing ratios
versus specific
humidities...**

$$\frac{\partial \rho_a}{\partial t} + \nabla(\rho_a \mathbf{u}) = 0 \quad \text{or} \quad \frac{d\rho_a}{dt} + \rho_a \nabla \mathbf{u} = 0$$

$$\frac{\partial \rho_v}{\partial t} + \nabla(\rho_v \mathbf{u}) = S \quad \text{or} \quad \frac{d\rho_v}{dt} + \rho_v \nabla \mathbf{u} = S$$

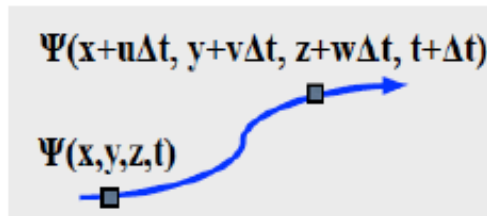
$$\text{mixing ratio : } q = \frac{\rho_v}{\rho_a}$$

$$\frac{dq}{dt} = \frac{S}{\rho_a}$$

$$\text{specific humidity : } Q = \frac{\rho_v}{\rho_v + \rho_a}$$

$$\frac{dQ}{dt} = \frac{\rho_a}{\rho_v + \rho_a} \frac{S}{\rho_v + \rho_a}$$

Lagrangian versus Eulerian formulation



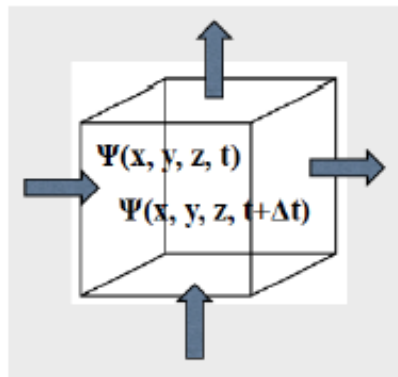
$$\frac{D\Psi}{Dt} = S$$

or

$$\frac{\partial \Psi}{\partial t} + \mathbf{u} \cdot \nabla \Psi = S$$

combined with dry air continuity equation:

$$\frac{\partial \rho_a}{\partial t} + \nabla(\rho_a \mathbf{u}) = 0$$



gives:

$$\frac{\partial \rho_a \Psi}{\partial t} + \nabla(\rho_a \mathbf{u} \Psi) = \rho_a S$$

For the anelastic system:

$$\frac{\partial \Psi}{\partial t} + \frac{1}{\rho_o} \nabla(\rho_o \mathbf{u} \Psi) = S$$

$$\rho_o = \rho_o(z)$$

Modeling of ice microphysics

Ice processes:

Ice initiation is the main problem:

**Primary ice nucleation - freezing of cloud droplets
homogeneously for temperatures colder than about -40 deg C
and heterogeneously by contact with ice-forming nucleus**

Secondary ice nucleation - the ice multiplication.

Unlike warm-rain microphysics, where cloud droplets and rain/drizzle drops are well separated in the radius space, growth of ice phase is continuous in size/mass space. Both diffusional and accretional growth are important.

Complexity of ice crystal shapes (“habits”).

OUTLINE:

Bulk ice physics modeling

- equilibrium approach: a simple extension of the warm-rain scheme
- non-equilibrium approach: more comprehensive schemes
- single-moment versus multi-moment schemes

Bin ice microphysics

Lagrangian (particle-based) methods

OUTLINE:

Bulk ice physics modeling

- equilibrium approach: a simple extension of the warm-rain scheme
- non-equilibrium approach: more comprehensive schemes
- single-moment versus multi-moment schemes

Bin ice microphysics

Lagrangian (particle-based) methods

Toward Cloud Resolving Modeling of Large-Scale Tropical Circulations: A Simple Cloud Microphysics Parameterization

WOJCIECH W. GRABOWSKI

National Center for Atmospheric Research, Boulder, Colorado*

(Manuscript received 9 September 1997, in final form 9 February 1998)

ABSTRACT

This paper discusses cloud microphysical processes essential for the large-scale tropical circulations and the tropical climate, as well as the strategy to include them in large-scale models that resolve cloud dynamics. The emphasis is on the ice microphysics, which traditional cloud models consider in a fairly complex manner and where a simplified approach is desirable. An extension of the classical warm rain bulk parameterization is presented. The proposed scheme retains simplicity of the warm rain parameterization (e.g., only two classes of condensed water are considered) but introduces two important modifications for temperatures well below freezing: 1) the saturation conditions are prescribed based on saturation with respect to ice, not water; and 2) growth characteristics and terminal velocities of precipitation particles are representative for ice particles, not raindrops. Numerical tests suggest that, despite its simplicity, the parameterization is able to capture essential aspects of the cloud microphysics important for the interaction between convection and the large-scale environment. As an example of the application of this parameterization, preliminary results of the two-dimensional cloud-resolving simulation of a Walker-like circulation are presented.

**Equilibrium approach: a simple extension
of the warm-rain scheme)**

J. Atmos. Sci.

Equilibrium approach (a simple extension of the warm-rain scheme)

SIMPLE BULK ICE MODEL (Grabowski JAS 1998):

$$\frac{D\theta}{Dt} = \frac{L_v\theta}{c_p T} (COND - DIFF)$$

$$\frac{Dq_v}{Dt} = -COND + DIFF$$

$$\frac{Dq_c}{Dt} = COND - AUTC - ACCR$$

$$\frac{Dq_p}{Dt} = \frac{1}{\rho} \frac{\partial}{\partial z} (\rho q_p v_t) + AUTC + ACCR - DIFF$$

θ - potential temperature

q_v - water vapor mixing ratio

q_c - cloud condensate (water or ice) mixing ratio

q_p - precipitation water (rain or snow) mixing ratio

$COND$ - condensation rate (saturation adjustment)

$DIFF$ - diffusional growth rate

$AUTC$ - "autoconversion" rate: $q_c \rightarrow q_p$

$ACCR$ - accretion rate: $q_c, q_p \rightarrow q_p$

saturation: $q_{vs} = \alpha q_{vw} + (1 - \alpha) q_{vi}$

cloud water: $q_w = \alpha q_c$; cloud ice: $q_i = (1 - \alpha) q_c$

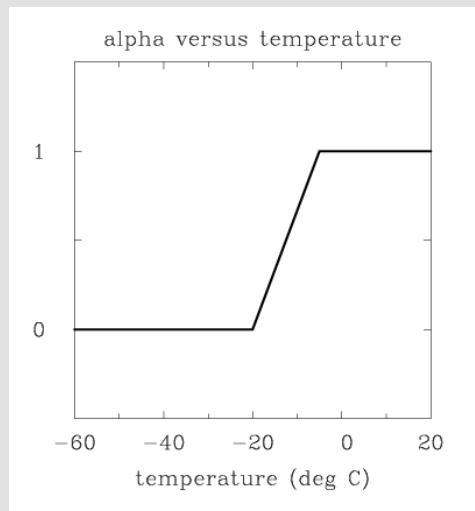
rain: $q_r = \alpha q_p$; snow: $q_s = (1 - \alpha) q_p$

$DIFF = DIFF_r + DIFF_s$

$AUTC = AUTC_r + AUTC_s$

$ACCR = ACCR_r + ACCR_s$

$v_t = \alpha v_t(q_r) + (1 - \alpha) v_t(q_s)$



$$\frac{\partial \rho_o \theta}{\partial t} + \nabla \cdot (\rho_o \mathbf{u} \theta) = \frac{L_v \theta_e}{c_p T_e} (\text{CON} + \text{DEP}) + D_\theta, \quad (1a)$$

$$\frac{\partial \rho_o q_v}{\partial t} + \nabla \cdot (\rho_o \mathbf{u} q_v) = -\text{CON} - \text{DEP} + D_{q_v}, \quad (1b)$$

$$\frac{\partial \rho_o q_c}{\partial t} + \nabla \cdot (\rho_o \mathbf{u} q_c) = \text{CON} - \text{ACC} - \text{AUT} + D_{q_c}, \quad (1c)$$

$$\frac{\partial \rho_o q_p}{\partial t} + \nabla \cdot [\rho_o (\mathbf{u} - V_T \mathbf{k}) q_p] = \text{ACC} + \text{AUT} + \text{DEP} + D_{q_p}. \quad (1d)$$

saturation: $q_{vs} = \alpha q_{vw} + (1 - \alpha)q_{vi}$

cloud water: $q_w = \alpha q_c$; cloud ice: $q_i = (1 - \alpha)q_c$

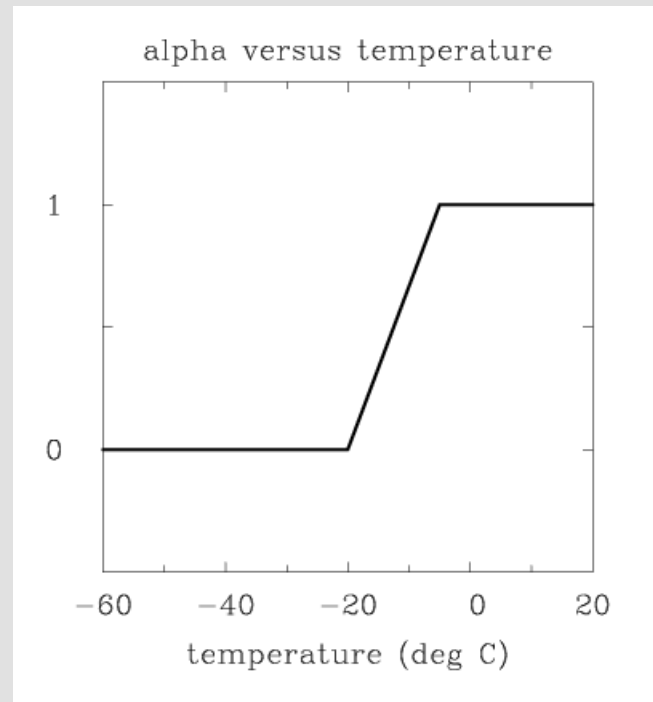
rain: $q_r = \alpha q_p$; snow: $q_s = (1 - \alpha)q_p$

$$DIFF = DIFF_r + DIFF_s$$

$$AUTC = AUTC_r + AUTC_s$$

$$ACCR = ACCR_r + ACCR_s$$

$$v_t = \alpha v_t(q_r) + (1 - \alpha)v_t(q_s)$$



$$q_{vs} = \frac{\varepsilon e_s}{p_e - e_s} \quad (2)$$

(see discussion in section 7 and appendix A of Lipps and Hemler 1982), where $\varepsilon = R_d/R_v$ (R_d and R_v are gas constants for the dry air and for the water vapor, respectively), p_e is the environmental pressure profile, and e_s is the saturated water vapor pressure given either by

$$e_s(T) = e_{oo} \exp \left[\frac{L_v}{R_v} \left(\frac{1}{T_{oo}} - \frac{1}{T} \right) \right] \quad (3a)$$

for the saturation over water or

$$e_s(T) = e_{oo} \exp \left[\frac{L_s}{R_v} \left(\frac{1}{T_{oo}} - \frac{1}{T} \right) \right] \quad (3b)$$

for the saturation over ice, where L_s denotes the latent heat of sublimation, $T = \theta(p_e/p_{oo})^{R_d/c_p}$, $p_{oo} = 10^5$ Pa, $e_{oo} = 611$ Pa, and $T_{oo} = 273.16$ K. The values of latent heats ($L_v = 2.53 \times 10^6$ J kg⁻¹, $L_s = 2.84 \times 10^6$ J kg⁻¹), assumed constant in (3), have been selected to provide as accurate values as possible of the saturated water vapor pressure over water and ice and their ratio over a wide range of temperatures.

precipitation (rain or snow),
 $N_0 = \text{const}$

$$n(D) = N_0 \exp(-\lambda D)$$

precipitation particles
mass-size and terminal
velocity-size relationships:

$$m = aD^b,$$
$$v_t = cD^d.$$

raindrops:

$$a = \frac{\pi}{6} \rho_w; \quad b = 3; \quad c = 130; \quad d = 0.5$$

snowflakes:

$$a = 2.5 \times 10^{-2}; \quad b = 2; \quad c = 4; \quad d = 0.25$$

$$\lambda = \left[\frac{aN_0 \Gamma(b+1)}{\rho_o q_p} \right]^{1/(b+1)}$$

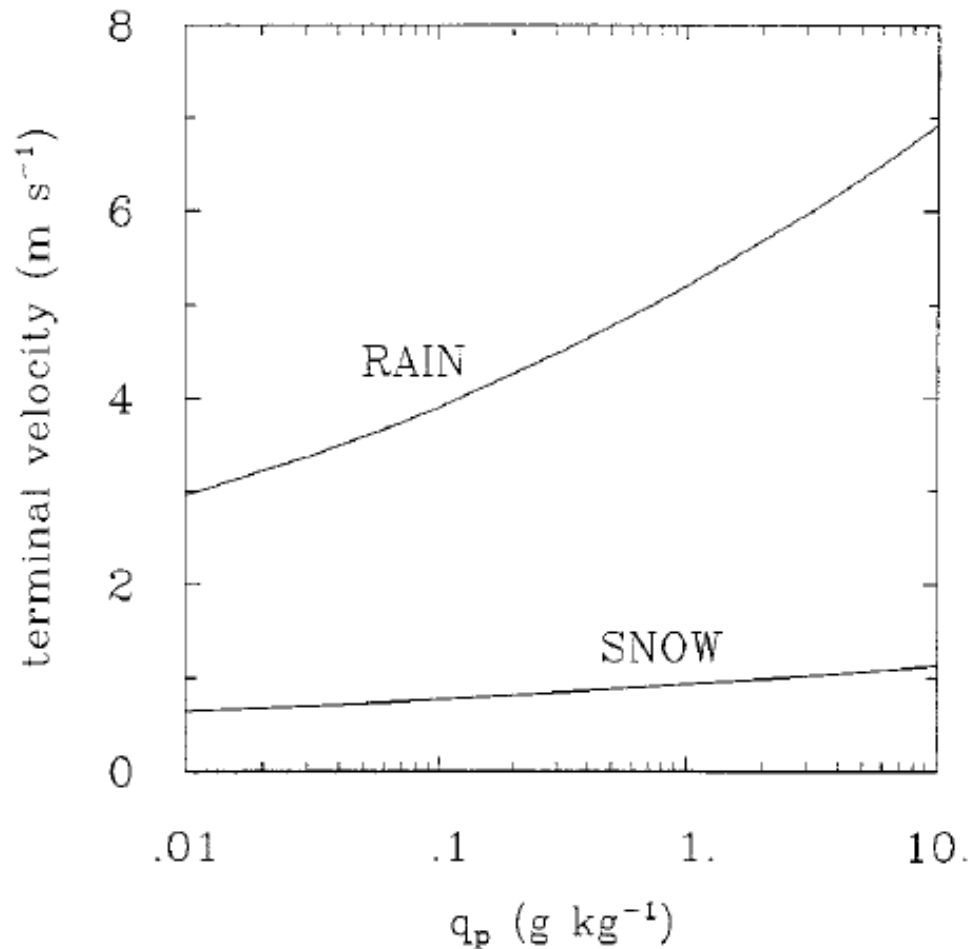


FIG. 2. Terminal velocity of rain and snow field as given by (17) as a function of the precipitation mixing ratio q_p .

RAIN:

Autoconversion: Berry's (1968) parameterization

$$\text{AUT} = 1.67 \times 10^{-5} \psi^2 \left(5 + \frac{0.036 N_d}{D_d \psi} \right)^{-1},$$

where

$$\psi = 10^3 \rho_o q_c$$

$$D_d = 0.146 - 5.964 \times 10^{-2} \ln \frac{N_d}{2000}, \quad (9)$$

which gives the relative dispersion of 0.33, 0.26, and 0.19 for droplet concentrations of 100, 300, and 1000 cm^{-3} . For the snow, the autoconversion term is para-

RAIN:

Autoconversion: Kogan (JAS 2013) parameterization

$$\left(\frac{\partial q_r}{\partial t}\right)_{\text{auto}} = 7.98 \times 10^{10} \times q_c^{4.22} N_c^{-3.01}, \quad (26)$$

where q_c and q_r are in kilograms per kilogram and N_c is per centimeters cubed.

SNOW:

cm^{-3} . For the snow, the autoconversion term is parameterized as

$$\text{AUT} = \frac{\rho_o q_c}{\tau_a}, \quad (10)$$

where τ_a is the conversion timescale assumed equal to a time required to grow an ice crystal by diffusion of water vapor in water saturated conditions up to a size of small precipitation particle (mass of 10^{-9} kg). This timescale is estimated using formulas for ice crystal growth developed by Koenig (1971) and approximated by a simple quadratic function decreasing from $\tau_a = 10^3$ s at 0°C to $\tau_a = 200$ s at -15°C and increasing back to $\tau_a = 10^3$ s at -30°C . For even colder temperatures, $\tau_a = 10^3$ s is used. Note that when the temperature is between T_w and T_i , q_c in (8) and (10) represents either cloud water part or cloud ice part of the cloud condensate, not the entire cloud condensate.

The precipitation growth terms (ACC, DEP) are estimated using characteristics of the particle with the average mass, that is,

$$\text{ACC} = \bar{n} \left(\frac{d\bar{m}}{dt} \right)_{\text{ACC}} \quad (11a)$$

$$\text{DEP} = \bar{n} \left(\frac{d\bar{m}}{dt} \right)_{\text{DEP}}, \quad (11b)$$

where \bar{n} is the mean concentration of precipitation particles

$$\bar{n} = \frac{N_o}{\lambda}; \quad (12)$$

\bar{m} is the mean mass of a precipitation particle,

$$\bar{m} = \frac{\rho_o q_p}{\bar{n}}; \quad (13)$$

and $(d\bar{m}/dt)_{\text{ACC}}$, $(d\bar{m}/dt)_{\text{DEP}}$ are growth rates of the mean particle due to accretion of cloud condensate and deposition of water vapor, respectively. The growth rates are estimated according to (e.g., Grabowski 1988)

for rain are

$$E = 0.8, \quad \alpha = 1, \quad \beta = 2,$$

and for the ice,

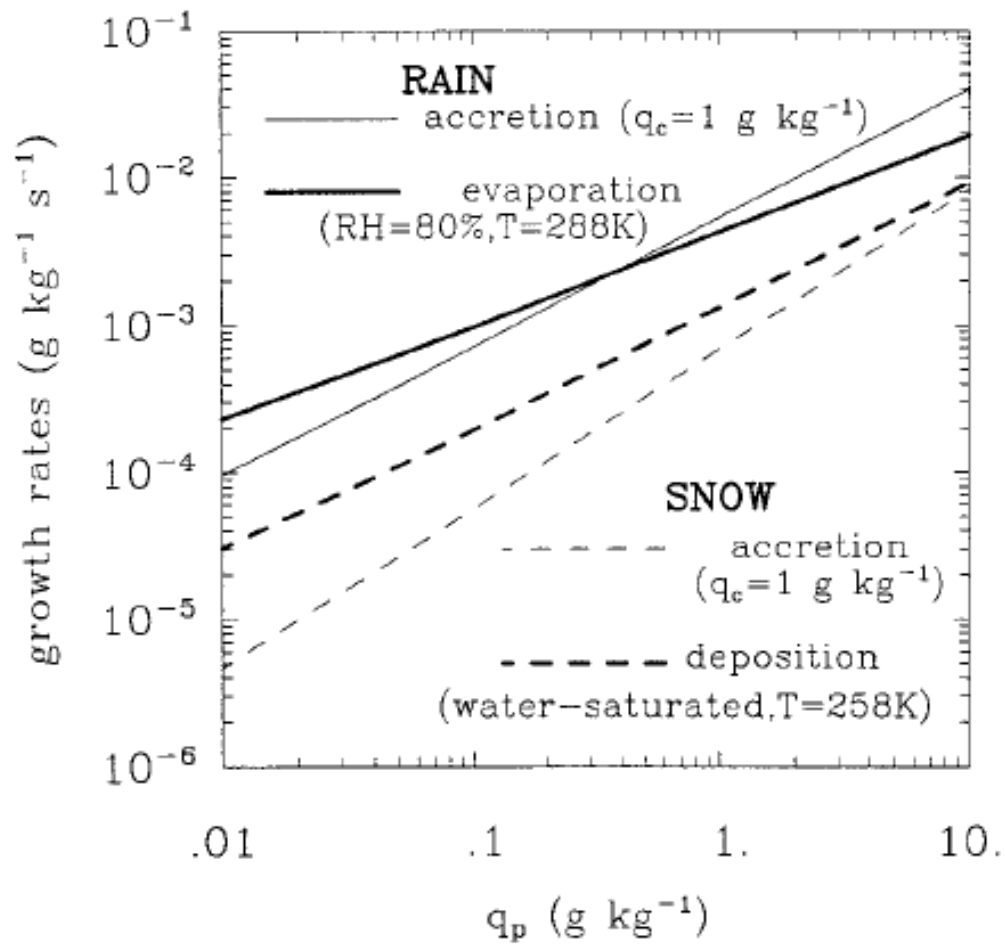
$$E = 0.2, \quad \alpha = 0.3, \quad \beta = 3.$$

$$\left(\frac{d\bar{m}}{dt} \right)_{\text{ACC}} = \frac{\pi \bar{D}^2}{4} v_t(\bar{D}) E \alpha \rho_o q_c \quad (14a)$$

$$\left(\frac{d\bar{m}}{dt} \right)_{\text{DEP}} = \frac{4\pi \bar{D}}{\beta} (S - 1) F G(T_e), \quad (14b)$$

where \bar{D} is the diameter of a particle with average mass [calculated from \bar{m} using (5a)], E is the collection efficiency, α is the ratio of the effective area of the precipitation particle and $\pi \bar{D}^2/4$ (i.e., 1 for raindrops and smaller than 1 for snow), β is a nondimensional factor that depends on precipitation particle geometry (e.g., $\beta = 2$ for a sphere, $\beta = \pi$ for an infinitely thin circular disc, $\beta \sim 3$ for a thin needle), $S = q_v/q_{vs}$ is the saturation ratio, F is the ventilation factor [$F \approx 0.78 + 0.27R_e^{1/2}$ for raindrops and $F \approx 0.65 + 0.39R_e^{1/2}$ for ice particles, $R_e = \bar{D}v_t(\bar{D})/\nu$ is the Reynolds number, $\nu \approx 2 \times 10^{-5} \text{ m}^2 \text{ s}^{-1}$ is the kinematic viscosity of air; Pruppacher and Klett (1978)], and $G(T_e)$ is the thermodynamic function [Pruppacher and Klett (1978), Eq. (13.28) and (13.71)] approximated as

$$G(T_e) = A \left(2.2 \frac{T_e}{e_s(T_e)} + \frac{2.2 \times 10^2}{T_e} \right)^{-1}, \quad (15)$$



SIMPLE BULK ICE MODEL (Grabowski JAS 1998):

$$\frac{D\theta}{Dt} = \frac{L_v\theta}{c_p T} (COND - DIFF)$$

$$\frac{Dq_v}{Dt} = -COND + DIFF$$

$$\frac{Dq_c}{Dt} = COND - AUTC - ACCR$$

$$\frac{Dq_p}{Dt} = \frac{1}{\rho} \frac{\partial}{\partial z} (\rho q_p v_t) + AUTC + ACCR - DIFF$$

OUTLINE:

Bulk ice physics modeling

- equilibrium approach - a simple extension of the warm-rain scheme
- non-equilibrium approach – more comprehensive schemes
- single-moment versus multi-moment schemes

Bin ice microphysics

Lagrangian (particle-based) methods

BULK MODEL WITH ICE MICROPHYSICS:

- potential temperature θ :

$$\frac{D\theta}{Dt} = \frac{L_v\theta_e}{c_p T_e} S_1 + \frac{L_s\theta_e}{c_p T_e} S_2 + \frac{L_f\theta_e}{c_p T_e} S_3$$

- water vapor mixing ratio q_v :

$$\frac{Dq_v}{Dt} = S_v$$

- cloud condensate variables q_c^i , $i = 1, N_c$ (typically, $N_c = 2$: cloud water, cloud ice):

$$\frac{Dq_c^i}{Dt} = S_c^i$$

- precipitating water variables q_p^i , $i = 1, N_p$: (typically, $N_p = 3$: rain, snow, graupel/hail):

$$\frac{Dq_p^i}{Dt} = \frac{1}{\rho} \frac{\partial}{\partial z} (\rho q_p^i v_t^i) + S_p^i$$

S – various sources/sinks due to phase changes

Single-moment schemes:

q – mass mixing ratios
(3rd moment of particle size distribution; PSD)

Double-moment schemes:

q – mass and number mixing ratios
(3rd and 1st moments of PSD)

...

BULK MODEL WITH ICE MICROPHYSICS:

- potential temperature θ :

$$\frac{d\theta}{dt} = \frac{L_v\theta_e}{c_p T_e} S_1 + \frac{L_s\theta_e}{c_p T_e} S_2 + \frac{L_f\theta_e}{c_p T_e} S_3$$

- water vapor mixing ratio q_v :

$$\frac{dq_v}{dt} = S_v$$

- cloud condensate variables q_c^i , $i = 1, N_c$ (typically, $N_c = 2$: cloud water, cloud ice):

$$\frac{dq_c^i}{dt} = S_c^i$$

- precipitating water variables q_p^i , $i = 1, N_p$: (typically, $N_p = 3$: rain, snow, graupel/hail):

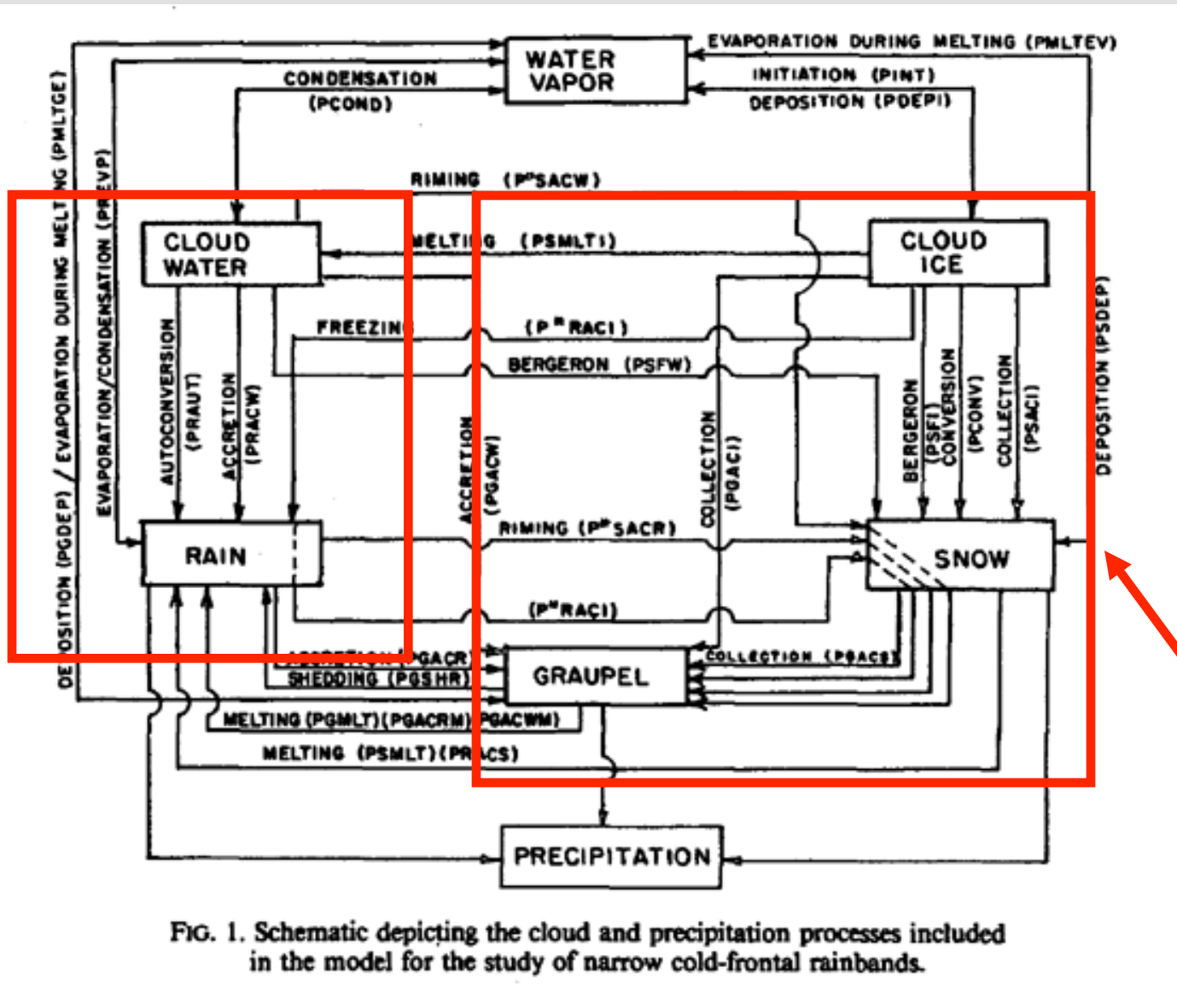
$$\frac{dq_p^i}{dt} = \frac{1}{\rho} \frac{\partial}{\partial z} (\rho q_p^i v_t^i) + S_p^i$$

Lin et al. 1983

Rutledge and Hobbs 1984

S – various sources/sinks due to phase changes

Traditional approach to bulk cloud microphysics



Warm-rain part

Ice part

FIG. 1. Schematic depicting the cloud and precipitation processes included in the model for the study of narrow cold-frontal rainbands.


BULK RAIN/ICE MODEL
(Lin et al. 1983, Rutledge and Hobbs 1984)


$$\frac{\partial \rho_o \theta}{\partial t} + \nabla \cdot (\rho_o \mathbf{u} \theta) = \frac{L_v \theta_e}{c_p T_e} S_1 + \frac{L_s \theta_e}{c_p T_e} S_2 + \frac{L_f \theta_e}{c_p T_e} S_3 + D_\theta$$


Water vapor  $\frac{\partial \rho_o q_v}{\partial t} + \nabla \cdot (\rho_o \mathbf{u} q_v) = S_4 + D_{q_v}$

Cloud water  $\frac{\partial \rho_o q_c}{\partial t} + \nabla \cdot (\rho_o \mathbf{u} q_c) = S_5 + D_{q_c}$

Cloud ice  $\frac{\partial \rho_o q_i}{\partial t} + \nabla \cdot (\rho_o \mathbf{u} q_i) = S_6 + D_{q_i}$

Rain  $\frac{\partial \rho_o q_r}{\partial t} + \nabla \cdot [\rho_o (\mathbf{u} - V_T^r \mathbf{k}) q_r] = S_7 + D_{q_r}$

Snow  $\frac{\partial \rho_o q_s}{\partial t} + \nabla \cdot [\rho_o (\mathbf{u} - V_T^s \mathbf{k}) q_s] = S_8 + D_{q_s}$

**Graupel
(or hail)**  $\frac{\partial \rho_o q_g}{\partial t} + \nabla \cdot [\rho_o (\mathbf{u} - V_T^g \mathbf{k}) q_g] = S_9 + D_{q_g}$

The main problem with such an approach to ice microphysics parameterization is that the ice scheme should produce various types of ice (cloud ice, snow, graupel) just by the physics of particle formation and growth.

Partitioning ice particles a priori into separate categories introduces unphysical “conversion rates” and may involve “thresholding behavior” (i.e., model solutions diverge depending whether the threshold is reached or not).

Unfortunately, the schemes designed in the 1980ies (with the logic taken from the warm rain physics...) are the mainstream of ice parameterization methods today...

Alternative approaches focusing on ice initiation and growth:

Koenig and Murray (JAM 1976) and its simplified version (Grabowski AR 1999)

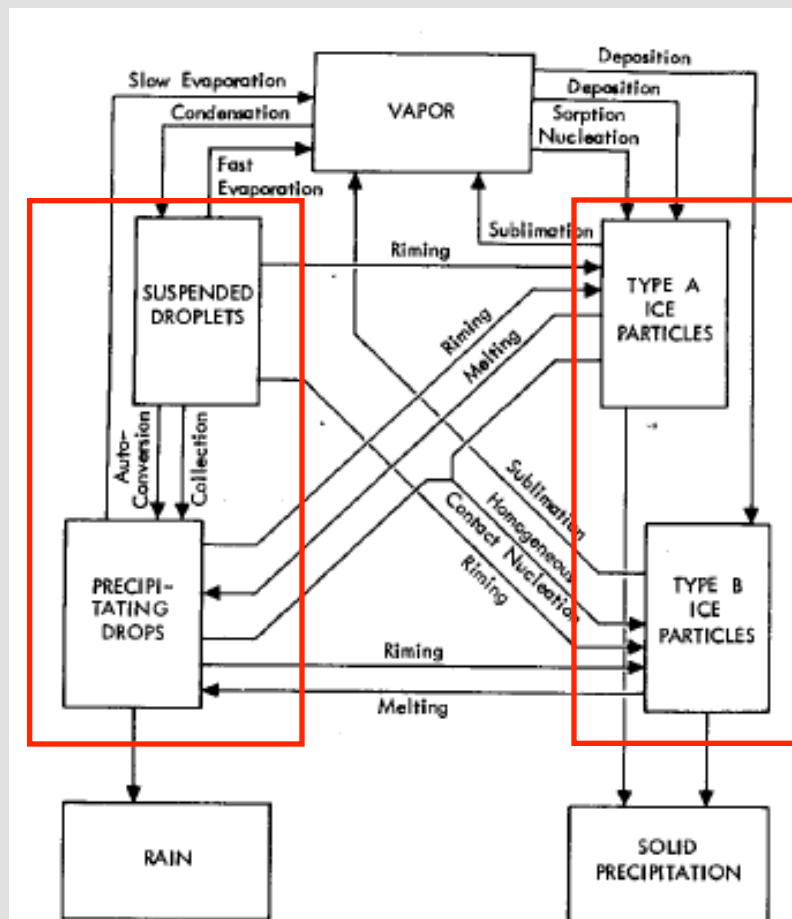
Morrison and Grabowski (JAS 2008) and ongoing development by Morrison and his colleagues (Prediction of bulk ice Particle Properties, P3, scheme)

Ice-Bearing Cumulus Cloud Evolution : Numerical Simulation and General Comparison Against Observations

L. RANDALL KOENIG AND FRANCIS W. MURRAY

The Rand Corporation, Santa Monica, Calif. 90406

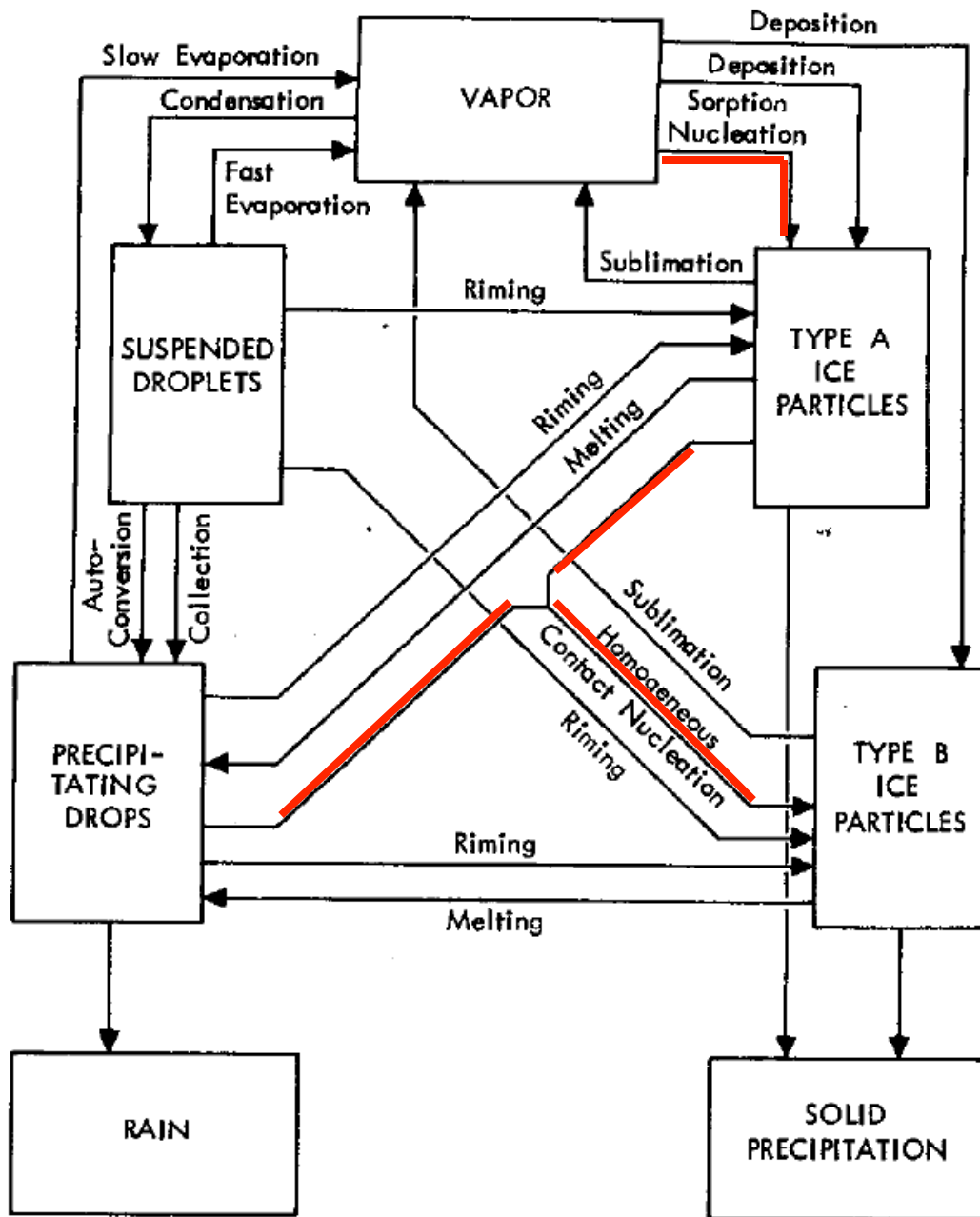
(Manuscript received 11 February 1976, in revised form 23 April 1976)



mass
mixing
ratios

mass and number
mixing ratios

FIG. 1. Schematic depiction of microphysical processes included in the model.



Ice initiation:

Ice A- initial source of ice (can be more complicated than "sorption nucleation")

Ice B – collisions between drizzle/rain drops and ice A

Physics of ice growth is the same for A and B:

- growth by diffusion of water vapor (based on laboratory experiments)
- growth by riming (collection of cloud droplets and drizzle/rain drops by ice crystals)

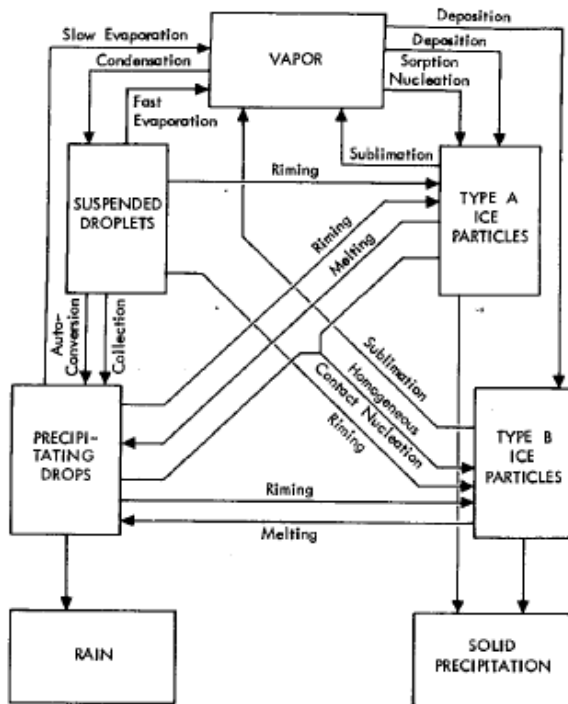


FIG. 1. Schematic depiction of microphysical processes included in the model.

A parameterization of cloud microphysics for long-term cloud-resolving modeling of tropical convection

Wojciech W. Grabowski

National Center for Atmospheric Research,¹ Boulder, CO 80307, USA

Received 15 March 1999; received in revised form 17 May 1999; accepted 7 June 1999

Follows the logic of Koenig and Murray approach with (some important) differences; ice A and B apply prescribed ice distributions based on observations in tropical anvils (ice A) and an exponential distribution (ice B).

$$\frac{\partial \rho_o \theta}{\partial t} + \nabla(\rho_o u \theta) = \mathcal{F}_\theta \equiv$$

$$\frac{L_v \theta_e}{c_p T_e} (\text{COND} - \text{REVP}) + \frac{L_s \theta_e}{c_p T_e} (\text{DEPA} + \text{DEPB} + \text{HOMA1})$$

$$+ \frac{L_f \theta_e}{c_p T_e} (\text{RIMA} + \text{RIMB} + \text{HOMA2} + \text{HETA} + \text{HETB1} - \text{MELA} - \text{MELB}) \quad (1a)$$

$$\frac{\partial \rho_o q_v}{\partial t} + \nabla(\rho_o u q_v) = \mathcal{F}_{q_v} \equiv -\text{COND} + \text{REVP} - \text{DEPA} - \text{DEPB} - \text{HOMA1}$$

$$(1b)$$

$$\frac{\partial \rho_o q_c}{\partial t} + \nabla(\rho_o u q_c) = \mathcal{F}_{q_c} \equiv \text{COND} - \text{AUTC} - \text{RCOL} - \text{RIMA} - \text{RIMB1}$$

$$- \text{HOMA2} - \text{HETA} \quad (1c)$$

$$\frac{\partial \rho_o q_r}{\partial t} + \nabla[\rho_o (u - \underline{V_r k}) q_r] = \mathcal{F}_{q_r} \equiv -\text{REVP} + \text{AUTC} + \text{RCOL} + \text{MELA}$$

$$+ \text{MELB} - \text{HETB1} - \text{RIMB2} \quad (1d)$$

$$\frac{\partial \rho_o q_A}{\partial t} + \nabla[\rho_o (u - \underline{V_A k}) q_A] = \mathcal{F}_{q_A} \equiv \text{HOMA} + \text{HETA} + \text{DEPA} + \text{RIMA}$$

$$- \text{MELA} - \text{HETB2} \quad (1e)$$

$$\frac{\partial \rho_o q_B}{\partial t} + \nabla[\rho_o (u - \underline{V_B k}) q_B] = \mathcal{F}_{q_B} \equiv \text{HETB} + \text{DEPB} + \text{RIMB} - \text{MELB} \quad (1f)$$

- COND ($q_v \rightarrow q_c$): condensation of water vapor to form cloud water;
- AUTC ($q_c \rightarrow q_r$): autoconversion of cloud water into rain (initiation of the rain field);
- RCOL ($q_c \rightarrow q_r$): collection of cloud water by rain water;
- REVP ($q_r \rightarrow q_v$): evaporation of rain;
- HETA ($q_c \rightarrow q_A$): heterogeneous nucleation of ice A (freezing of cloud droplets);
- HOMA = HOMA1 + HOMA2 ($q_v, q_c \rightarrow q_A$): homogeneous nucleation of ice A;
- HETB = HETB1 + HETB2 ($q_r, q_A \rightarrow q_B$): nucleation of ice B due to interaction of rain with ice A;
- DEPA ($q_v \rightarrow q_A$): growth of ice A due to deposition of water vapor;
- DEPB ($q_v \rightarrow q_B$): growth of ice B due to deposition of water vapor;
- RIMA ($q_c \rightarrow q_A$): growth of ice A due to accretion of cloud water (i.e., growth by riming);
- RIMB = RIMB1 + RIMB2 ($q_c, q_r \rightarrow q_B$): growth of ice B by accretion of cloud water and rain;
- MELA ($q_A \rightarrow q_r$): melting of ice A to form rain; and
- MELB ($q_B \rightarrow q_r$): melting of ice B to form rain.

See Appendix A in Grabowski 1999 for details of each term formulation.

TABLE 1. Numerical tests performed using the kinematic setup and the GATE setup. The table shows experiment acronym, a brief description, and a comparison of CPU time based on single processor Cray J90 run with the time for the REFER experiment taken as 1.

Experiment	Description	CPU usage	
		Kinematic	Dynamic
G99 REFER	Microphysical scheme includes cloud water, rain, and two classes of ice	1.0	1.0
WRAIN	Warm rain microphysical scheme (cloud water and rain)	0.12	0.70
G98 SIMP1	Microphysical scheme described in section 3, threshold temperatures of -5° and -20°C	0.13	0.76
SIMP2	Microphysical scheme described in section 3, threshold temperatures of 0° and -10°C	0.13	0.76

Kinematic
(prescribed-
flow) model

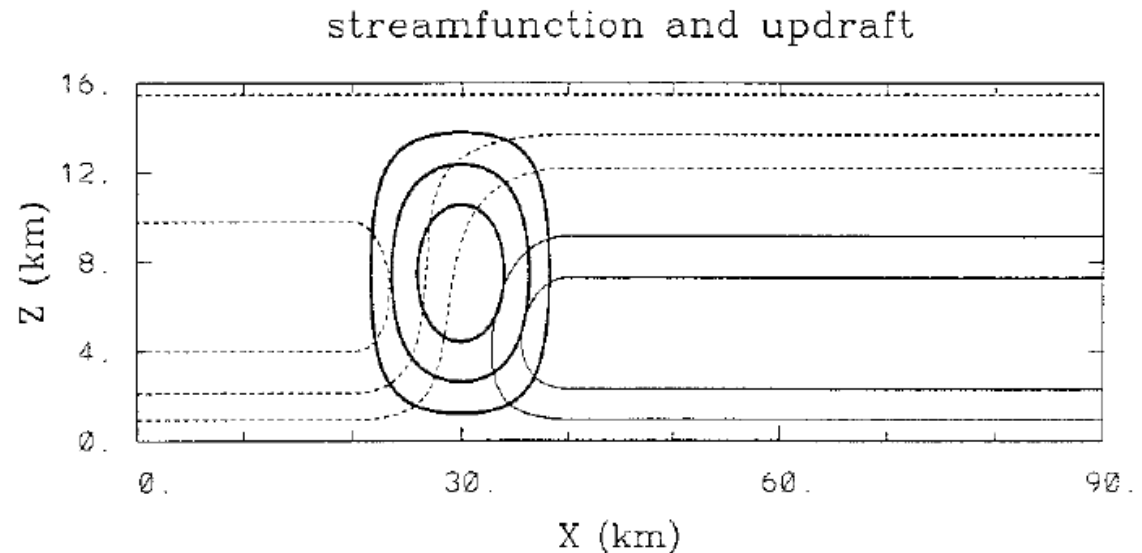


FIG. 3. Streamfunction pattern [thin lines, solid (dashed) for positive (negative) values] used in the kinematic test. Contour interval is $10^4 \text{ kg m}^{-1} \text{ s}^{-1}$. Corresponding vertical velocity field is also shown using thick contours with contour interval of 2 m s^{-1} .

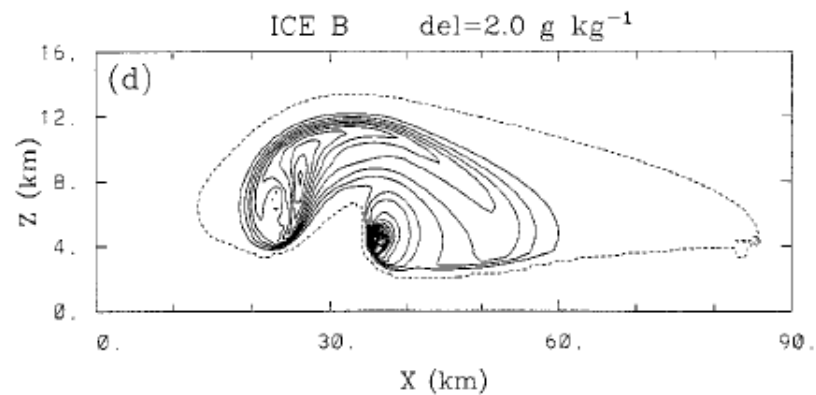
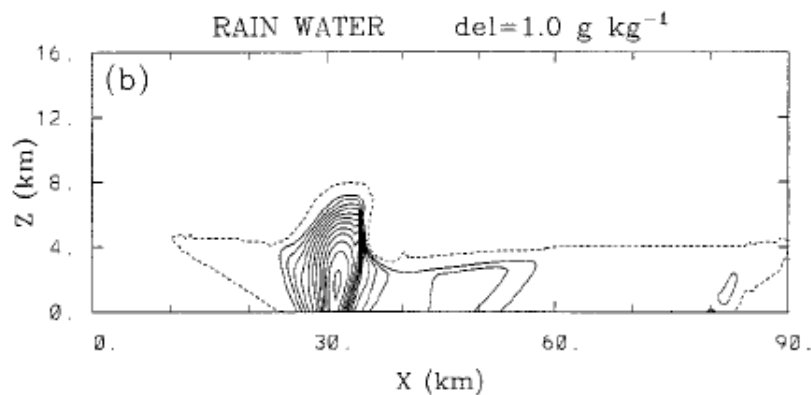
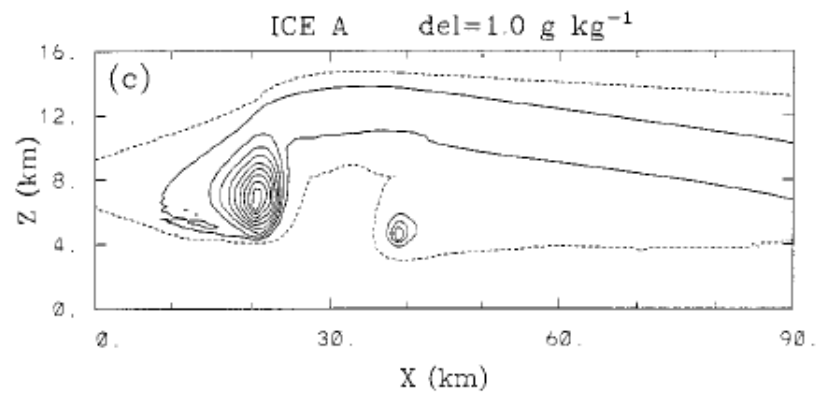
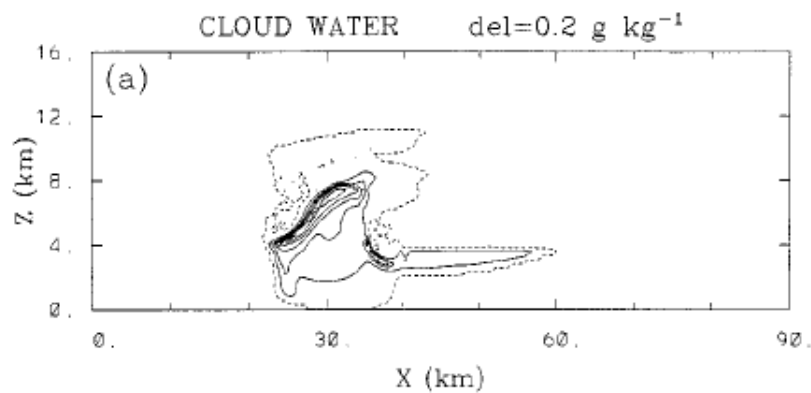


FIG. 4. Isolines of the condensate fields for the experiment REFER. The panels show (a) cloud water, (b) rain, (c) ice A, and (d) ice B mixing ratios with contour intervals of (a) 0.2 g kg^{-1} , (b, c) 1.0 g kg^{-1} , and (d) 2.0 g kg^{-1} . The dashed contours are for mixing ratios of 0.01 g kg^{-1} .

G99

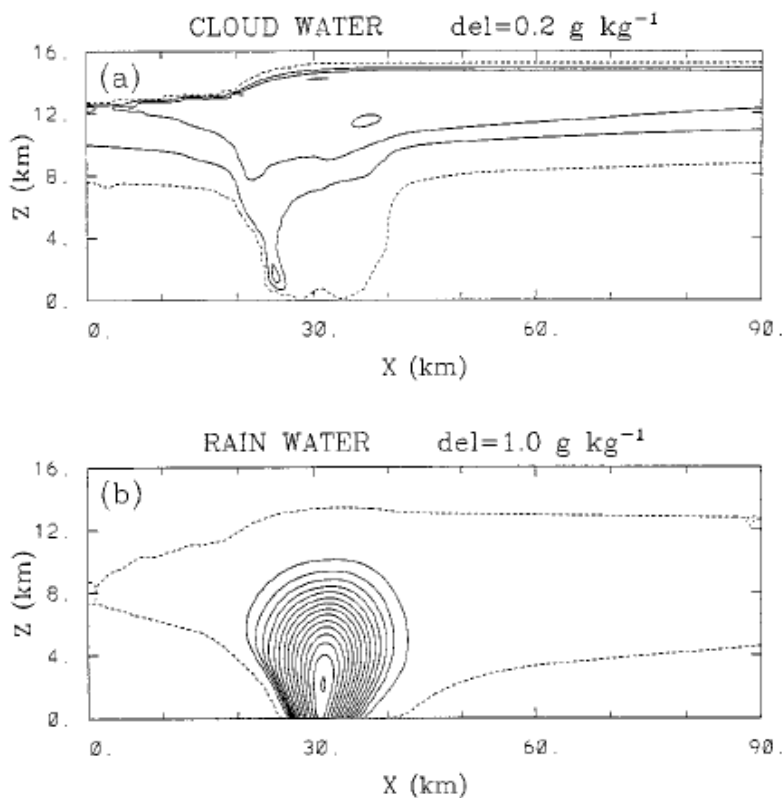


FIG. 5. Isolines of the condensate fields for the experiment WRAIN. The panels show (a) cloud water and (b) rain mixing ratios with contour intervals of (a) 0.2 g kg^{-1} and (b) 1.0 g kg^{-1} . The dashed contours are for mixing ratios of 0.01 g kg^{-1} .

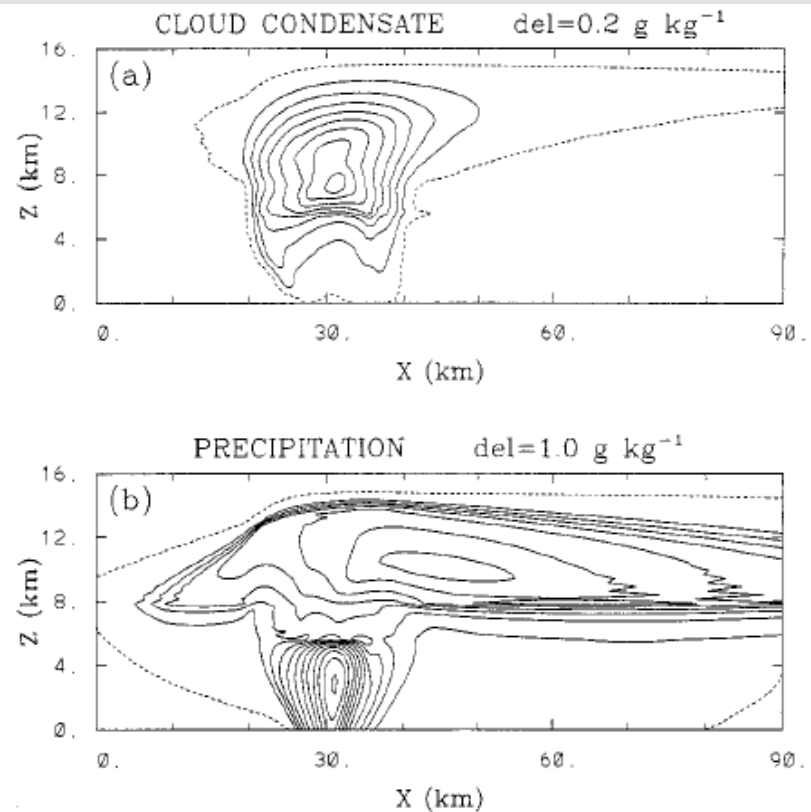


FIG. 6. Isolines of the condensate fields for the experiment SIMP1. The panels show (a) cloud condensate and (b) precipitation mixing ratios with contour intervals of (a) 0.2 g kg^{-1} and (b) 1.0 g kg^{-1} . The dashed contours are for mixing ratios of 0.01 g kg^{-1} .

warm rain

G98

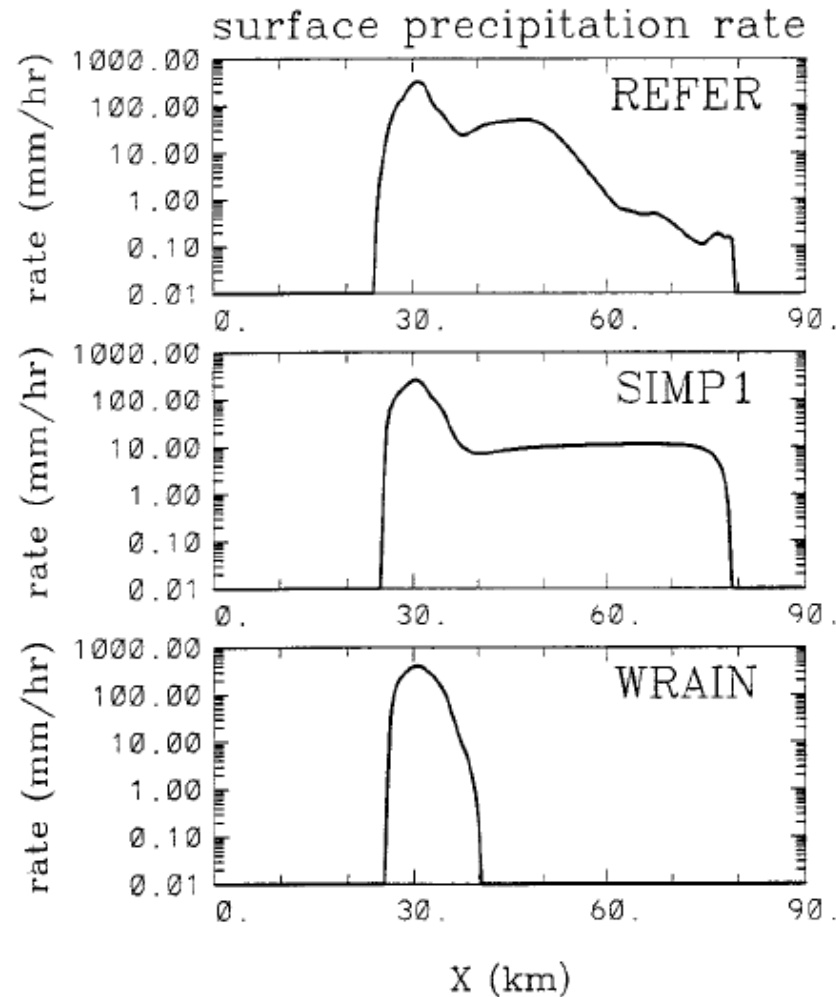


FIG. 7. Distribution of the surface precipitation intensity in mm h^{-1} across the domain at time $t = 4 \text{ h}$ for the simulation REFER, SIMP1, and WRAIN. Precipitation rates smaller than 0.01 mm h^{-1} are not shown.

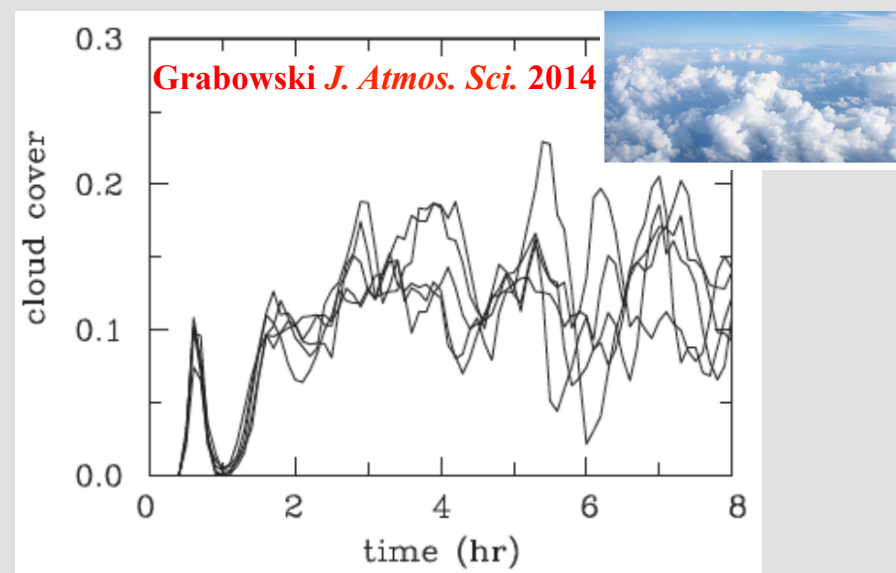
G99

G98

warm rain

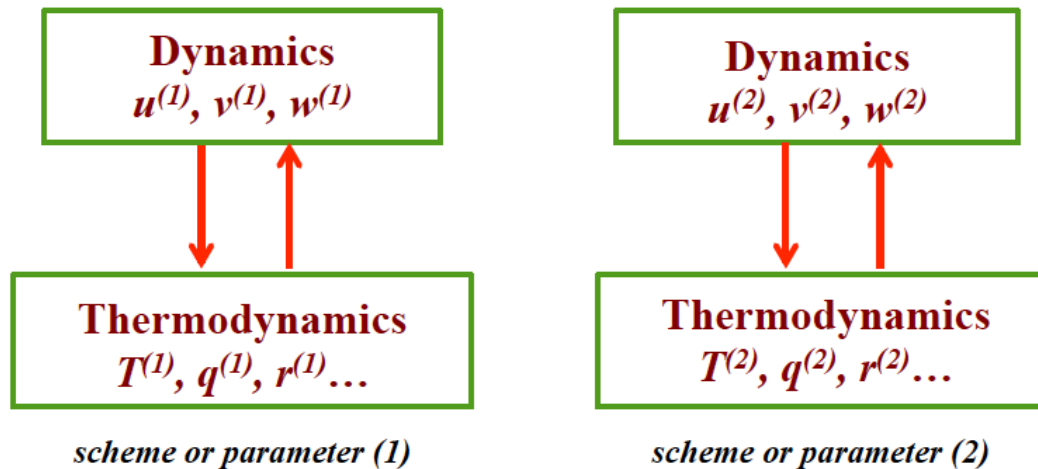
**How to quantify the impact of
microphysics on cloud dynamics?**

Because of the nonlinear fluid dynamics, separating physical impacts from the effects of different flow realizations (“the butterfly effect”; Ed Lorenz) is nontrivial.



Evolution of cloud cover in 5 simulations of shallow cumulus cloud field. The only difference is in random small temperature and moisture perturbations at $t=0$.

Traditional approach: parallel simulations with different microphysical schemes or scheme parameters

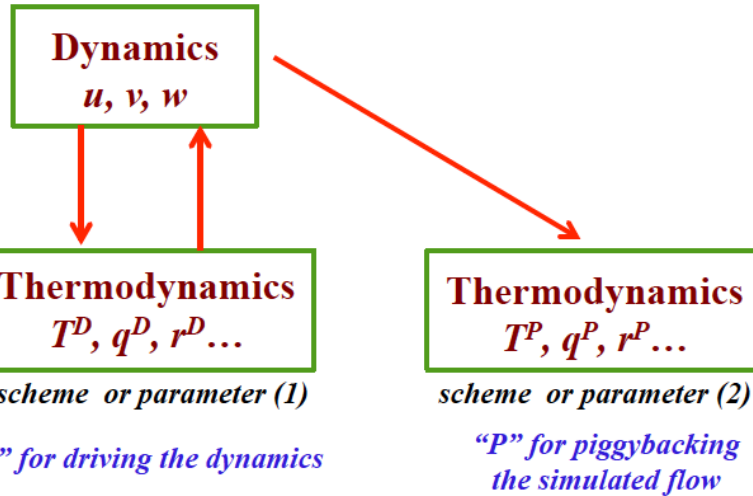


The separation is traditionally done by performing parallel simulations where each simulation applies modified model physics.

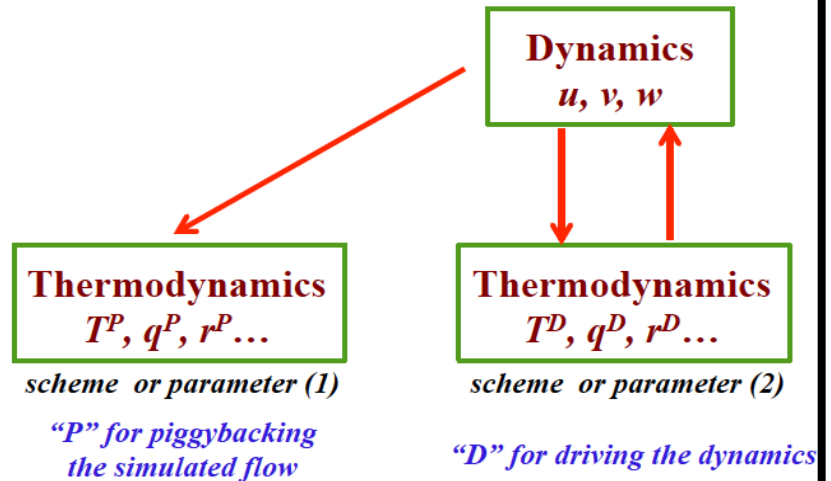
Novel modeling methodology: *the piggybacking*



Microphysical piggybacking; 1st step:



Microphysical piggybacking; 2nd step:

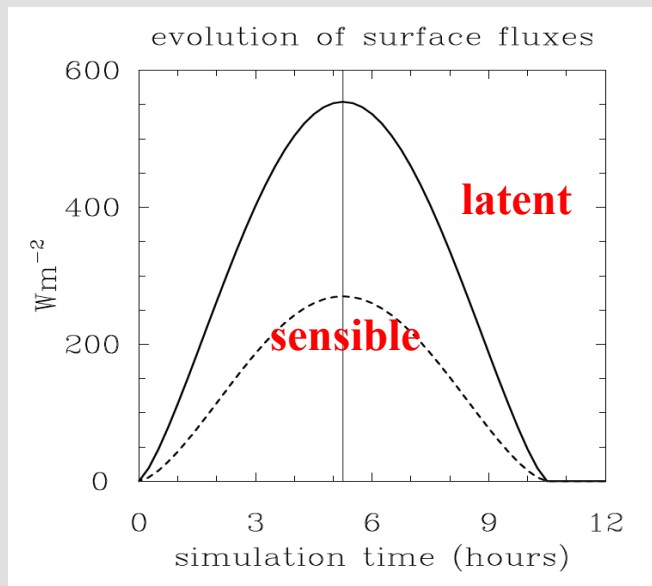


The novel piggybacking methodology is being applied in modeling studies that investigate the impact of cloud microphysics on cloud dynamics, see references below.

- Grabowski, W. W., 2014: Extracting microphysical impacts in large-eddy simulations of shallow convection. *J. Atmos. Sci.* 71, 4493-4499.
- Grabowski, W. W., 2015: Untangling microphysical impacts on deep convection applying a novel modeling methodology. *J. Atmos. Sci.*, 72, 2446-2464.
- Grabowski, W. W., and D. Jarecka, 2015: Modeling condensation in shallow nonprecipitating convection. *J. Atmos. Sci.*, 72, 4661-4679.
- Grabowski, W. W., and H. Morrison, 2016: Untangling microphysical impacts on deep convection applying a novel modeling methodology. Part II: Double-moment microphysics. *J. Atmos. Sci.* (in press).

Daytime convective development over land: A model intercomparison based on LBA observations

By W. W. GRABOWSKI^{1*}, P. BECHTOLD², A. CHENG³, R. FORBES⁴, C. HALLIWELL⁴,
M. KHAIROUTDINOV⁵, S. LANG⁶, T. NASUNO⁷, J. PETCH⁸, W.-K. TAO⁶, R. WONG⁸,
X. WU⁹ and K.-M. XU³



Grabowski (*JAS* 2015) simulations:

Extended to 12 hrs

50 x 50 km² horizontal domain, 400 m gridlength

24 km deep domain, 81 levels, stretched grid

1. Contrasting simulations applying different microphysical schemes: separating dynamical and microphysical effects.

2. Contrasting simulations assuming clean and polluted conditions (with droplet concentration of 100/1,000 per cc for **pristine/polluted) and the same microphysical scheme: exploring dynamical basis of deep convection invigoration in polluted environments.**

Two microphysics schemes:

Grabowski 1998 (G98) – simple ice: **SIM**

Grabowski 1999 (G99) – more complex ice: **IAB**

G98

$$\frac{\partial \rho_o \theta}{\partial t} + \nabla \cdot (\rho_o \mathbf{u} \theta) = \frac{L_v \theta_e}{c_p T_e} (\text{CON} + \text{DEP}) + D_{\theta}, \quad (1a)$$

$$\frac{\partial \rho_o q_v}{\partial t} + \nabla \cdot (\rho_o \mathbf{u} q_v) = -\text{CON} - \text{DEP} + D_{q_v}, \quad (1b)$$

$$\frac{\partial \rho_o q_c}{\partial t} + \nabla \cdot (\rho_o \mathbf{u} q_c) = \text{CON} - \text{ACC} - \text{AUT} + D_{q_c}, \quad (1c)$$

$$\frac{\partial \rho_o q_p}{\partial t} + \nabla \cdot [\rho_o (\mathbf{u} - V_T \mathbf{k}) q_p] = \text{ACC} + \text{AUT} + \text{DEP} + D_{q_p}. \quad (1d)$$

q_c – cloud condensate

q_p – precipitation

freezing/melting not considered: saturation adjustment applies always latent heat of condensation, even at cold temperatures

G99

$$\begin{aligned} \frac{\partial \rho_o \theta}{\partial t} + \nabla \cdot (\rho_o \mathbf{u} \theta) = \mathcal{F}_{\theta} \equiv \\ \frac{L_v \theta_e}{c_p T_e} (\text{COND} - \text{REVP}) + \frac{L_s \theta_e}{c_p T_e} (\text{DEPA} + \text{DEPB} + \text{HOMA1}) \\ + \frac{L_t \theta_e}{c_p T_e} (\text{RIMA} + \text{RIMB} + \text{HOMA2} + \text{HETA} + \text{HETB1} - \text{MELA} - \text{MELB}) \end{aligned} \quad (1a)$$

$$\frac{\partial \rho_o q_v}{\partial t} + \nabla \cdot (\rho_o \mathbf{u} q_v) = \mathcal{F}_{q_v} \equiv -\text{COND} + \text{REVP} - \text{DEPA} - \text{DEPB} - \text{HOMA1} \quad (1b)$$

$$\begin{aligned} \frac{\partial \rho_o q_c}{\partial t} + \nabla \cdot (\rho_o \mathbf{u} q_c) = \mathcal{F}_{q_c} \equiv \text{COND} - \text{AUTC} - \text{RCOL} - \text{RIMA} - \text{RIMB1} \\ - \text{HOMA2} - \text{HETA} \end{aligned} \quad (1c)$$

$$\begin{aligned} \frac{\partial \rho_o q_r}{\partial t} + \nabla \cdot [\rho_o (u - V_T k) q_r] = \mathcal{F}_{q_r} \equiv -\text{REVP} + \text{AUTC} + \text{RCOL} + \text{MELA} \\ + \text{MELB} - \text{HETB1} - \text{RIMB2} \end{aligned} \quad (1d)$$

$$\begin{aligned} \frac{\partial \rho_o q_A}{\partial t} + \nabla \cdot [\rho_o (u - V_A k) q_A] = \mathcal{F}_{q_A} \equiv \text{HOMA} + \text{HETA} + \text{DEPA} + \text{RIMA} \\ - \text{MELA} - \text{HETB2} \end{aligned} \quad (1e)$$

$$\frac{\partial \rho_o q_B}{\partial t} + \nabla \cdot [\rho_o (u - V_B k) q_B] = \mathcal{F}_{q_B} \equiv \text{HETB} + \text{DEPB} + \text{RIMB} - \text{MELB} \quad (1f)$$

q_c - cloud water

q_r - rain

q_{iA} - ice A

q_{iB} - ice B

freezing/melting included

G98

$$\frac{\partial \rho_o \theta}{\partial t} + \nabla \cdot (\rho_o \mathbf{u} \theta) = \frac{L_v \theta_e}{c_p T_e} (\text{CON} + \text{DEP}) + D_\theta, \quad (1a)$$

$$\frac{\partial \rho_o q_v}{\partial t} + \nabla \cdot (\rho_o \mathbf{u} q_v) = -\text{CON} - \text{DEP} + D_{q_v}, \quad (1b)$$

$$\frac{\partial \rho_o q_c}{\partial t} + \nabla \cdot (\rho_o \mathbf{u} q_c) = \text{CON} - \text{ACC} - \text{AUT} + D_{q_c}, \quad (1c)$$

$$\frac{\partial \rho_o q_p}{\partial t} + \nabla \cdot [\rho_o (\mathbf{u} - V_T \mathbf{k}) q_p] = \text{ACC} + \text{AUT} + \text{DEP} + D_{q_p}. \quad (1d)$$

q_c – cloud condensate

q_p – precipitation

freezing/melting not considered: saturation adjustment applies always latent heat of condensation, even at cold temperatures

G99

$$\frac{\partial \rho_o \theta}{\partial t} + \nabla \cdot (\rho_o \mathbf{u} \theta) = \mathcal{S}_\theta \equiv$$

$$\frac{L_v \theta_e}{c_p T_e} (\text{COND} - \text{REVP}) + \frac{L_s \theta_e}{c_p T_e} (\text{DEPA} + \text{DEPB} + \text{HOMA1})$$

$$+ \frac{L_t \theta_e}{c_p T_e} (\text{RIMA} + \text{RIMB} + \text{HOMA2} + \text{HETA} + \text{HETB1} - \text{MELA} - \text{MELB}) \quad (1a)$$

$$\frac{\partial \rho_o q_v}{\partial t} + \nabla \cdot (\rho_o \mathbf{u} q_v) = \mathcal{S}_{q_v} \equiv \text{CON} + \text{HETB1} - \text{DEPA} - \text{DEPB} - \text{HOMA1} \quad (1b)$$

$$\frac{\partial \rho_o q_c}{\partial t} + \nabla \cdot (\rho_o \mathbf{u} q_c) = \mathcal{S}_{q_c} \equiv \text{COND} - \text{AUTC} - \text{RCOL} - \text{RIMA} - \text{RIMB1} - \text{HOMA2} - \text{HETA} \quad (1c)$$

$$\frac{\partial \rho_o q_r}{\partial t} + \nabla \cdot [\rho_o (u - V_T k) q_r] = \mathcal{S}_{q_r} \equiv -\text{REVP} + \text{AUTC} + \text{RCOL} + \text{MELA} + \text{MELB} - \text{HETB1} - \text{RIMB2} \quad (1d)$$

$$\frac{\partial \rho_o q_A}{\partial t} + \nabla \cdot [\rho_o (u - V_A k) q_A] = \mathcal{S}_{q_A} \equiv \text{HOMA} + \text{HETA} + \text{DEPA} + \text{RIMA} - \text{MELA} - \text{HETB2} \quad (1e)$$

$$\frac{\partial \rho_o q_B}{\partial t} + \nabla \cdot [\rho_o (u - V_B k) q_B] = \mathcal{S}_{q_B} \equiv \text{HETB} + \text{DEPB} + \text{RIMB} - \text{MELB} \quad (1f)$$

q_c - cloud water

q_r - rain

q_{iA} - ice A

q_{iB} - ice B

freezing/melting included

Single-moment bulk schemes with saturation adjustment...

Warm-rain representation the same in both...

Two microphysics schemes:

Grabowski 1998 (G98) – simple ice: SIM

Grabowski 1999 (G99) – more complex ice: IAB

Two collections of simulations:

C1: 12 piggybacking simulations with SIM and IAB:

3 pristine ensemble members for D-SIM/P-IAB and 3 for D-IAB/P-SIM

3 polluted ensemble members for D-SIM/P-IAB and 3 for D-IAB/P-SIM

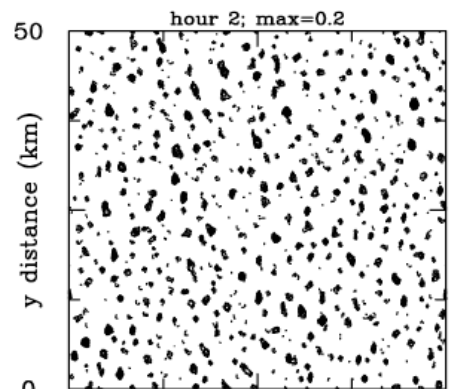
C2: 12 piggybacking simulations with polluted and pristine:

3 SIM ensemble members for D100/P1000 and 3 for D1000/P100

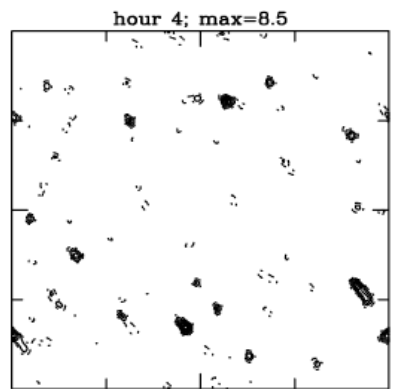
3 IAB ensemble members for D100/P1000 and 3 for D1000/P100

Example of model results: maps of the total water path (liquid plus ice);
a single simulations from IAB ensemble

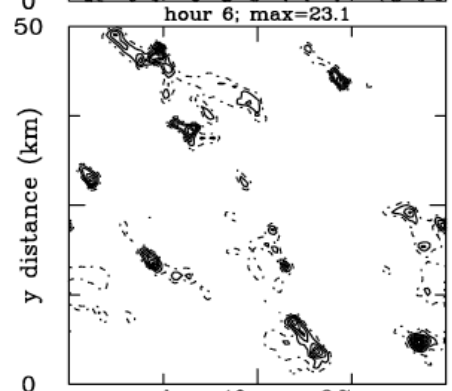
2 hr



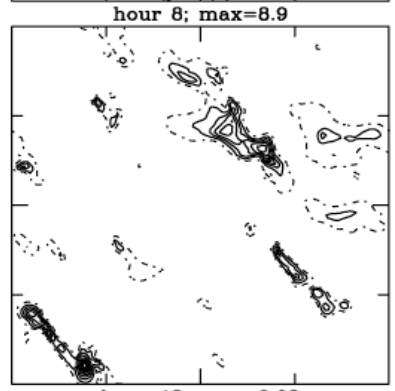
4 hr



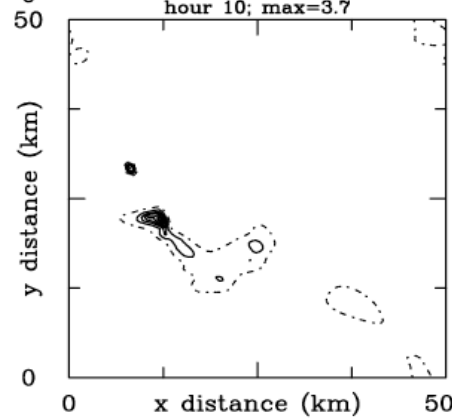
6 hr



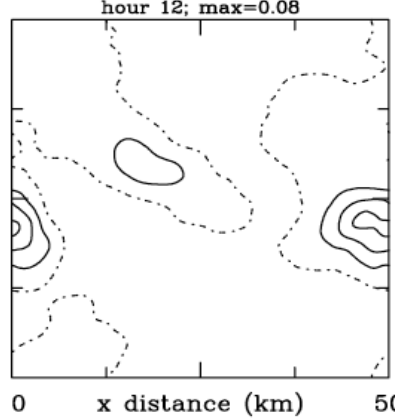
8 hr



10 hr

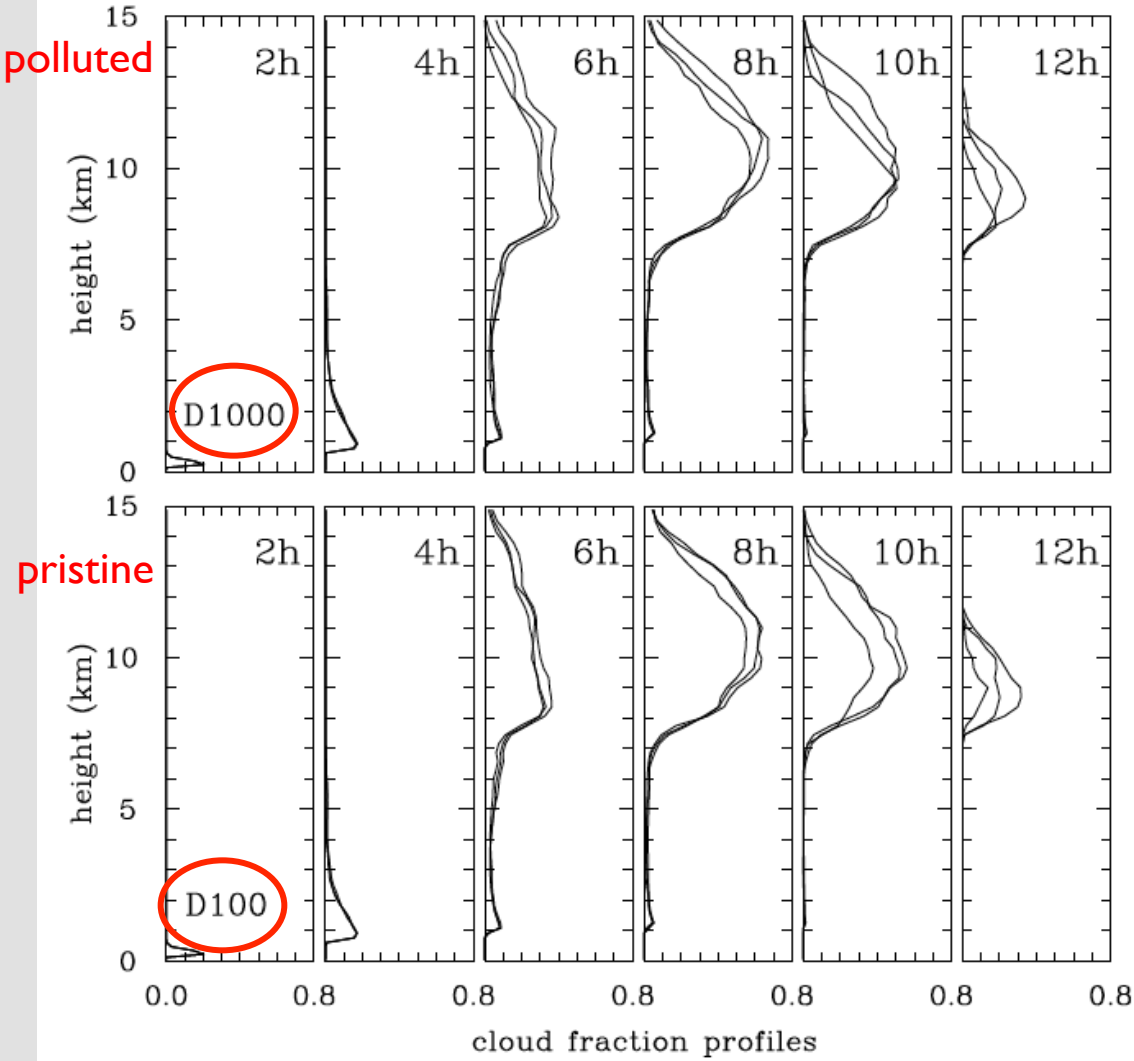


12 hr

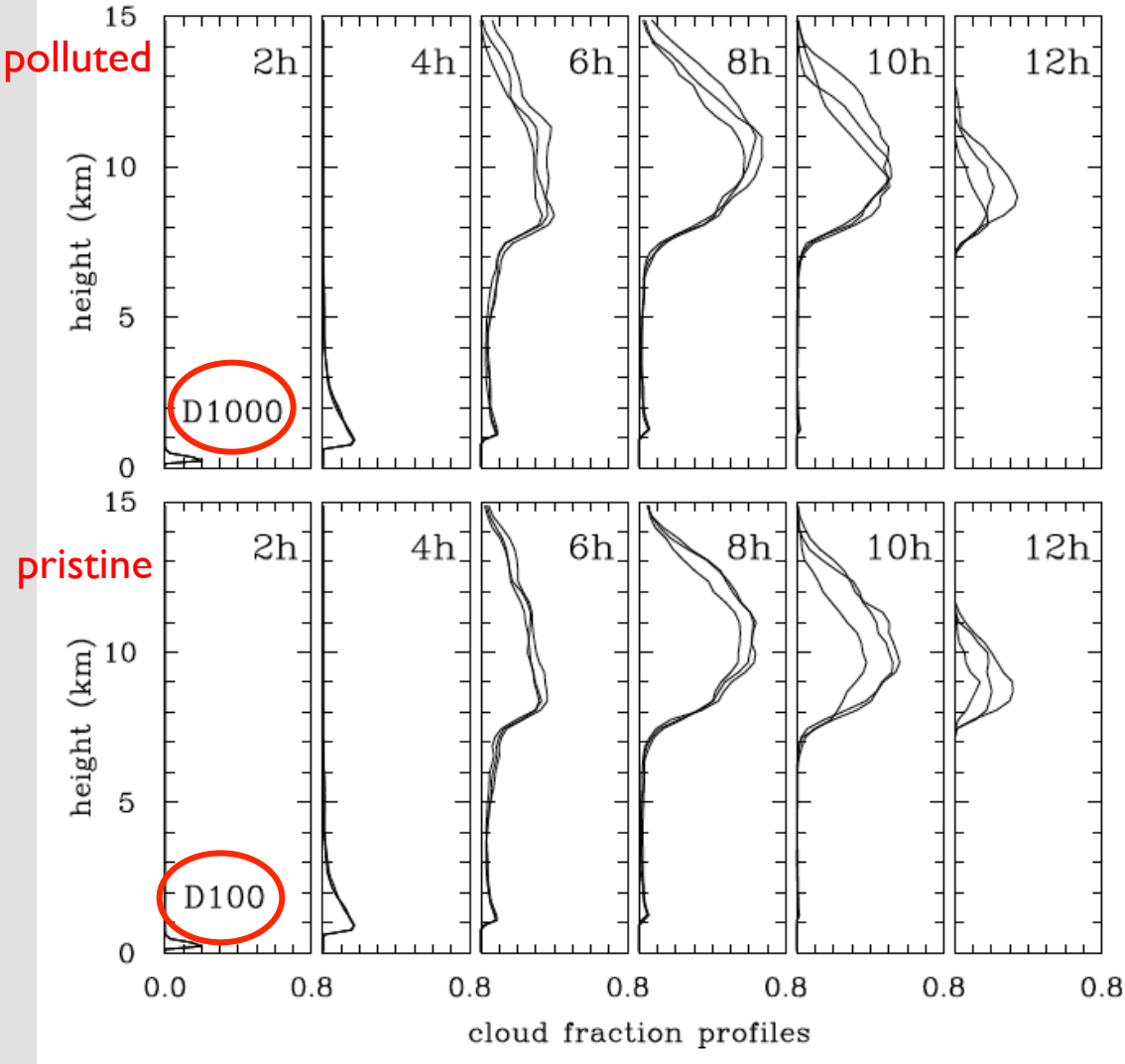


contour interval: 0.1 x maximum

Example of model results: cloud fraction profiles from IAB ensemble

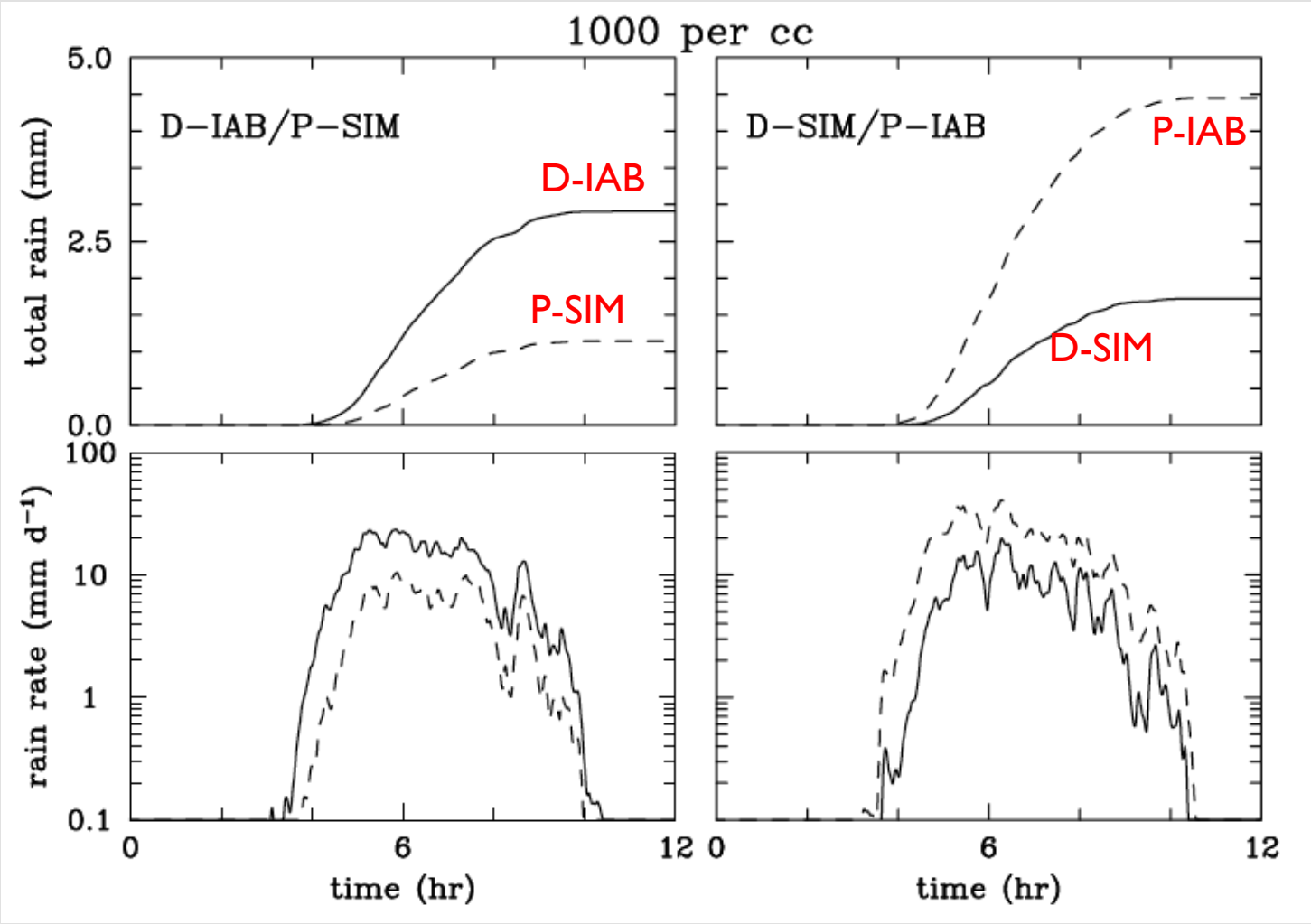


Example of model results: cloud fraction profiles from IAB ensemble

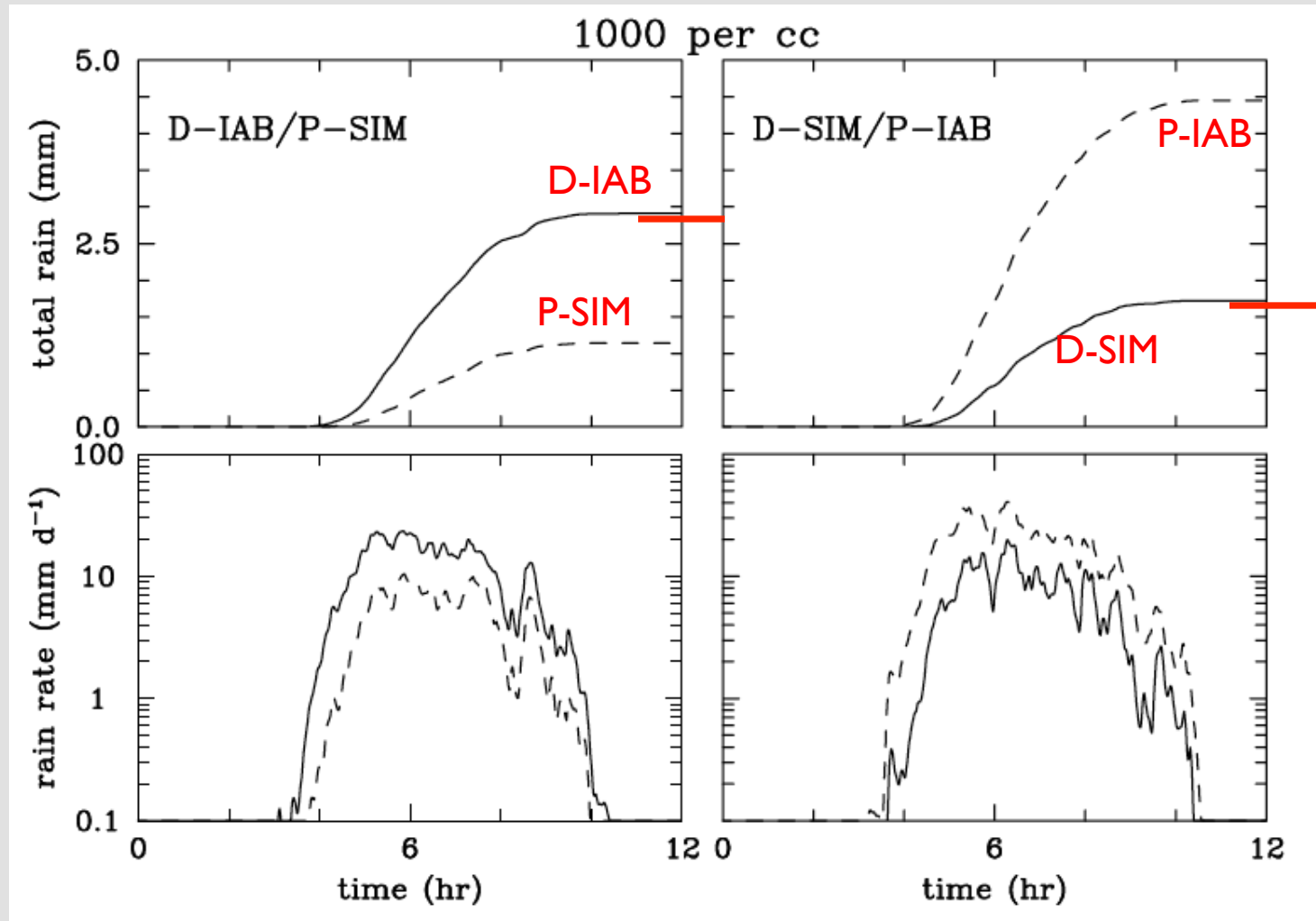


Droplet concentration seems to have an insignificant effect...

Piggybacking with different schemes: D-IAB/P-SIM versus D-SIM/P-IAB

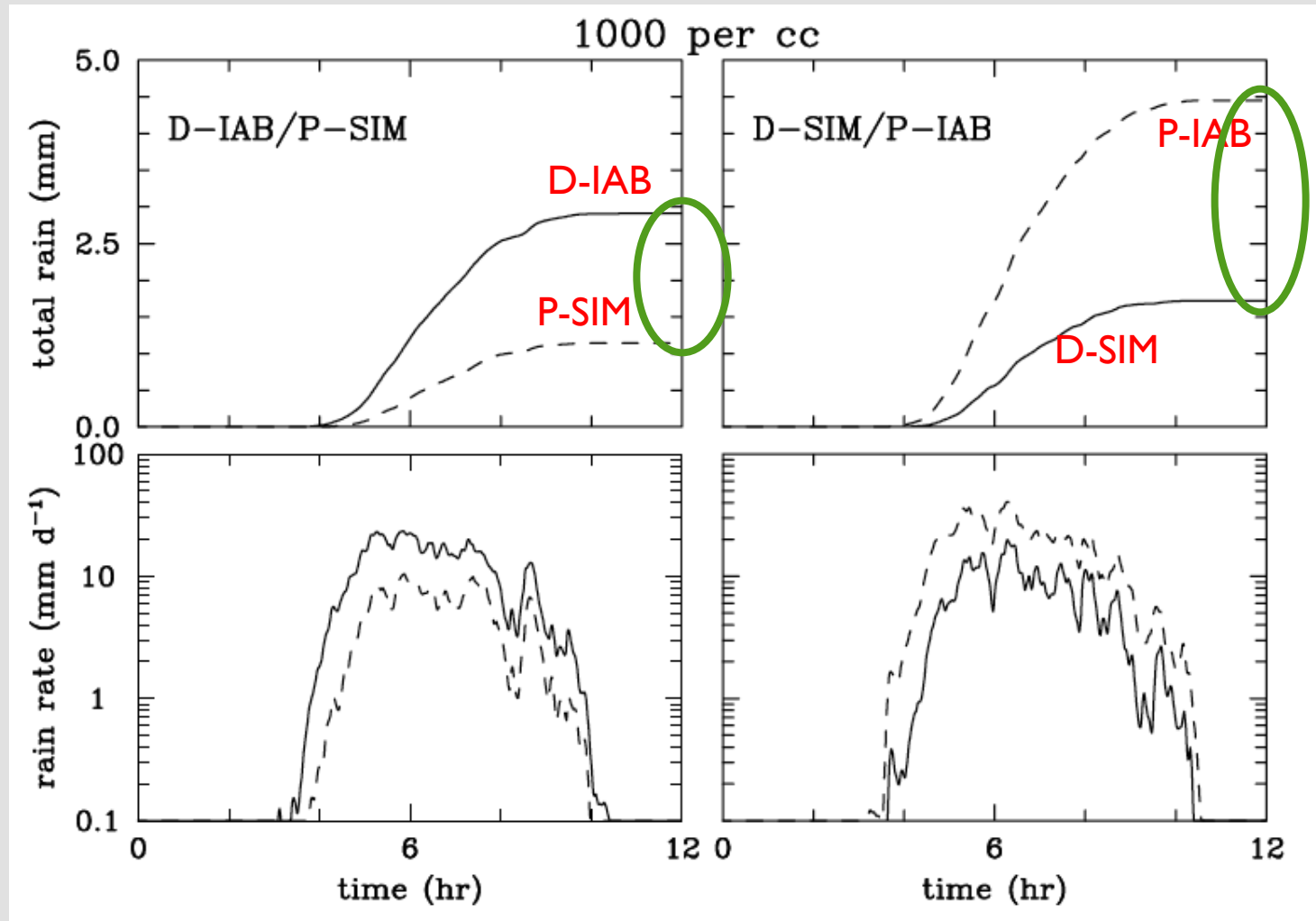


Piggybacking with different schemes: D-IAB/P-SIM versus D-SIM/P-IAB



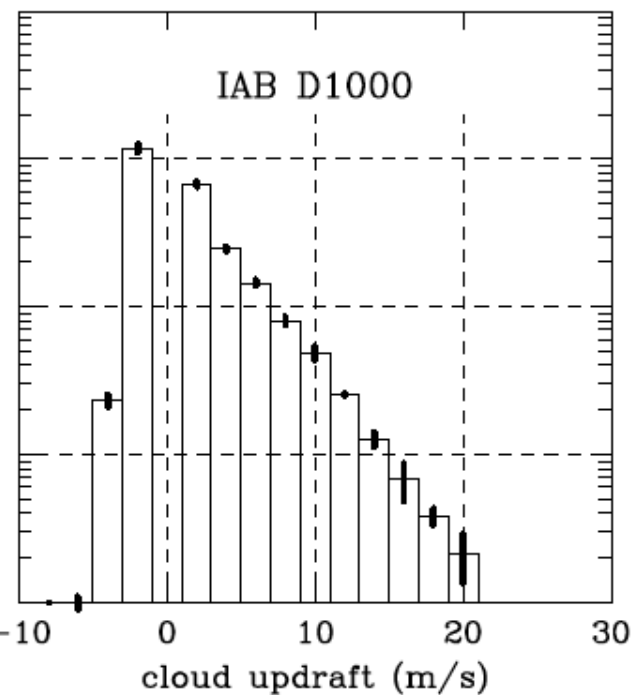
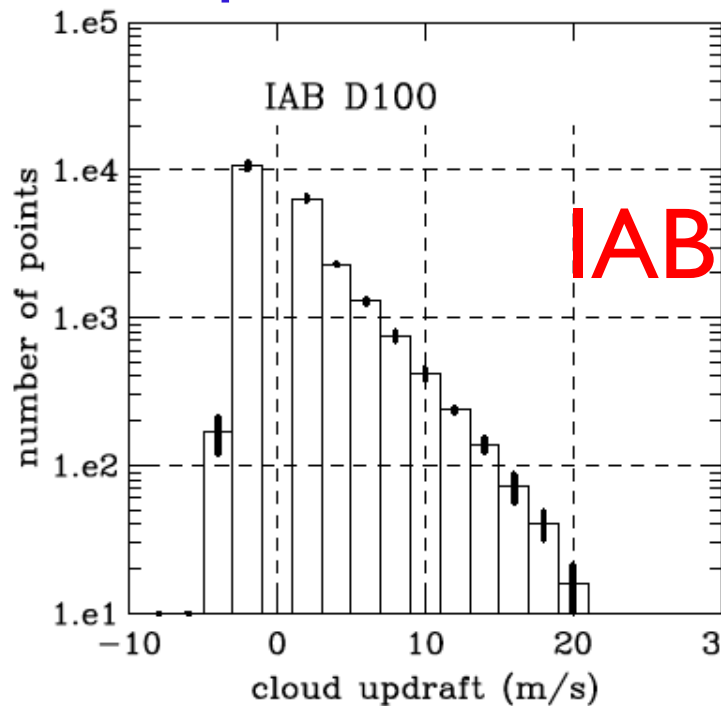
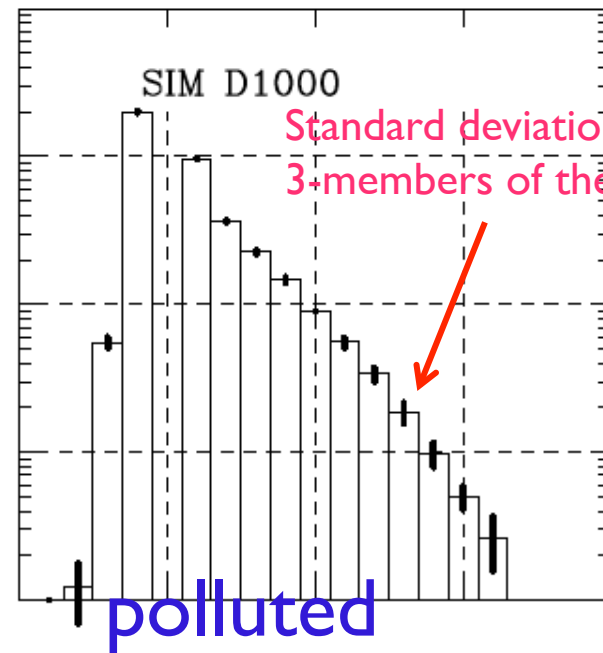
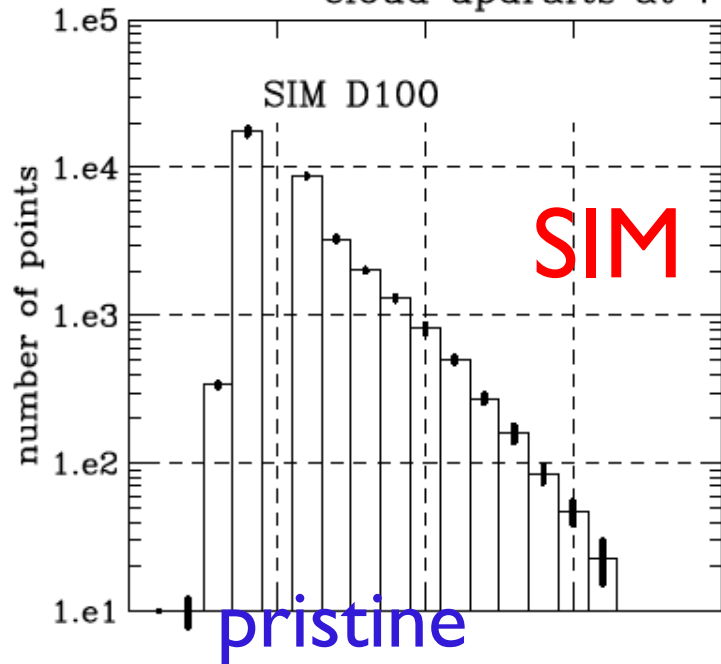
IAB produces almost twice as much surface rain as SIM...

Piggybacking with different schemes: D-IAB/P-SIM versus D-SIM/P-IAB

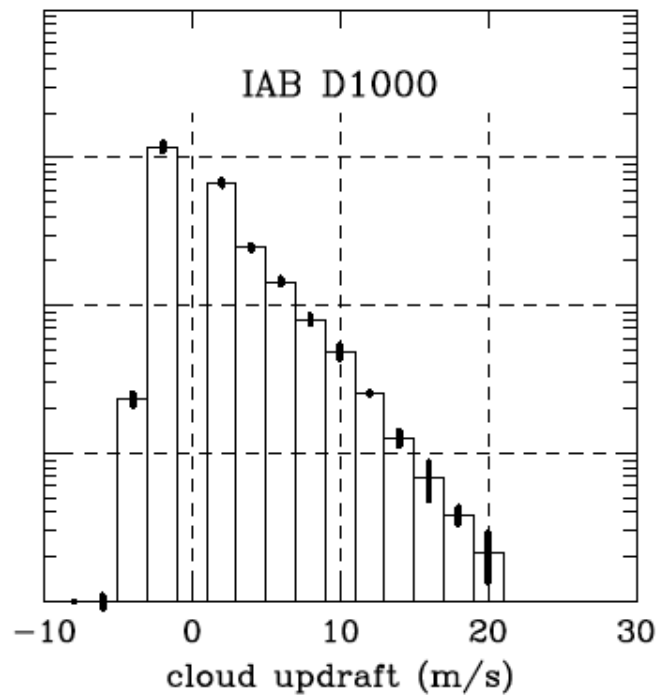
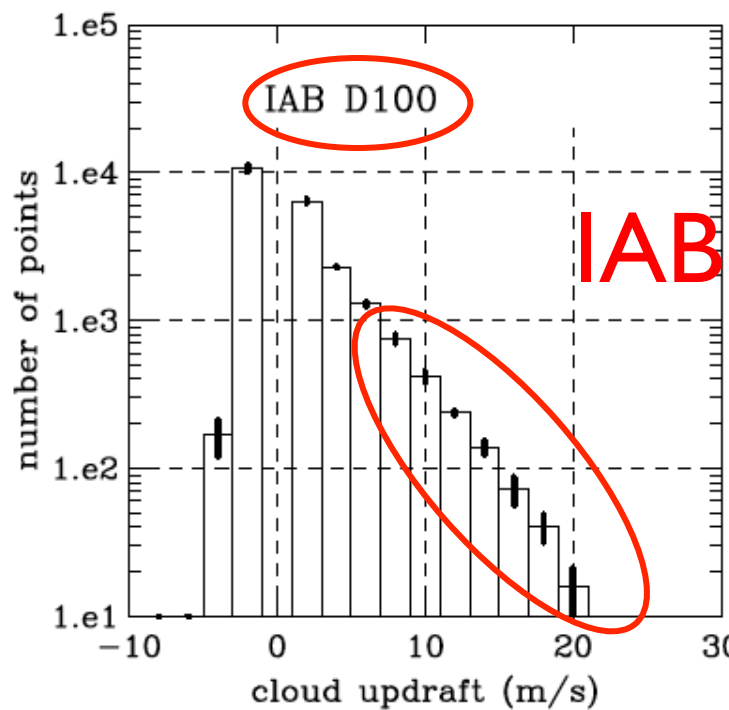
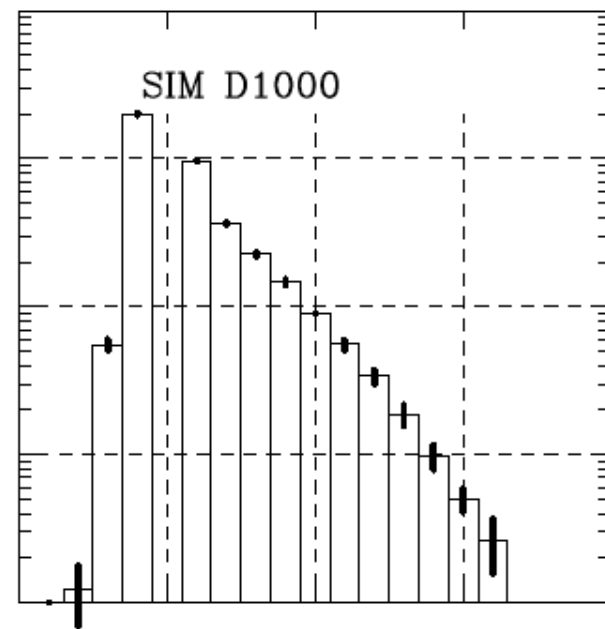
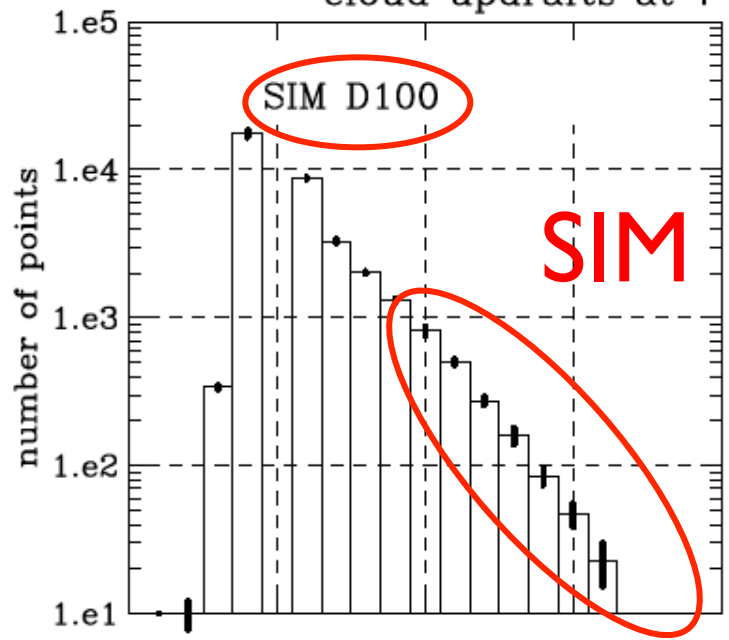


Differences between left and right panel suggest modified dynamics between SIM and IAB driving...

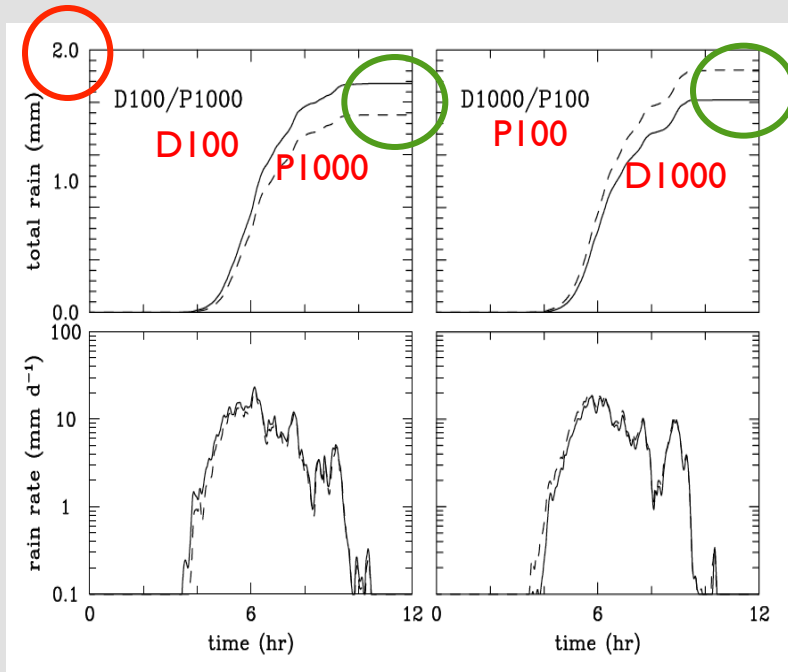
cloud updrafts at 7 km; 6th and 7th hour



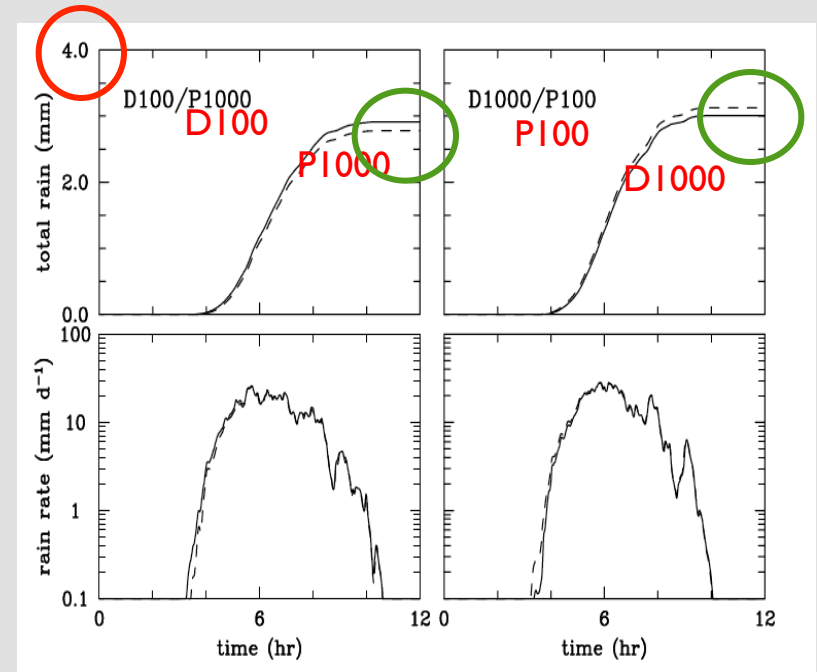
cloud updrafts at 7 km; 6th and 7th hour



SIM



IAB



IAB produces significantly more surface rain than SIM...
Pristine simulations still produce more rain...
Differences (D-P and P-D) are similar (except for the sign)...

OUTLINE:

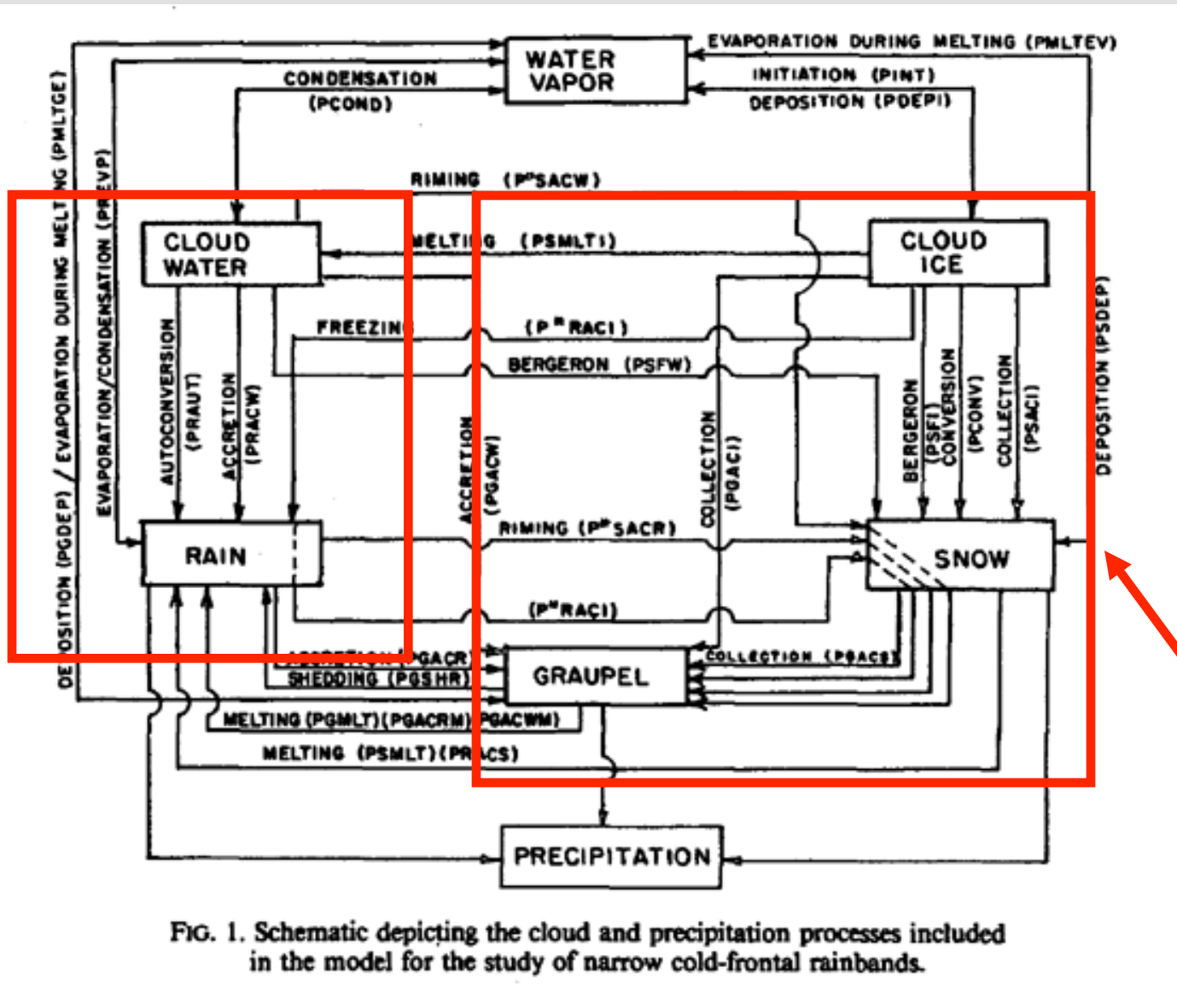
Bulk ice physics modeling

- equilibrium approach - a simple extension of the warm-rain scheme
- non-equilibrium approach – more comprehensive schemes
- single-moment versus multi-moment schemes

Bin ice microphysics

Lagrangian (particle-based) methods

Traditional approach to bulk cloud microphysics



Warm-rain part

Ice part

FIG. 1. Schematic depicting the cloud and precipitation processes included in the model for the study of narrow cold-frontal rainbands.


BULK RAIN/ICE MODEL
(Lin et al. 1983, Rutledge and Hobbs 1984)


$$\frac{\partial \rho_o \theta}{\partial t} + \nabla \cdot (\rho_o \mathbf{u} \theta) = \frac{L_v \theta_e}{c_p T_e} S_1 + \frac{L_s \theta_e}{c_p T_e} S_2 + \frac{L_f \theta_e}{c_p T_e} S_3 + D_\theta$$


Water vapor  $\frac{\partial \rho_o q_v}{\partial t} + \nabla \cdot (\rho_o \mathbf{u} q_v) = S_4 + D_{q_v}$

Cloud water  $\frac{\partial \rho_o q_c}{\partial t} + \nabla \cdot (\rho_o \mathbf{u} q_c) = S_5 + D_{q_c}$

Cloud ice  $\frac{\partial \rho_o q_i}{\partial t} + \nabla \cdot (\rho_o \mathbf{u} q_i) = S_6 + D_{q_i}$

Rain  $\frac{\partial \rho_o q_r}{\partial t} + \nabla \cdot [\rho_o (\mathbf{u} - V_T^r \mathbf{k}) q_r] = S_7 + D_{q_r}$

Snow  $\frac{\partial \rho_o q_s}{\partial t} + \nabla \cdot [\rho_o (\mathbf{u} - V_T^s \mathbf{k}) q_s] = S_8 + D_{q_s}$

**Graupel
(or hail)**  $\frac{\partial \rho_o q_g}{\partial t} + \nabla \cdot [\rho_o (\mathbf{u} - V_T^g \mathbf{k}) q_g] = S_9 + D_{q_g}$

TRADITIONAL ICE MICROPHYSICS:

cloud ice: q_i

snow: q_s

graupel / hail: q_g

-

EXTENDING TRADITIONAL APPROACH TO 2-MOMENT ICE MICROPHYSICS:

cloud ice: q_i, N_i

snow: q_s, N_s

graupel / hail: q_g, N_g

-
Is such an approach justified?

WRF model V3.2 schemes...

Microphysics schemes in V3.2

mp_physics	Scheme	Cores	Mass Variables	Number Variables
1	Kessler	ARW	Qc Qr	
2	Lin (Purdue)	ARW	Qc Qr Qi Qs Qg	
3	WSM3	ARW	Qc Qr	
4	WSM5	ARW NMM	Qc Qr Qi Qs	
5 (/85)	EtaFerrier(/HWRF)	ARW NMM	Qc Qr Qs (Qt*)	
6	WSM6	ARW NMM	Qc Qr Qi Qs Qg	
7	Goddard	ARW	Qc Qr Qi Qs Qg	
8 (/98)	Thompson(/old)	ARW NMM	Qc Qr Qi Qs Qg	Ni Nr (/Ni)
9	Milbrandt 2-mom	ARW	Qc Qr Qi Qs Qg Qh	Nc Nr Ni Ns Ng Nh
10	Morrison 2-mom	ARW	Qc Qr Qi Qs Qg	Nr Ni Ns Ng
14	WDM5	ARW	Qc Qr Qi Qs	Nn** Nc Nr
16	WDM6	ARW	Qc Qr Qi Qs Qg	Nn** Nc Nr

* Advects only total condensate ** Nn= CCN number

Not really!

The ice scheme should produce various types of ice (cloud ice, snow, graupel) just by the physics of particle growth. Partitioning ice particles a priori into separate categories introduces unphysical “conversion rates” and may involve “thresholding behavior” (i.e., model solutions diverge depending whether the threshold is reached or not).

A two-moment three-variable ice scheme:

$$\frac{\partial N}{\partial t} + \frac{1}{\rho_a} \nabla \cdot [\rho_a (\mathbf{u} - \underline{V_N \mathbf{k}}) N] = \mathcal{F}_N$$

Number concentration of ice crystals, N

$$\frac{\partial q_{dep}}{\partial t} + \frac{1}{\rho_a} \nabla \cdot [\rho_a (\mathbf{u} - \underline{V_q \mathbf{k}}) q_{dep}] = \mathcal{F}_{q_{dep}}$$

Mixing ratio of ice mass grown by diffusion of water vapor, q_{dep}

$$\frac{\partial q_{rim}}{\partial t} + \frac{1}{\rho_a} \nabla \cdot [\rho_a (\mathbf{u} - \underline{V_q \mathbf{k}}) q_{rim}] = \mathcal{F}_{q_{rim}}$$

Mixing ratio of ice mass grown by riming (accretion of liquid water), q_{rim}

Case without riming



- Growth by vapor deposition



- Growth by aggregation

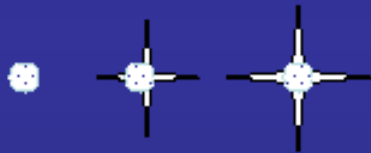
- Growth by vapor deposition

Smooth transition from small spherical ice to larger nonspherical crystals to aggregates.

Case with riming

Stage 1: Unrimed crystal

- Particle dimension and mass determined by vapor deposition



- Vapor depositional growth

Stage 2: Partially-rimed crystal

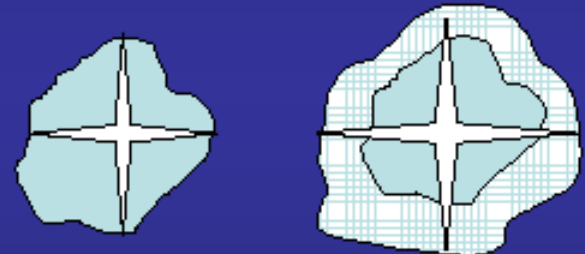
- Particle dimension determined by vapor deposition
- Mass determined by vapor deposition and riming



- Riming of crystal interstices
- Vapor depositional growth

Stage 3: Graupel

- Particle dimension determined by vapor deposition and riming
- Mass determined by vapor deposition and riming



- Complete filling-in of interstices with rime
- Further growth by riming and vapor deposition

Prediction of both riming and vapor deposition mass allows for realistic particle evolution during growth.

Ice particles assumed to follow gamma distribution (3 parameters: N_o , μ , λ)

$$N(D) = N_o D^\mu e^{-\lambda D}$$

$$N = \int_0^\infty N(D) dD$$

$$q_{dep} + q_{rim} \equiv q = \int_0^\infty m(D) N(D) dD$$

$$\frac{\partial N}{\partial t} + \frac{1}{\rho_a} \nabla \cdot [\rho_a (\mathbf{u} - V_N \mathbf{k}) N] = \mathcal{F}_N$$

$$\frac{\partial q_{dep}}{\partial t} + \frac{1}{\rho_a} \nabla \cdot [\rho_a (\mathbf{u} - V_q \mathbf{k}) q_{dep}] = \mathcal{F}_{q_{dep}}$$


$$\frac{\partial q_{rim}}{\partial t} + \frac{1}{\rho_a} \nabla \cdot [\rho_a (\mathbf{u} - V_q \mathbf{k}) q_{rim}] = \mathcal{F}_{q_{rim}}$$


$$\mu = 0.076 \lambda^{0.8} - 2 ; \quad 0 \leq \mu \leq 6$$

Diagnostic relationship based on cloud observations (Heymsfield 2003)

Morrison and Grabowski (JAS 2008)

Ice particle mass-dimension (m-D) and projected-area-dimension (A-D) relationships are based on observed characteristics of ice crystals, aggregates, and graupel particles (from aircraft and ground-based observations).


$$m = \alpha D^{\beta}$$


$$A = \sigma D^{\gamma}$$

rimed mass fraction F_r :

$$F_r = \frac{q_{rim}}{q_{dep} + q_{rim}} \approx \frac{m_{rim}}{m_{dep} + m_{rim}}$$

assumed constant across the spectrum of ice particles

$F_r = 0$ — ice particle grown by diffusion/aggregation

$F_r \rightarrow 1$ — graupel (or hail)

$0 < F_r < 1$ — rimed ice particle:

size D given by the mass grown by diffusion $m_{dep} = (1 - F_r)m$;

$m = m_{rim} + m_{dep}$ is the total mass of ice particle

Morrison and Grabowski (JAS 2008)

Ice crystals/snowflakes grown by diffusion of water vapor and aggregation

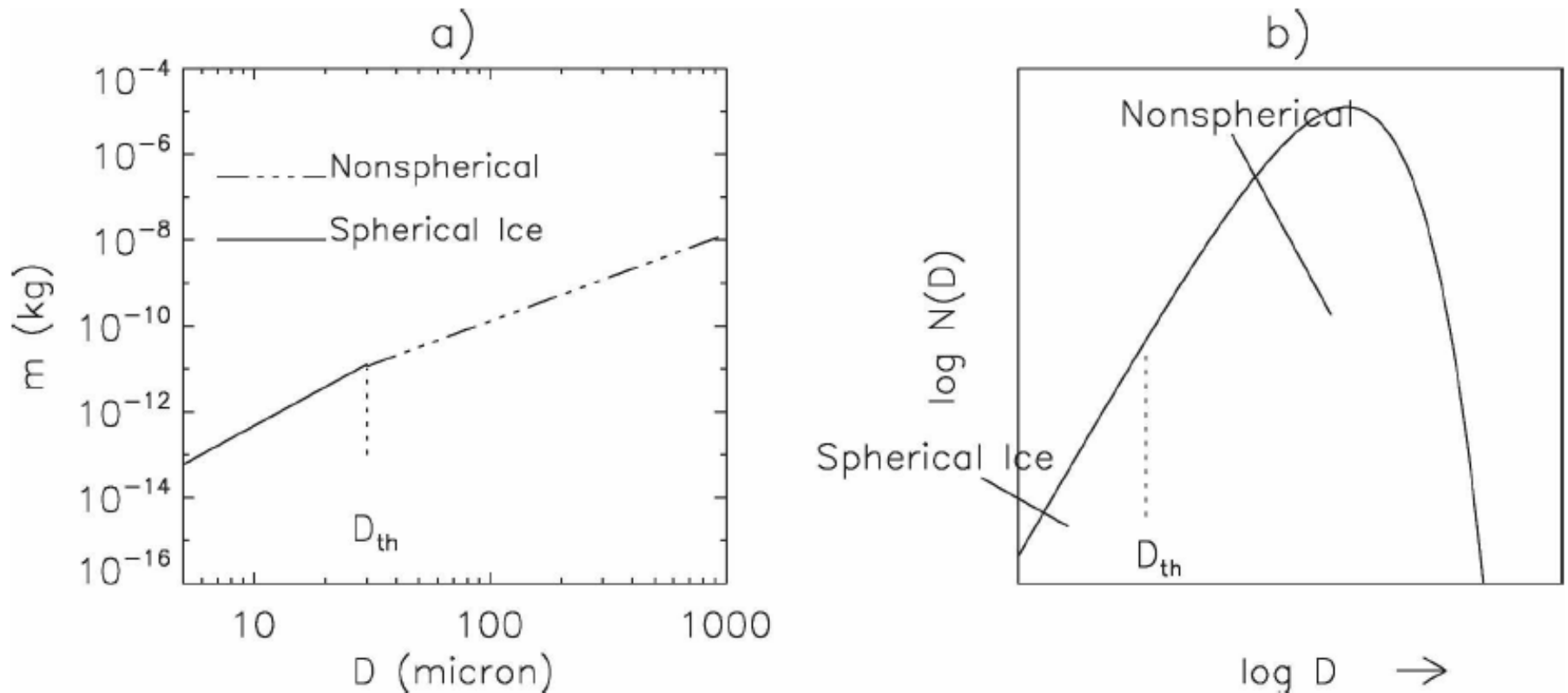


FIG. 1. (a) Mass–dimension relationships in unrimed conditions for solid spherical ice and unrimed nonspherical ice using parameters in Table 1 and critical particle dimension D_{th} . (b) Schematic diagram of the gamma particle size distribution $N(D)$ divided into two regions based on D_{th} .

Ice crystals/snowflakes grown by diffusion of water vapor/ aggregation and by riming

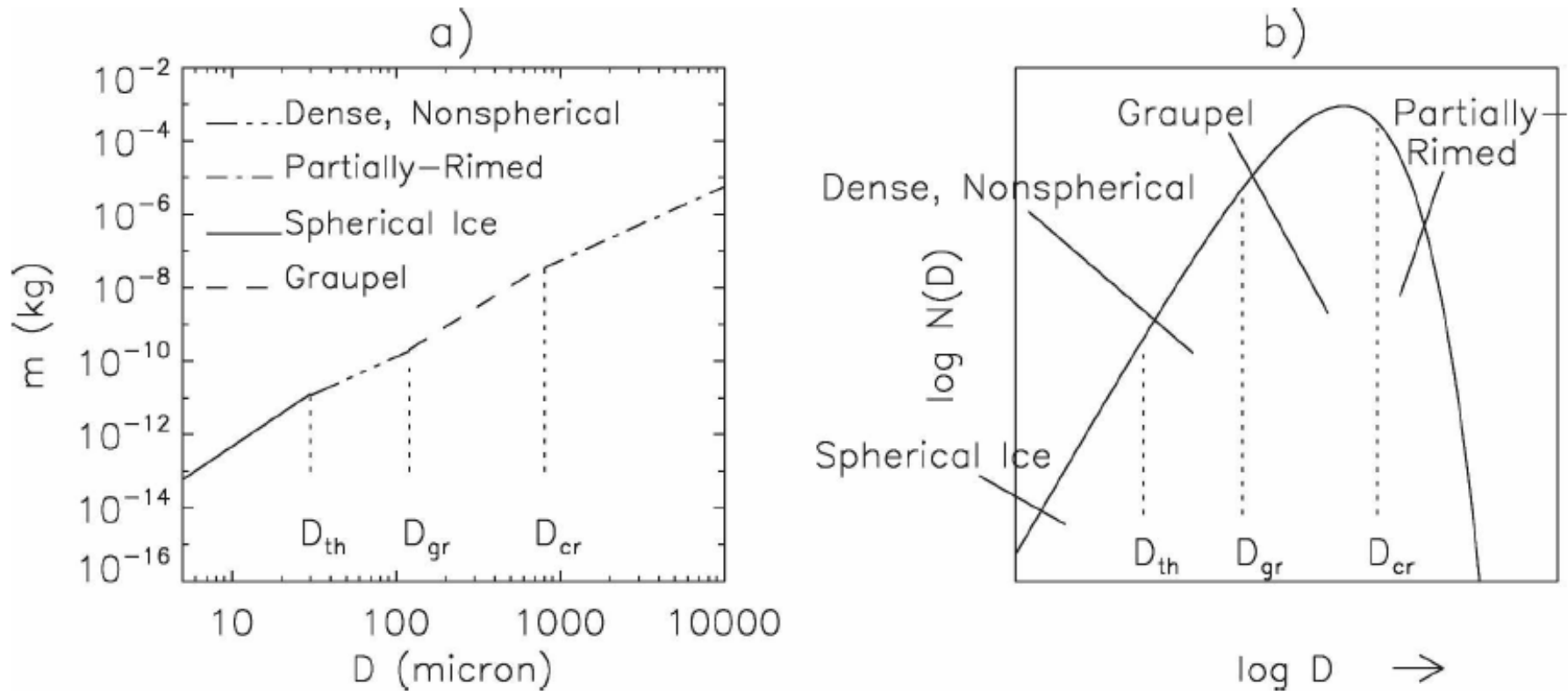
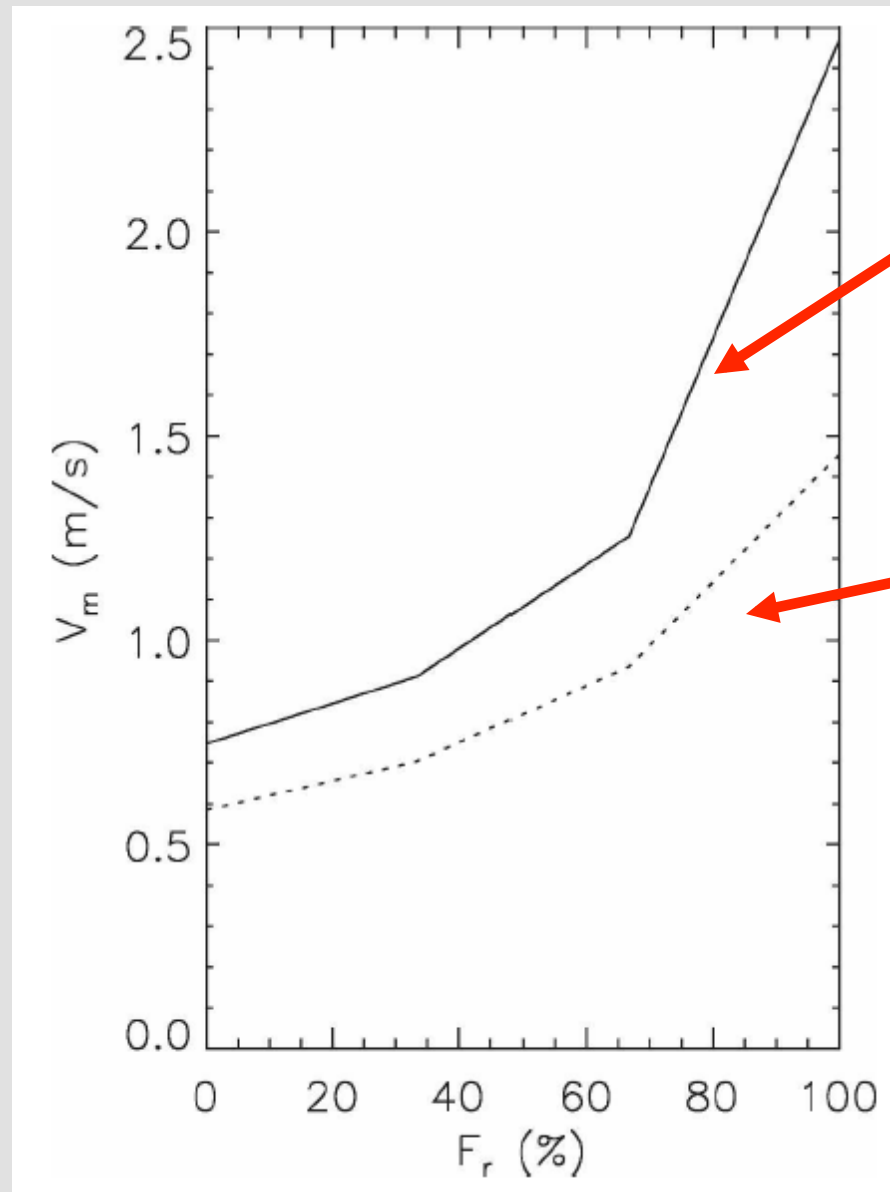


FIG. 2. (a) Mass–dimension relationships in rimed conditions for solid spherical ice, graupel, dense nonspherical ice, and partially rimed ice using parameters in Table 1, and critical dimensions D_{th} , D_{gr} , and D_{cr} . The m – D relationship shown in this example is calculated using a rimed mass fraction of 0.75. (b) Schematic diagram of the gamma particle size distribution $N(D)$ divided into four regions based on D_{th} , D_{gr} , and D_{cr} .

Parameterization of ice mass fallspeed. Note gradual increase with the rimed fraction F_r



1 g/kg; 3 l/L

0.1 g/kg; 3 l/L

Morrison and Grabowski (JAS 2008)

Example of the application of the new ice scheme: precipitation development in a small convective cloud [2D (x-z) prescribed-flow framework with a low-level convergence, upper-level divergence, evolving-in-time updraft, and weak vertical shear]

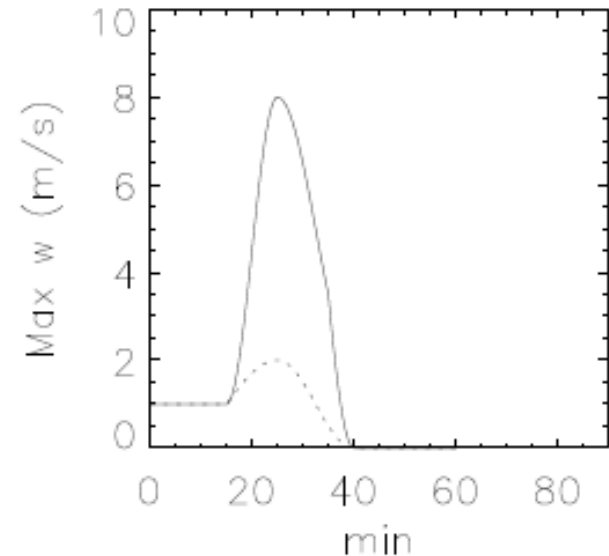
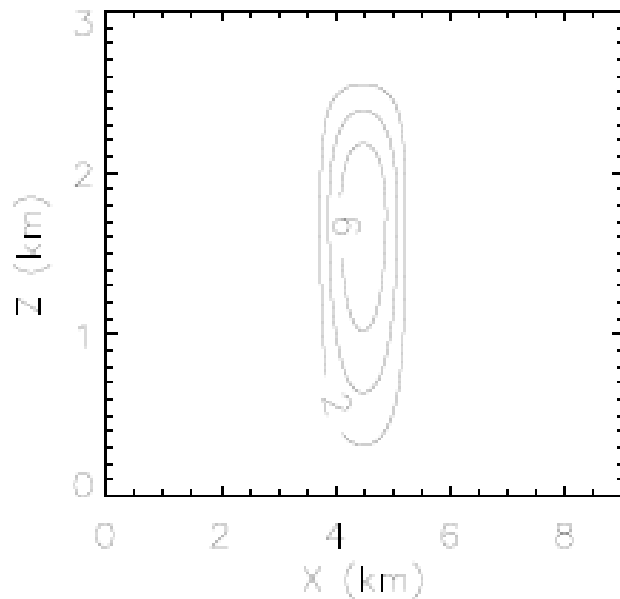
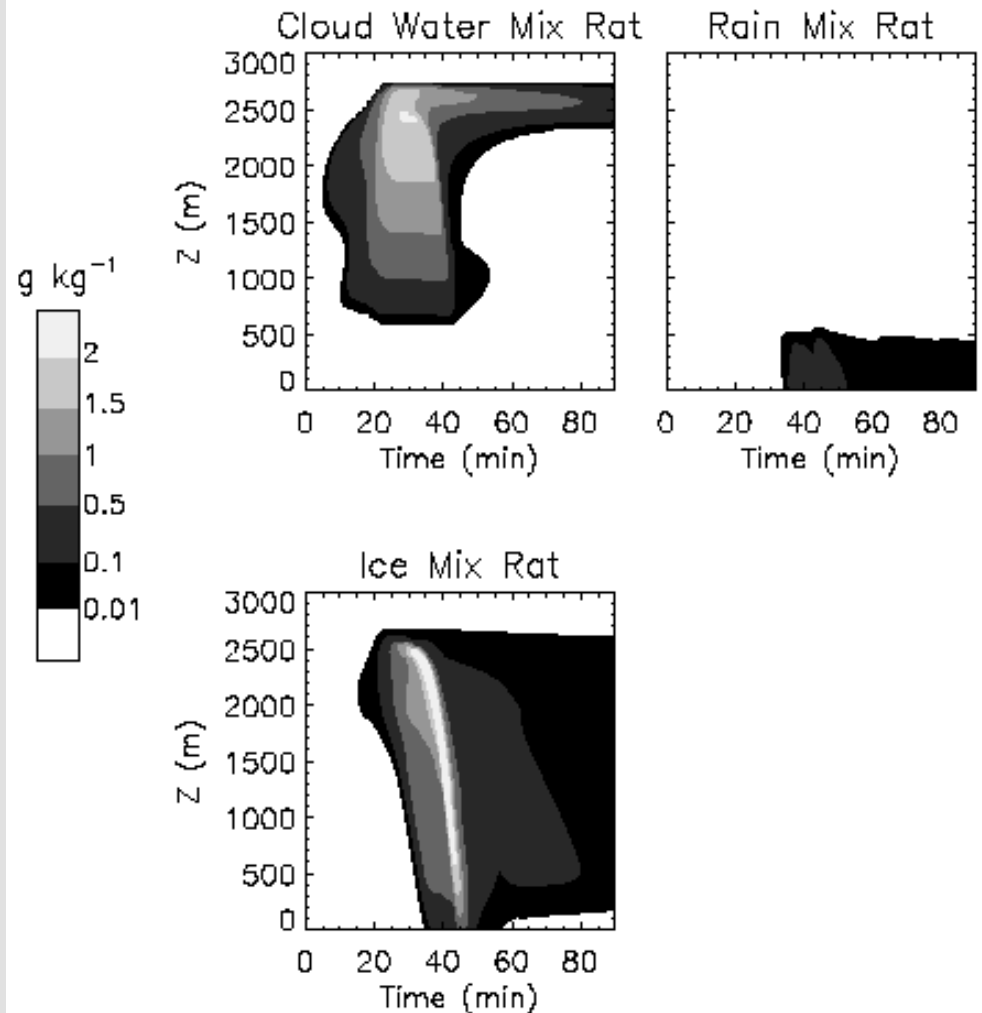
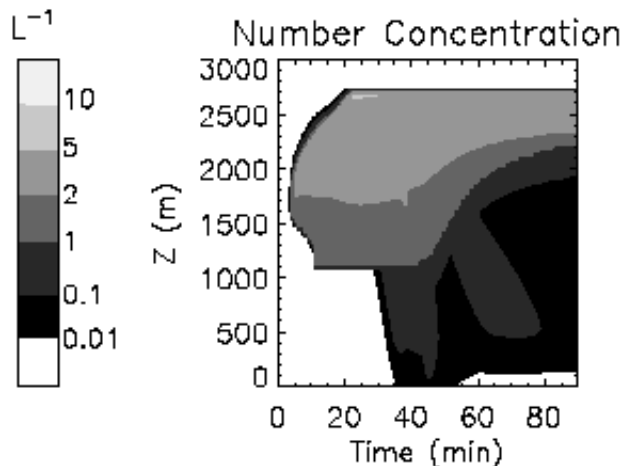
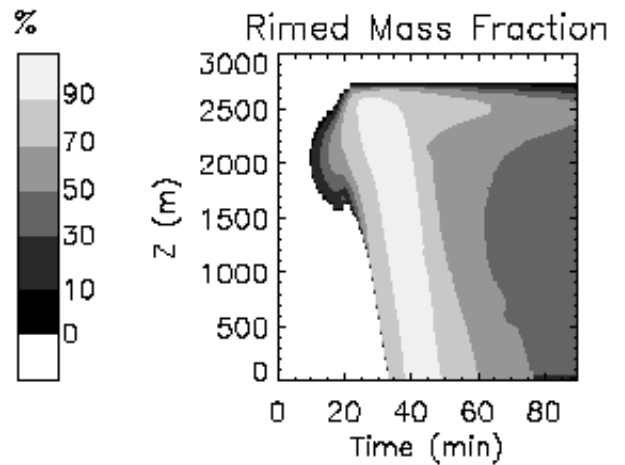


Figure 4: Maximum updraft velocity w in the X-Z plane as a function of time for peak updraft strength of 8 m/s (solid) and 2 m/s (dotted).

Morrison and Grabowski (JAS 2008)

Example of results: evolutions of horizontal maximum at each level



Morrison and Grabowski (JAS 2008)

Table 2: Time- and domain-average cloud liquid water path LWP (g m^{-2}), ice water path IWP (g m^{-2}), water optical depth τ_c (unitless), ice optical depth τ_i (unitless), total cloud optical depth τ_{tot} (unitless), and surface precipitation rate $PREC$ (mm/hr) for simulations with maximum updraft speed w of either 2 or 8 m s^{-1} . “NEW” and “TRADITIONAL” refer to simulations using the new and traditional ice microphysics schemes, respectively. “TH-HIGH” and “TH-LOW” refer to sensitivity tests using the traditional scheme but with the threshold ice/snow and droplet mixing ratios for graupel production during droplet collection increased or decreased, respectively (see text for details). “S1” and “H07” refer to sensitivity tests with the new scheme using the m-D relationship for side planes or from Heymsfield et al. (2007), respectively. The averaging period is from $t = 25$ to 90 min.

Run	Max w	LWP	IWP	τ_c	τ_i	τ_{tot}	$PREC$
NEW	8	228.4	237.1	26.7	8.6	35.3	0.68
TRADITIONAL	8	92.9	317.9	12.1	32.6	44.7	0.76
TH-HIGH	8	52.8	719.3	7.4	111.0	118.4	0.62
TH-LOW	8	474.7	137.5	52.6	2.8	55.4	0.46
S1	8	288.8	198.0	33.3	4.6	37.9	0.64
H07	8	477.0	136.5	52.1	2.4	54.5	0.52
NEW	2	49.8	85.3	7.1	4.5	11.6	0.23
TRADITIONAL	2	16.8	140.4	2.7	20.9	23.6	0.20
TH-HIGH	2	15.4	169.4	2.5	26.4	28.9	0.20
TH-LOW	2	122.8	34.3	16.0	0.8	16.8	0.14

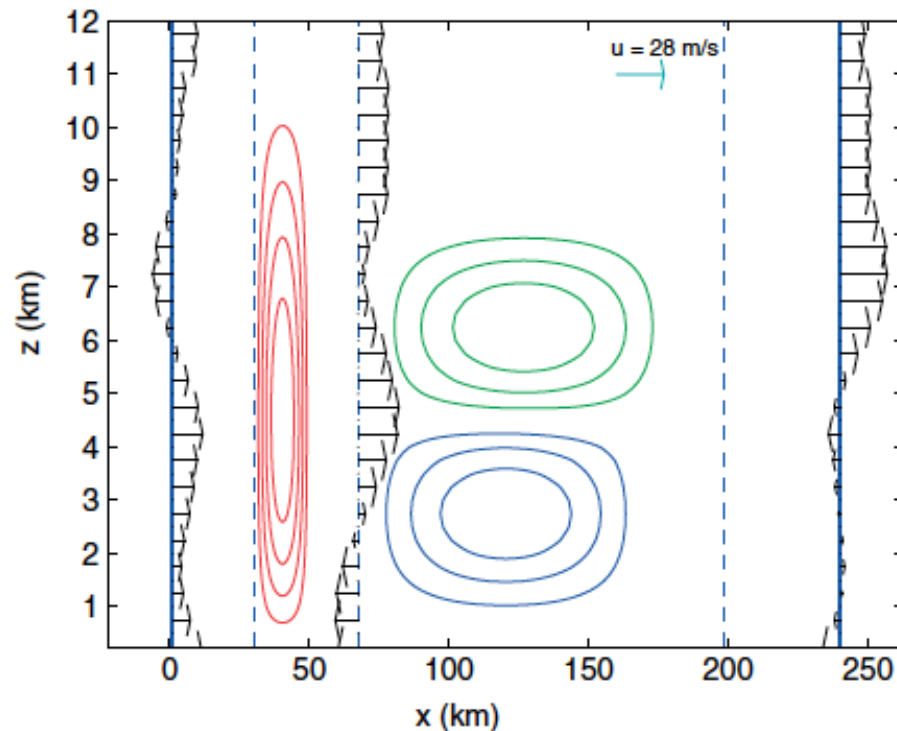
Notes and Correspondence

The impact of atmospheric aerosols on precipitation from deep organized convection: A prescribed-flow model study using double-moment bulk microphysics

Joanna Slawinska,^{a,*} Wojciech W. Grabowski^b and Hugh Morrison^b

^a*Institute of Geophysics, University of Warsaw, Poland*

^b*National Center for Atmospheric Research, Boulder, Colorado, USA*



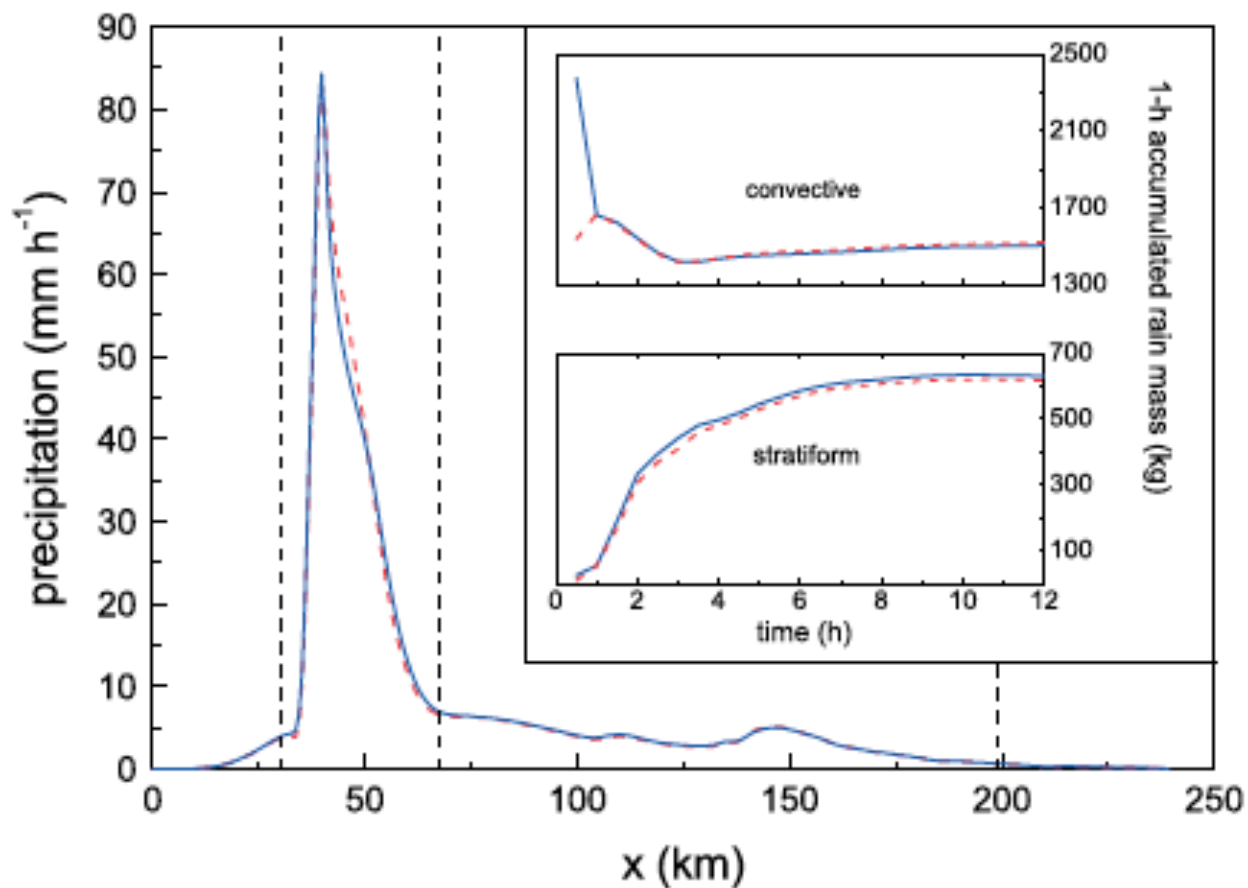


Figure 2. Spatial distribution of the steady-state surface precipitation for the whole area, with convective and stratiform boundaries shown as dashed vertical lines. The inserted figure shows time evolution of the area-integrated surface precipitation separated into convective and stratiform regions for 'pristine' (dashed lines) and 'polluted' (solid lines) base simulations. This figure is available in colour online at www.interscience.wiley.com/journal/qj

Table III. Description of all simulations analyzed in this paper, the one-hour accumulated rain mass R and the percentage of convective precipitation $\%C$. The simulations are referred to by the number given in the first column.

Simulations	'Pristine'		'Polluted'		
	R	$\%C$	R	$\%C$	
1	Base	2193	69.0	2196	68.5
2	75% qv	1790	68.8	1793	67.5
3	125% qv	2589	70.5	2590	69.8
4	$\theta = \theta - 5\text{ K}$	2451	64.7	2447	63.9
5	$\theta = \theta + 5\text{ K}$	1934	70.4	1935	69.4
6	10% ice nucleation	2187	69.4	2189	68.9
7	1000% ice nucleation	2192	67.0	2195	66.0
8	autoconversion: B1994	2195	67.5	2199	66.4
9	autoconversion: KK2000	2181	69.3	2190	68.5
10	smaller coefficient of ice-cloud droplet collision	2194	67.7	2195	66.8
11	smaller coefficient of ice-raindrop collision	2193	69.0	2196	68.5
12	enhanced raindrop breakup	2195	74.1	2196	74.4
13	50% stratiform updraft	2062	74.8	2065	74.2
14	150% stratiform updraft	2260	65.2	2265	64.6
15	without downdraft	2973	67.7	2979	67.8
16	50% downdraft	2561	67.3	2561	67.1
17	150% downdraft	1874	69.4	1876	68.0
18	without downdraft + 50% stratiform updraft	2853	73.5	2845	73.7
19	wider stratiform	2202	69.7	2204	69.2
20	narrower stratiform	2192	68.3	2195	67.8
21	stratiform closer to convective	2203	67.8	2206	67.4
22	70% convective updraft	1403	68.1	1406	67.2
23	130% convective updraft	3012	67.8	3016	67.1
24	1000% shear	2037	68.7	2042	67.3
25	1000% shear + 130% convective updraft	2862	66.6	2865	65.3

“thermodynamics”

“microphysics”

“dynamics”

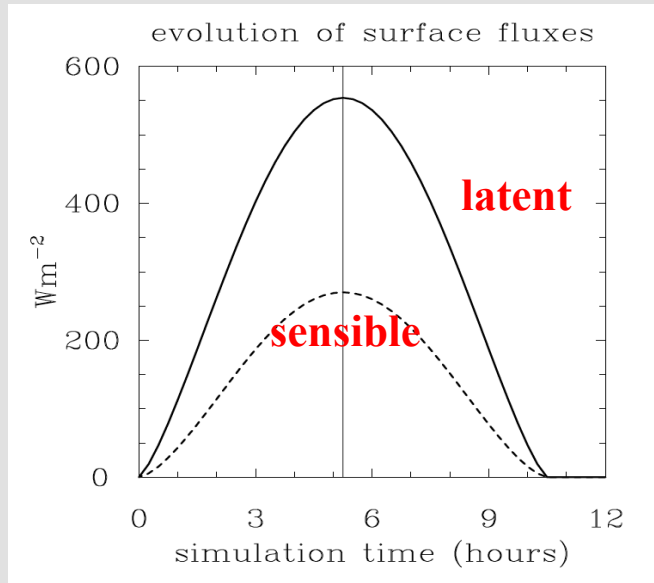
Many tests can be run at a very small cost...

Table III. Description of all simulations analyzed in this paper, the one-hour accumulated rain mass R and the percentage of convective precipitation $\%C$. The simulations are referred to by the number given in the first column.

	Simulations	'Pristine'		'Polluted'	
		R	$\%C$	R	$\%C$
1	Base	2193	69.0	2196	68.5
2	75% qv	1790	68.8	1793	67.5
3	125% qv	2589	70.5	2590	69.8
4	$\theta = \theta - 5$ K	2451	64.7	2447	63.9
5	$\theta = \theta + 5$ K	1934	70.4	1935	69.4
6	10% ice nucleation	2187	69.4	2189	68.9
7	1000% ice nucleation	2192	67.0	2195	66.0
8	autoconversion: B1994	2195	67.5	2199	66.4
9	autoconversion: KK2000	2181	69.3	2190	68.5
10	smaller coefficient of ice-cloud droplet collision	2194	67.7	2195	66.8
11	smaller coefficient of ice-raindrop collision	2193	69.0	2196	68.5
12	enhanced raindrop breakup	2195	74.1	2196	74.4
13	50% stratiform updraft	2062	74.8	2065	74.2
14	150% stratiform updraft	2260	65.2	2265	64.6
15	without downdraft	2973	67.7	2979	67.8
16	50% downdraft	2561	67.3	2561	67.1
17	150% downdraft	1874	69.4	1876	68.0
18	without downdraft + 50% stratiform updraft	2853	73.5	2845	73.7
19	wider stratiform	2202	69.7	2204	69.2
20	narrower stratiform	2192	68.3	2195	67.8
21	stratiform closer to convective	2205	67.8	2206	67.4
22	70% convective updraft	1403	68.1	1406	67.2
23	130% convective updraft	3012	67.8	3016	67.1
24	1000% shear	2837	68.7	2842	67.3
25	1000% shear + 130% convective updraft	2862	66.6	2865	65.3

Daytime convective development over land: A model intercomparison based on LBA observations

By W. W. GRABOWSKI^{1*}, P. BECHTOLD², A. CHENG³, R. FORBES⁴, C. HALLIWELL⁴,
M. KHAIROUTDINOV⁵, S. LANG⁶, T. NASUNO⁷, J. PETCH⁸, W.-K. TAO⁶, R. WONG⁸,
X. WU⁹ and K.-M. XU³



Simulations with double-moment bulk microphysics of Morrison and Grabowski (*JAS* 2007, 2008a,b):

N_c, q_c - cloud water
 N_r, q_r - drizzle/rain water
 N_i, q_{id}, q_{ir} - ice

Important differences from single-moment bulk schemes:

1. Supersaturation is allowed.
2. Ice concentration linked to droplet and drizzle/rain concentrations.

Simulations with double-moment bulk microphysics of Morrison and Grabowski (*JAS* 2007, 2008a,b):

PRI: pristine case, CCN of 100 per cc

POL: polluted case, CCN of 1,000 per cc

The same IN for POL and PRI

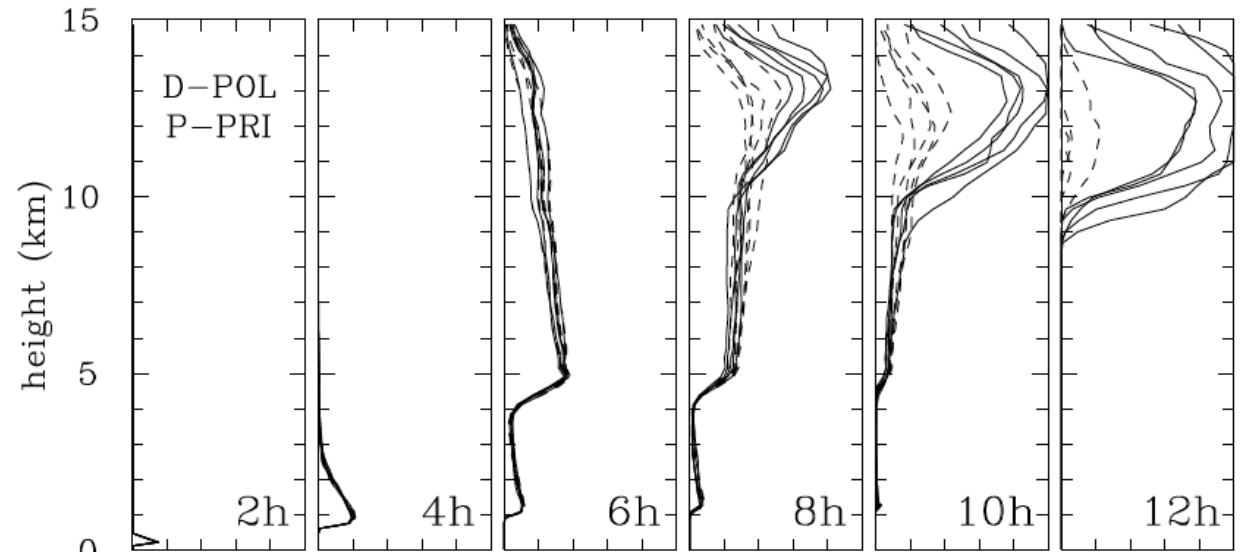
Piggybacking: D-PRI/P-POL: PRI drives, POL piggybacks

D-POL/P-PRI: POL drives, PRI piggybacks

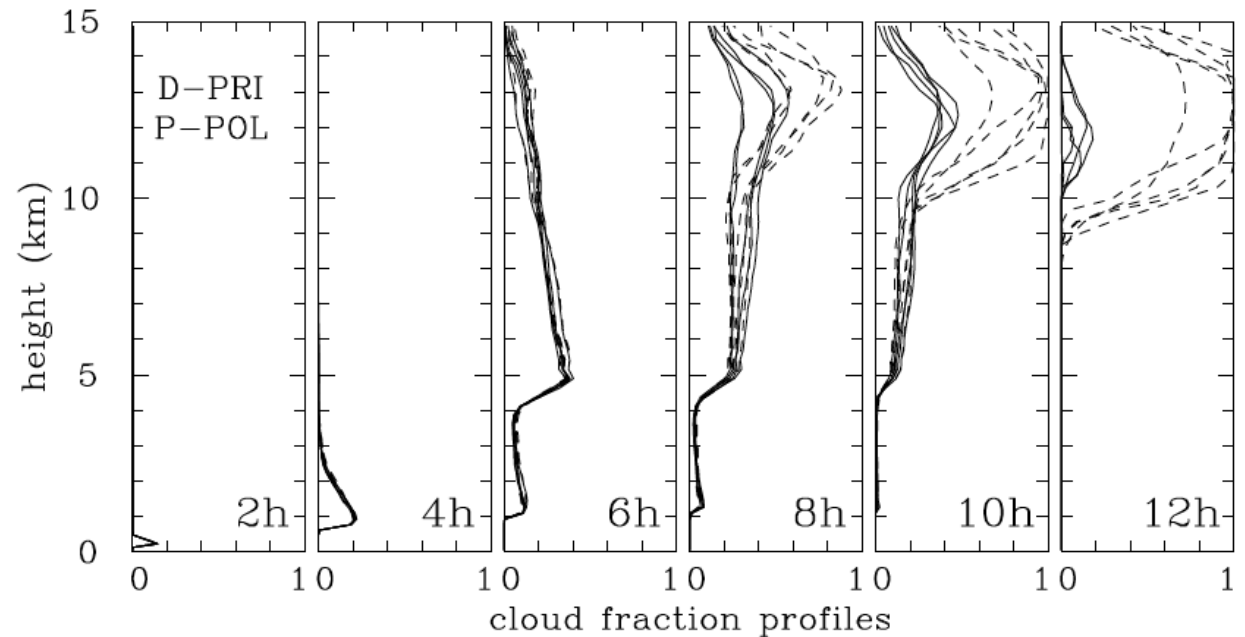
Five-member ensemble for each

solid lines: driving set
dashed lines: piggybacking set

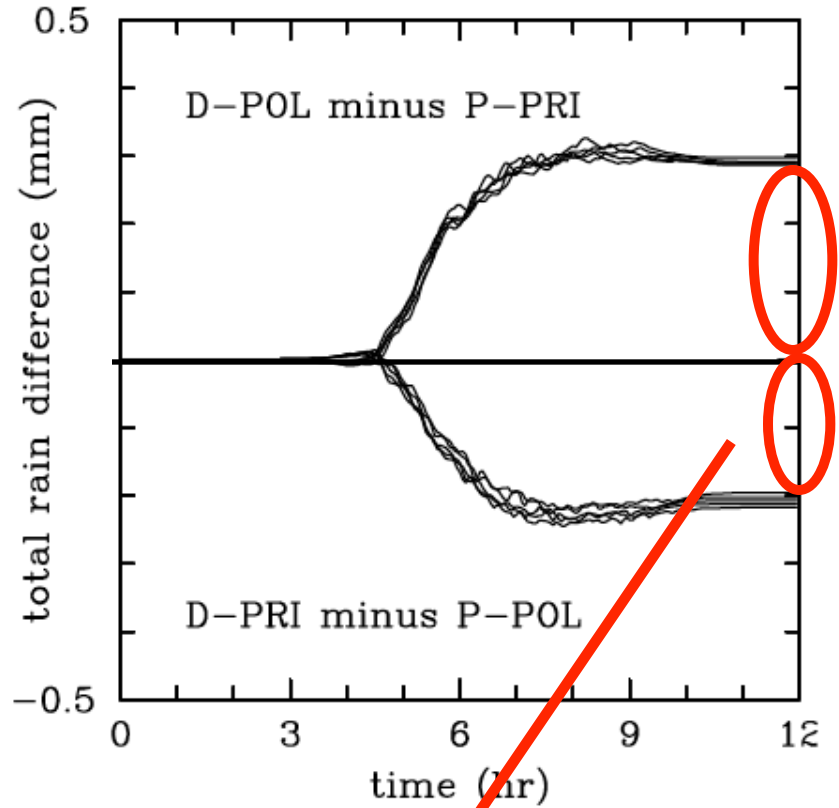
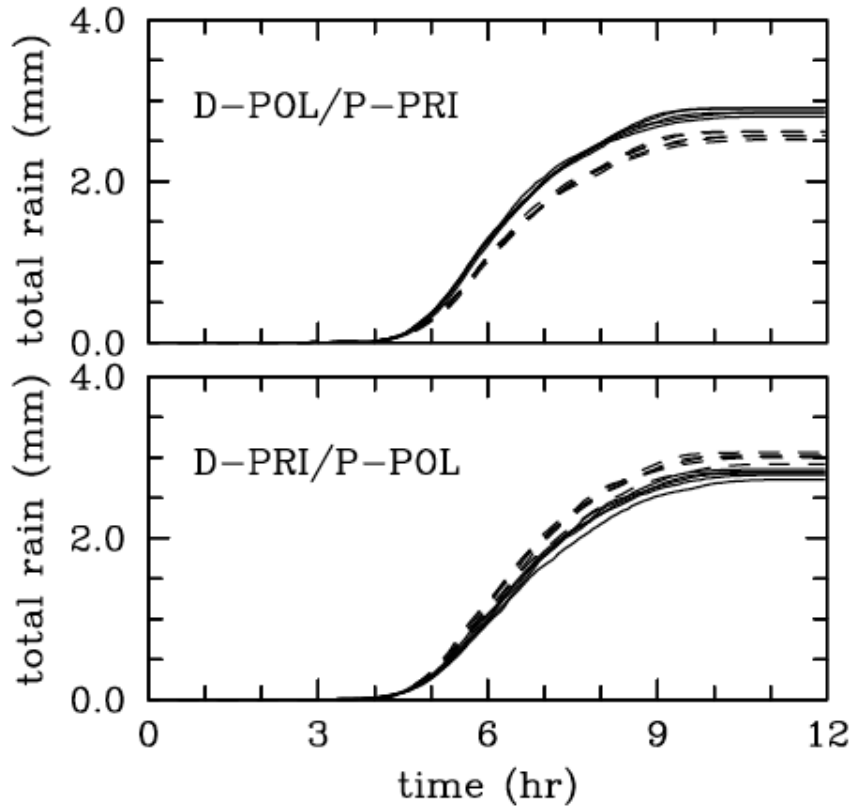
POL drives,
PRI piggybacks



PRI drives,
POL piggybacks



solid lines: driving set
dashed lines: piggybacking set

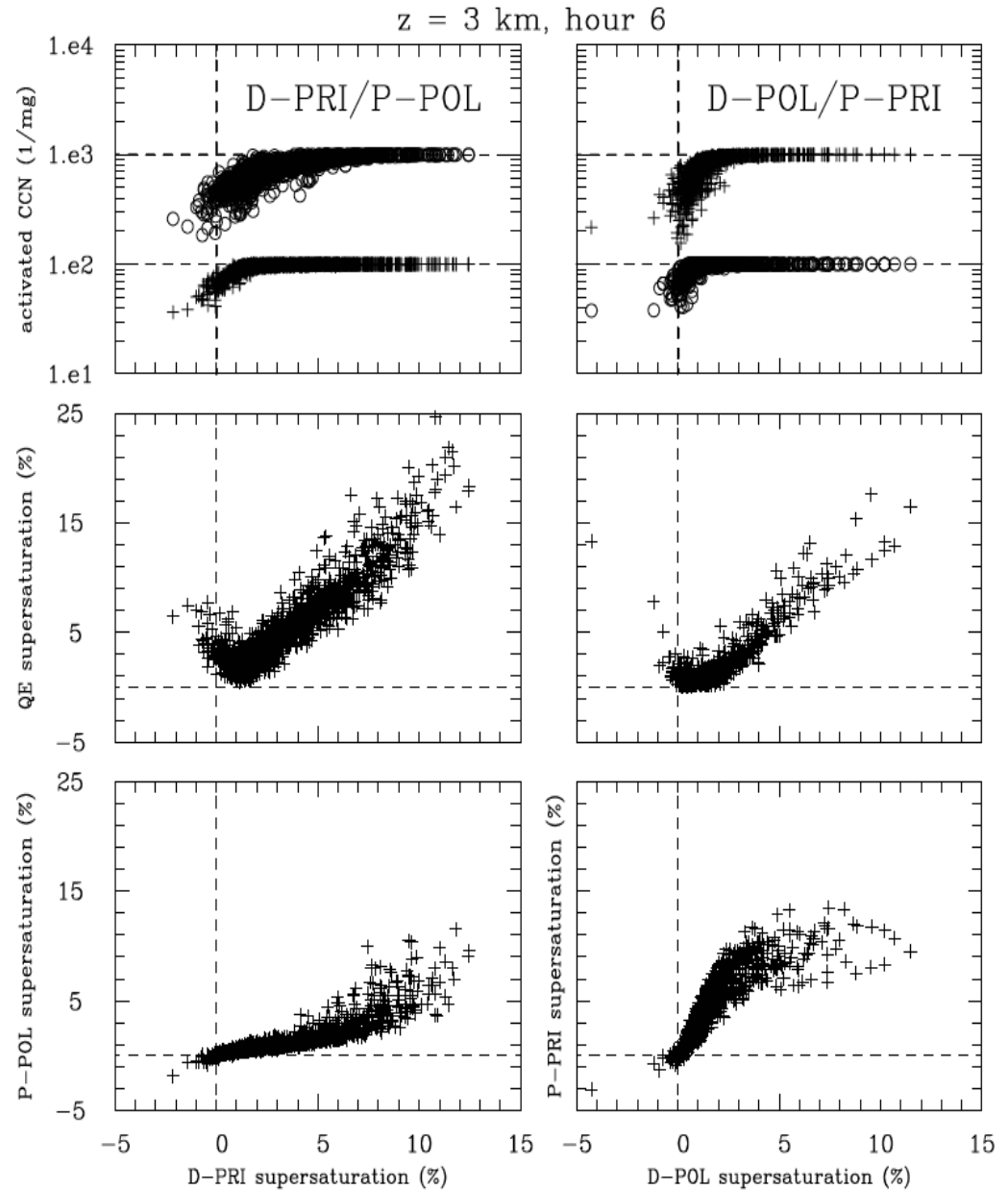


impact on the cloud dynamics?

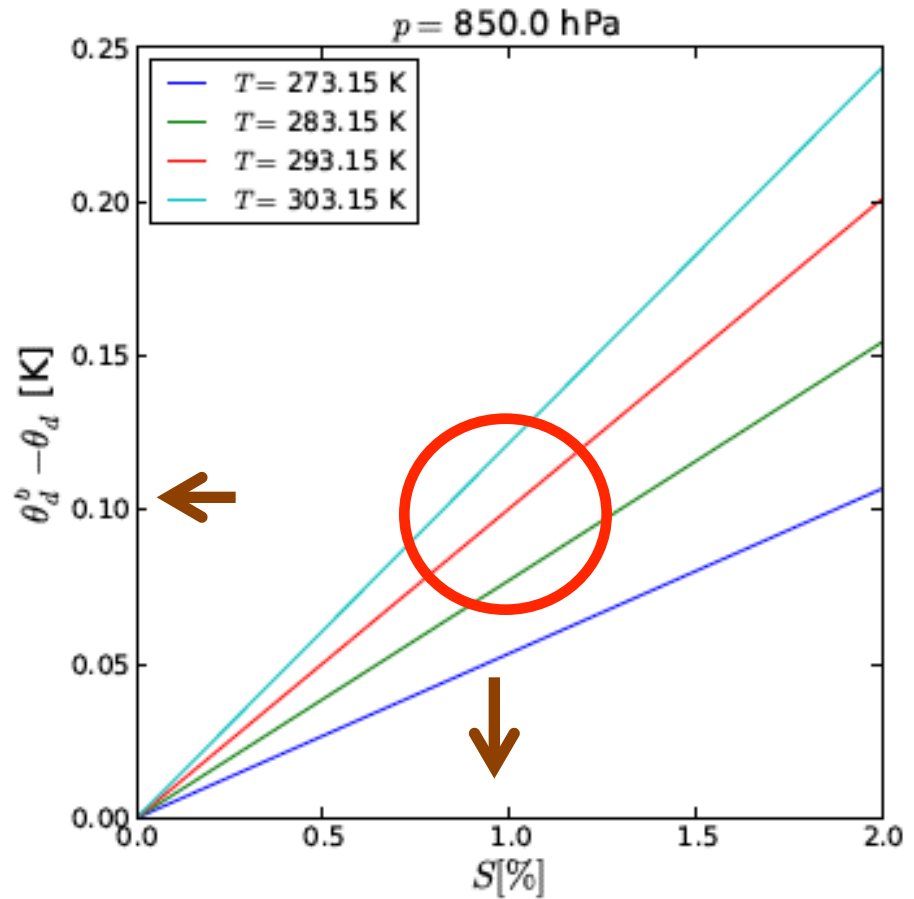
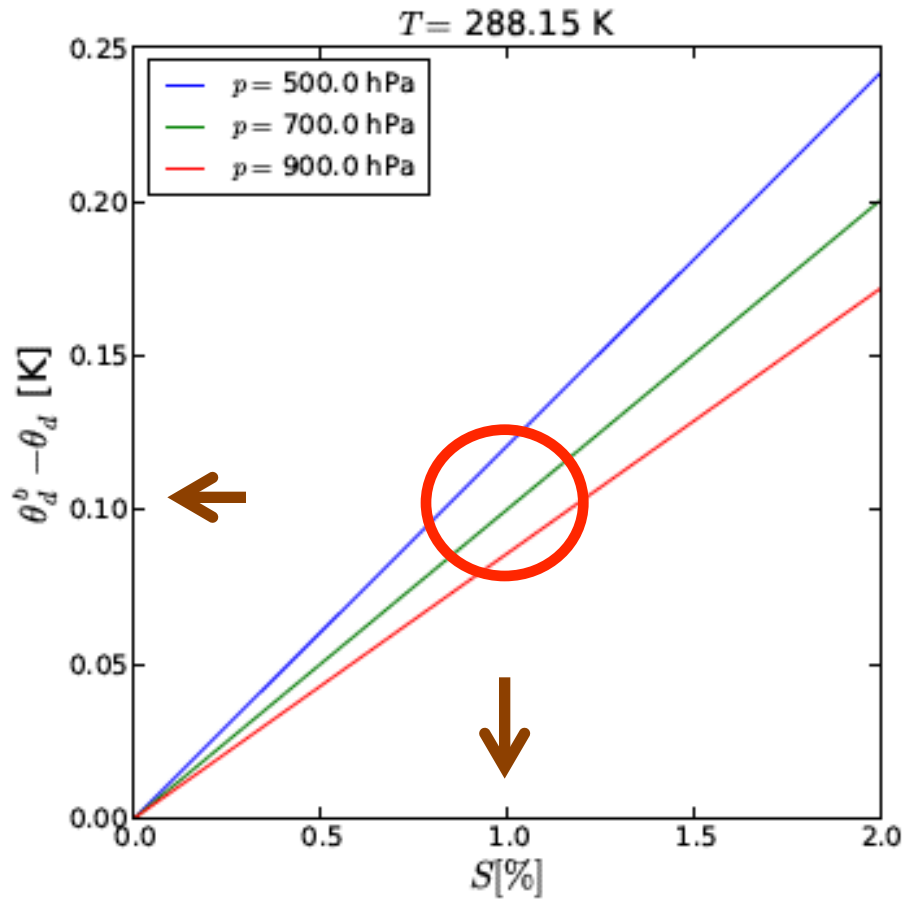
Local supersaturation, QE supersaturation, and activated CCN

$$S_{qe} \sim w \tau$$

$$\tau \sim (N_c r_c + N_r r_r)^{-1}$$

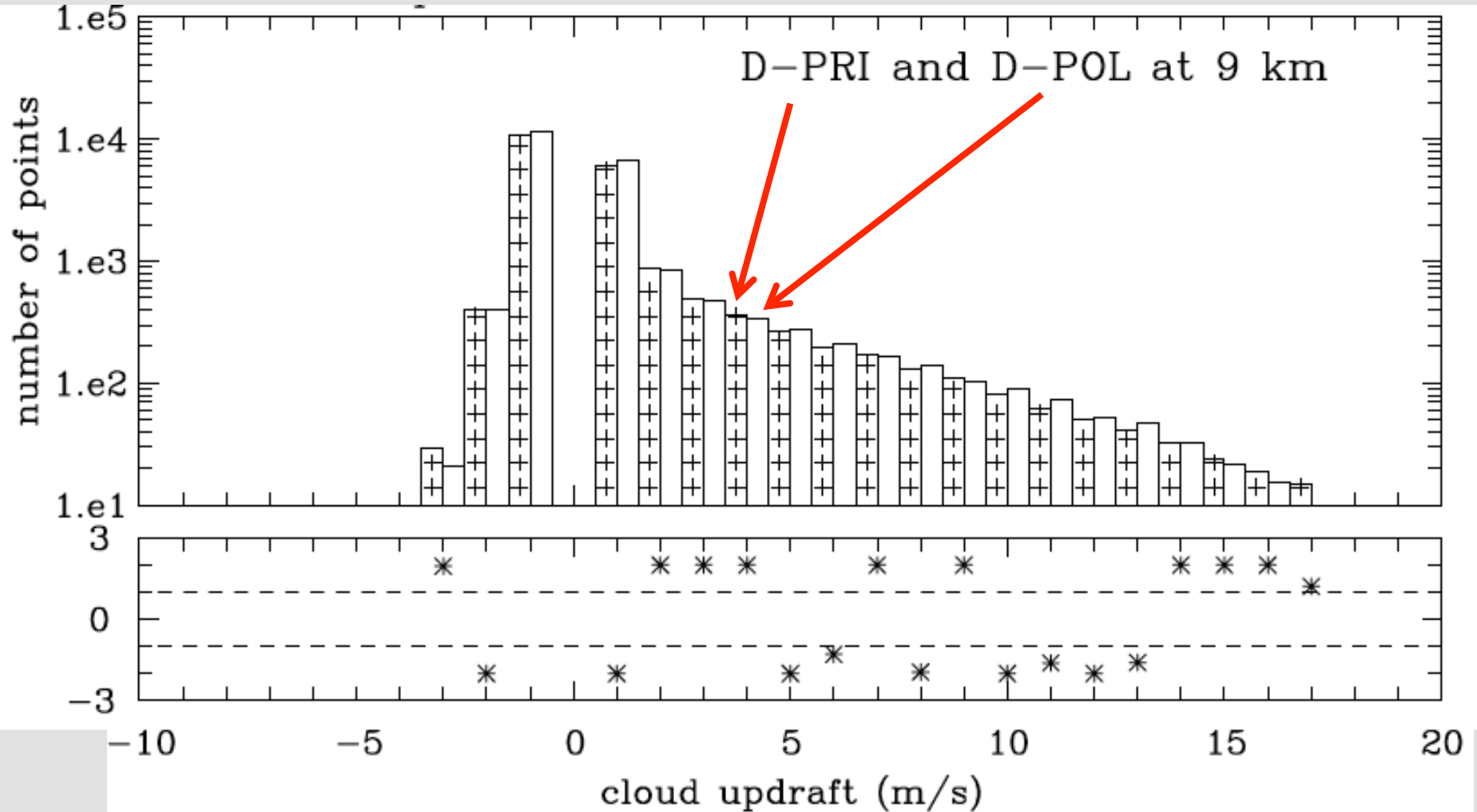


Comparing Θ_d with finite supersaturation with Θ_d at $S=0$, Θ_d^b

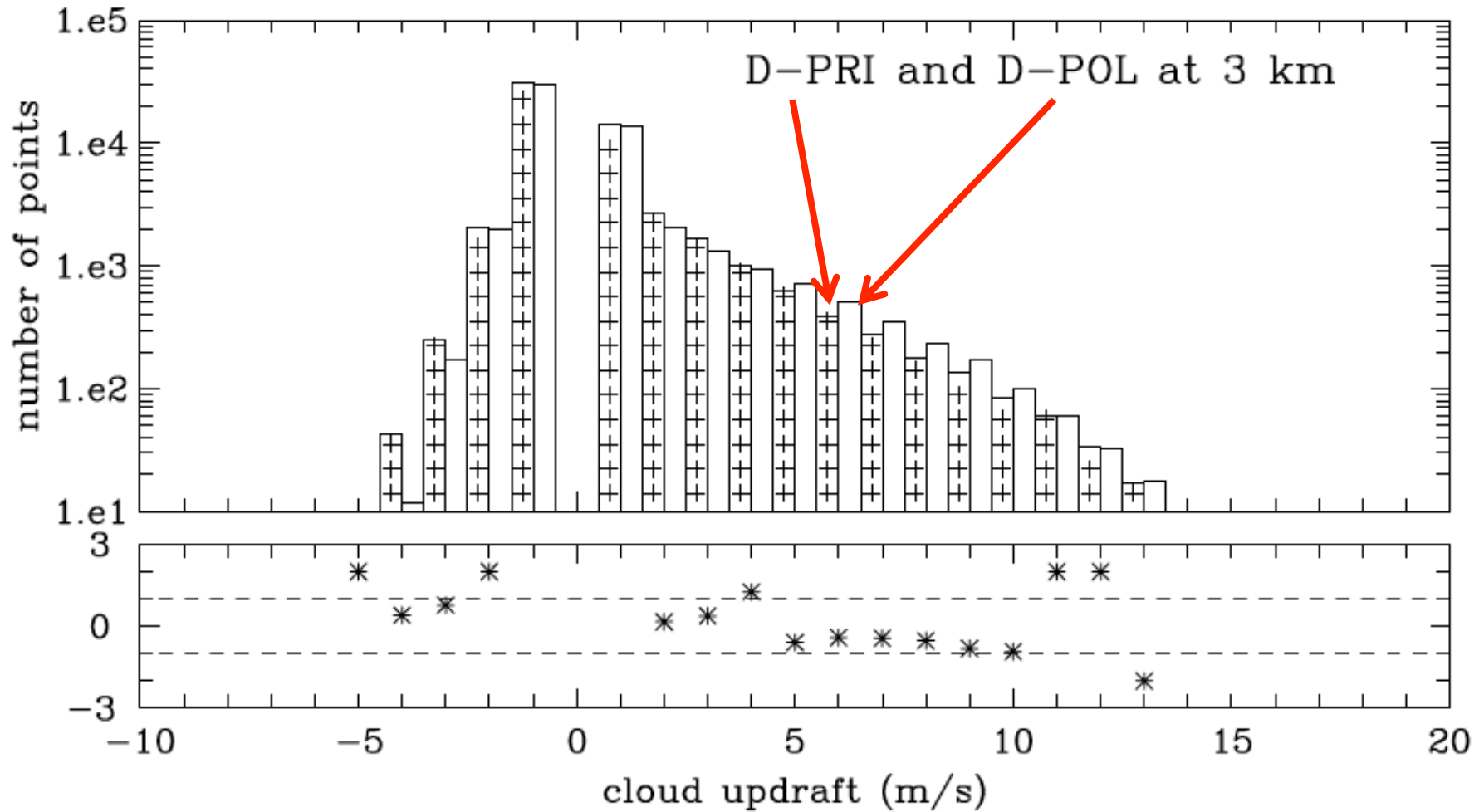


1% supersaturation \approx 0.1 K density temperature reduction

Vertical velocity statistics for D-PRI and D-POL at 9 km, measure of statistical significance of the D-PRI and D-POL difference



Vertical velocity statistics for D-PRI and D-POL at 3 km, measure of statistical significance of the D-PRI and D-POL difference



Conclusions for this part:

The piggybacking methodology clarifies the dynamic basis of convective invigoration in polluted environments.

- single-moment bulk schemes: no dynamical effect, 5-15% more surface rain in pristine cases;

- double-moment bulk scheme: small modification of the cloud dynamics in the warm-rain zone due to differences in the supersaturation field, ~10% more rain in polluted cases; significant *microphysical* impact on convective anvils.

Bulk schemes with saturation adjustment are likely inappropriate for deep convection.

Bin ice microphysics?

Traditional approach to bin cloud microphysics

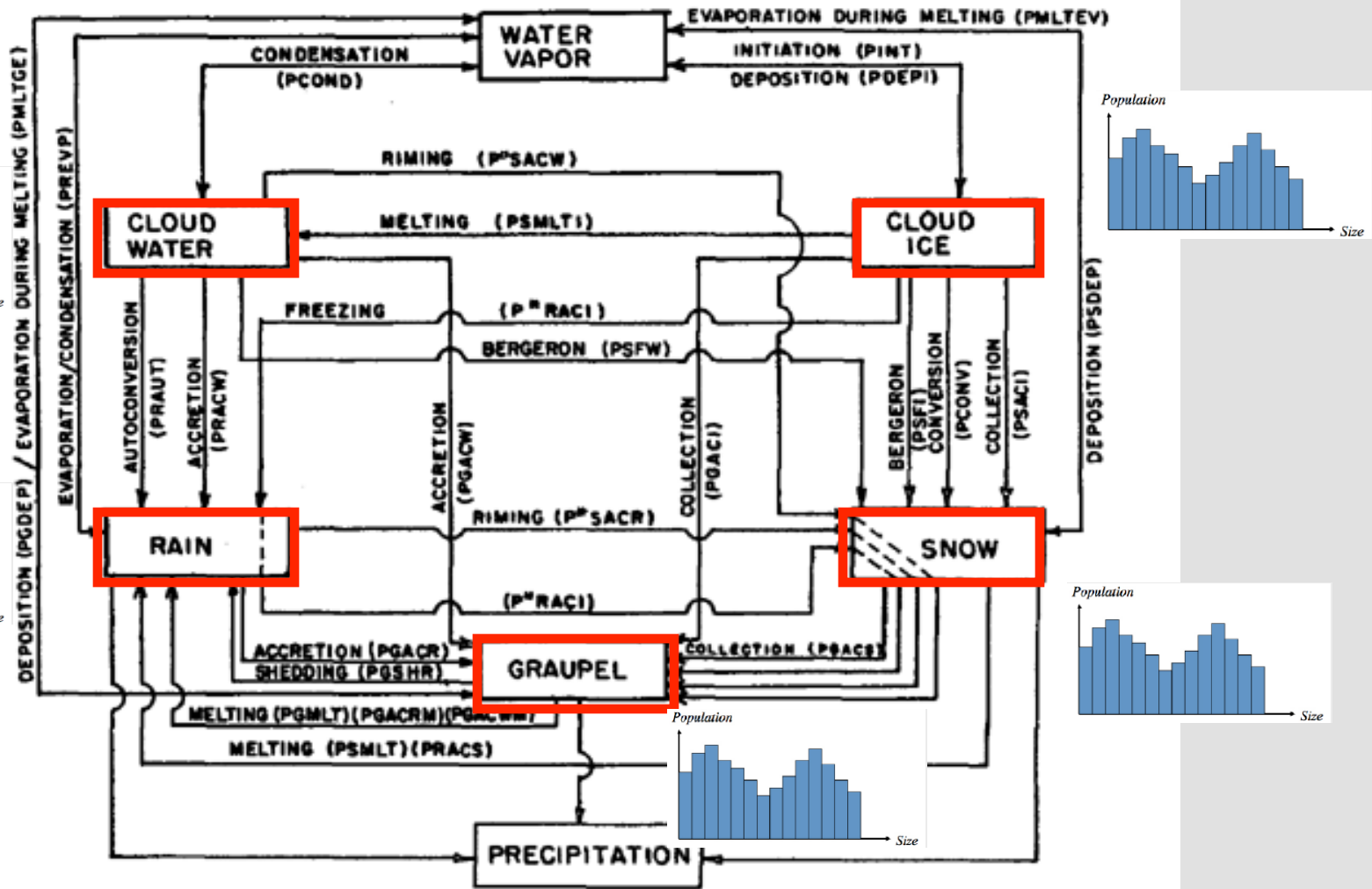


FIG. 1. Schematic depicting the cloud and precipitation processes included in the model for the study of narrow cold-frontal rainbands.

Does this approach make sense?

Does this approach make sense?

Can the approach applied in the 2-moment scheme of Morrison and Grabowski (2008) be expanded to the bin ice microphysics?

Can the approach applied in the 2-moment scheme of Morrison and Grabowski (2008) be expanded to the bin ice microphysics?

MAY 2010

MORRISON AND GRABOWSKI

1337

An Improved Representation of Rimed Snow and Conversion to Graupel in a Multicomponent Bin Microphysics Scheme

HUGH MORRISON AND WOJCIECH W. GRABOWSKI

National Center for Atmospheric Research, Boulder, Colorado*

(Manuscript received 13 July 2009, in final form 22 January 2010)

ABSTRACT

New trend: Lagrangian treatment of the condensed phase:

The super-droplet method for the numerical simulation of clouds and precipitation: A particle-based and probabilistic microphysics model coupled with a non-hydrostatic model

S. Shima,^{a*} K. Kusano,^c A. Kawano,^a T. Sugiyama^a and S. Kawahara^b

Cloud-aerosol interactions for boundary layer stratocumulus in the Lagrangian Cloud Model

M. Andrejczuk,¹ W. W. Grabowski,² J. Reisner,³ and A. Gadian¹

Large-Eddy Simulations of Trade Wind Cumuli Using Particle-Based Microphysics with Monte Carlo Coalescence

SYLWESTER ARABAS

Institute of Geophysics, Faculty of Physics, University of Warsaw, Warsaw, Poland

SHIN-ICHIRO SHIMA

Graduate School of Simulation Studies, University of Hyogo, Kobe, and Japan Agency for Marine-Earth Science and Technology, Kanagawa, Japan

A new method for large-eddy simulations of clouds with Lagrangian droplets including the effects of turbulent collision

T Riechelmann^{1,3}, Y Noh² and S Raasch¹

Eulerian dynamics, energy and water vapor transport:

$$\frac{\partial(u\rho)}{\partial t} + \frac{\partial(uu\rho)}{\partial x} + \frac{\partial(wu\rho)}{\partial z} = -\frac{\partial p'}{\partial x} + \Phi_{m,x} + \frac{\partial(\kappa\rho\tau^{11})}{\partial x} + \frac{\partial(\kappa\rho\tau^{13})}{\partial z},$$

$$\frac{\partial(w\rho)}{\partial t} + \frac{\partial(uw\rho)}{\partial x} + \frac{\partial(ww\rho)}{\partial z} = -\frac{\partial p'}{\partial z} - \rho'g + \Phi_{m,z} + \frac{\partial(\kappa\rho\tau^{31})}{\partial x} + \frac{\partial(\kappa\rho\tau^{33})}{\partial z},$$

$$\frac{\partial(\theta\rho)}{\partial t} + \frac{\partial(u\theta\rho)}{\partial x} + \frac{\partial(w\theta\rho)}{\partial z} = \frac{\theta\rho L}{TC_p} f_{cond} + f_{surface-energy} + f_{rad} + \frac{\partial F_{\theta x}}{\partial x} + \frac{\partial F_{\theta z}}{\partial z},$$

$$\frac{\partial(q_v\rho)}{\partial t} + \frac{\partial(uq_v\rho)}{\partial x} + \frac{\partial(wq_v\rho)}{\partial z} = -f_{cond} + f_{surface-gas} + \frac{\partial F_{q_v x}}{\partial x} + \frac{\partial F_{q_v z}}{\partial z},$$

Lagrangian physics of “super-particles”

a single “super-particle” represents a number of the same airborne particles (aerosol, droplet, ice, etc.) with given attributes

$$\frac{dx_i}{dt} = v_i$$

$$\frac{dv_i}{dt} = \frac{1}{\tau_p} (v_i^* - v_i) + g\delta_{i,2}$$

$$\frac{dr}{dt} = \frac{G}{r} (S^* - S_{eq})$$

Coupling

$$\Phi_{m,x} = \sum_{id} m_{id} \frac{M_{id}}{\Delta V} \frac{(u^* - u_{id})}{\tau_{p,id}}$$

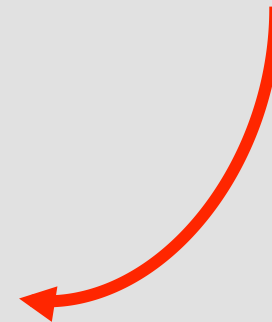
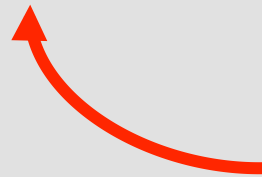
$$\Phi_{m,z} = \sum_{id} m_{id} \frac{M_{id}}{\Delta V} \frac{(w^* - w_{id})}{\tau_{p,id}}$$

$$f_{cond} = \sum_{id} \frac{M_{id}}{\Delta V} \frac{dm_{id}}{dt}$$

m_{id} – mass of the super-particle

M_{id} – concentration of super-particles

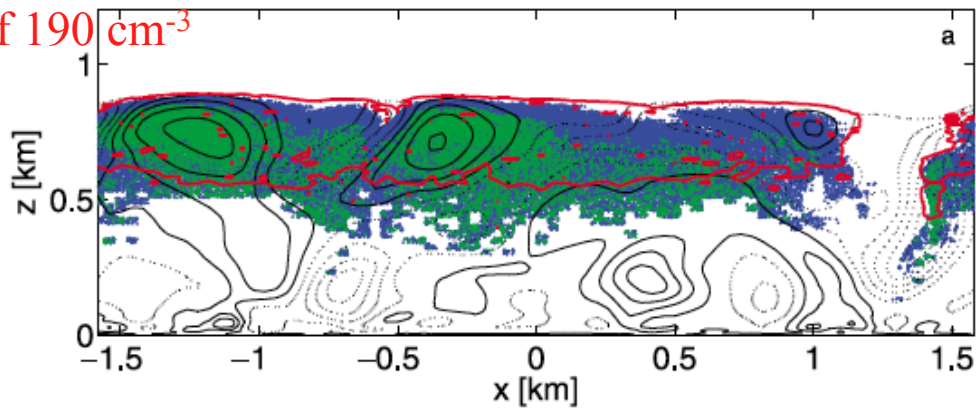
ΔV – volume of the gridbox



Why Lagrangian SD approach is appealing?

- no numerical diffusion due to advection;
- but sampling errors: one needs ~ 100 particles per gridbox for simple problems, many more with a longer list of attributes for appropriate sampling of the parameter space;
- straightforward for condensational growth of cloud droplets (initial sampling of the CCN distribution, growth/activation/evaporation of aerosol/droplet) – *ideal for entrainment/mixing!*
- more complex for collisions (collision of two SDs creates a new SD: two methods in the literature to deal with this...);
- seems ideal to couple with sophisticated subgrid-scale models to represent effects of turbulence (e.g., randomly choose thermodynamic environment within a gridbox, use LEM approach, etc);
- easy representation of ice particle habits and diffusional versus accretional growth.

CCN of 190 cm^{-3}



CCN of 1295 cm^{-3}

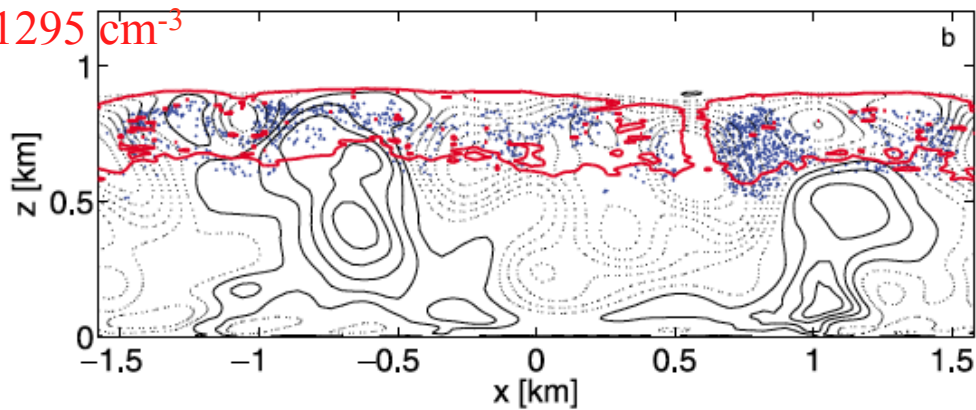
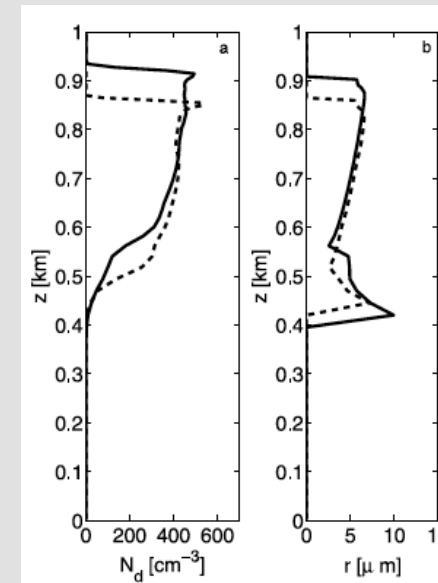
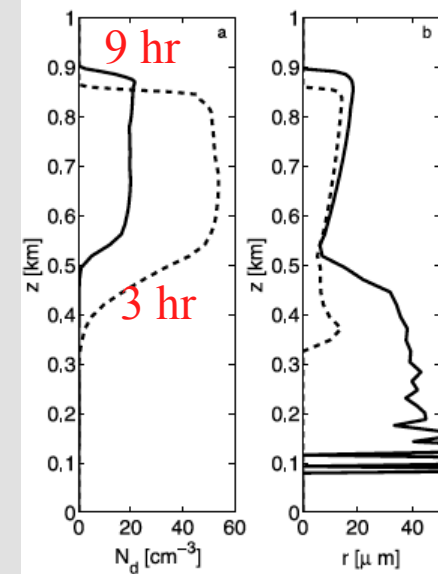


Figure 3. Vertical cross sections through model domain after 9 h of simulations: cross sections at (a) $y = -1180 \text{ m}$ for LOW and (b) $y = 420 \text{ m}$ for HIGH. Solid lines indicate positive velocities starting from 0.1 m/s with contour interval 0.2 m/s ; dotted lines represent negative velocity starting from -0.1 m/s with the interval -0.2 m/s . The red line presents condensed water contour of 0.1 g/kg . Blue/green dots represent the locations of droplets bigger than $50/90 \mu\text{m}$.



Summary of the warm-rain and ice lectures:

A wide range of modeling approaches exists that one can use in modeling various aspects of cloud dynamics and microphysics. Most of them are within the framework of Eulerian modeling, but use of Lagrangian microphysics is rapidly expanding.

The selection of specific method needs to be tailored to the specific problem one would like to study. If multiscale dynamics (e.g., convectively coupled waves in the Tropics) is the focus, application of as simple microphysics as possible makes sense (to use the computer time to widen the range of spatial scales). If small-scale dynamics–microphysics interactions is the focus, more emphasis on microphysics is needed.

The multiscale nature of clouds (the range of spatial scales), difficulties of cloud observations (in-situ and remote sensing), and increasing appreciation of the role of clouds in weather and climate make the cloud physics an appealing area of research.